Dissertation zur Erlangung des Doktorgrades

der Fakultät für Chemie und Pharmazie

der Ludwig-Maximilians-Universität München

Critical Role of Transcription Cofactor PC4 in Mammals

Na Li

aus

Henan, China

2010

Erklärung

Diese Dissertation wurde im Sinne von §13 Abs. 3 bzw. 4 der Promotionsordnung vom 29. Januar 1998 von Herrn Prof. Dr. Meisterernst betreut.

Ehrenwörtliche Versicherung

Diese Dissertation wurde selbständig und ohne unerlaubte Hilfe erarbeitet.

München, am 11.01.2010

_____

Na Li

Dissertation eingereicht am: 11.01.2010

1. Gutachter: Prof. Dr. Meisterernst

2. Gutachter: Prof. Dr. Wolf

Mündliche Prüfung am: 15.03.2010

ACKNOWLEDGEMENTS

I am very grateful to Prof. Dr. Michael Meisterernst for giving me the opportunity to work with him and for guiding me in the field of transcription. I am thankful for his constant support and guidance throughout my work.

I am grateful to Prof. Dr. Eckhard Wolf for taking the part of referee.

I am thankful to all the current and former lab members, especially, Ulrike Niehues for taking care of mice and all the technical help.
I would like to thank former member Dr. Wera Roth who was initially involved in designing the conditional knockout-targeting vector for this project and also for constant guidance.
I thank former member Gertraud Stelzer for making a lot of contribution to generating the constitutive knockout mouse model.
Many thanks to Dr. Thomas Albert for the critical comments on this manuscript.
I enjoyed all the scientific and non-scientific discussions with my friends Ming, Tasneem and Caroline and thank them for the pleasant atmosphere in the lab.

I am grateful to all the collaborators who contributed to this work,
Prof. Dr. Hans R. Schöler, who provided me the opportunity to work in his lab and utilize the facilities at the Max PIanck Institute for Molecular Biomedicine, and Dr. Guangming Wu from his lab, who helped me to generate knockout ES cell lines and also taught me many techniques related to this work.
Prof. Dr. Jörn Walter and Mark Wossidlo, who helped in mouse zygotes immunostaining.
Prof. Dr. Heinrich Leonhardt and Dr. Ursula Zimber-Strobl, who gave me a lot of invaluable help and advice.

Finally, I would like to thank my husband and my family for their love, support and all the encouragement throughout these years.

SUMMARY

PC4 is a small protein with unique DNA-binding properties that affects transcription and has presumptive roles in DNA repair and genome stability. It was originally isolated from a cofactor fraction termed the ‘‘upstream stimulatory activity’’ (USA) of HeLa cell nuclear extracts. The cofactor has been shown to broadly enhance RNA polymerase II-driven gene transcription in the presence of activators (e.g., hormone receptors, viral activators, cell-specific and ubiquitous activators). Although such data imply that PC4 is a very important factor *in vivo*, human tumor cell lines with PC4 knockdowns are without obvious phenotypes. To further study the *in vivo* role of PC4, we constructed constitutive and conditional knockout mouse models as well as knockout embryonic stem cells. Mammalian PC4 is here shown to be an essential factor during early embryogenesis. $PC4^{-/-}$ embryos develop normally until E5.5, but then degenerated around E7.5. PC4 knockout ES cell lines were generated from $PC4^{-/-}$ blastocysts (E3.5), which develop normally from 2-cell stage embryos. All PC4 knockout ES cell lines displayed a severe proliferation deficit phenotype, which could be partially rescued by re-expression of human PC4. The reduced proliferation was not due to an increase in cell apoptosis. Occasionally, PC4 knockout ES cells undergo tetraploidy apparently as a survival mechanism to circumvent the loss of PC4. Knocking down PC4 in mouse embryonic fibroblasts also resulted in reduced proliferation rates. These data indicate that PC4 is important for cell proliferation in embryos. Moreover, *in vitro* embryoid body formation and *in vivo* teratoma formation assays provided preliminary evidence for an important role of PC4 in differentiation. Differentiated ES cells displayed alterations in germ-layer specific gene expression, that are in agreement with morphological abnormalities observed in histological analyses of $PC4^{-/-}$ embryos at E6.5 and E7.5. Thus, depletion of PC4 results in reduced proliferation and impaired differentiation, the consequence of which appears to be of gastrulation arrest in early embryos.

In an attempt to understand the underlying mechanisms of this phenotype, differential gene expression in ES knockout and wild-type cells was studied. Microarray and qRT-PCR analyses revealed more than 2 fold alterations in expression of many genes in knockout ES cells as compared with wild-type cells. These include enhanced expression of *p21*, *Rb1*, *and Ddit4l*, and lower expression of *Sfmbt2*, *Tdrd12*, and *Dppa3*, suggesting a specific direct or indirect physiological role of the cofactor.

Nevertheless, the previously proposed role of PC4 in *p53* expression and function was not confirmed using the knockout model. Taken together, this work represents the first description of the physiological functions of PC4 during mammalian embryogenesis.

PUBLICATION

Oliver Mortusewicz, Wera Roth, **Na Li**, M. Cristina Cardoso, Michael Meisterernst, Heinrich Leonhardt.

Recruitment of RNA polymerase II cofactor PC4 to DNA damage sites.

The Journal of Cell Biology, 2008, 183 (5):769-76.

TABLE OF CONTENTS

1. INTRODUCTION

1.1 The process of gene expression

The genome of an organism has been called “the blueprint for life”. Through the process of gene expression, the master plan is realized. During this process, genetic information is transferred from deoxyribonucleic acid (DNA) to ribonucleic acid (RNA) (transcription) and then from RNA to protein (translation) to bring the genome to life. These two processes, transcription and translation, are physically separated in eukaryotes by a membrane that surrounds the nucleus; transcription occurs in the nucleus, whereas translation is a cytoplasmic event.

Transcription of protein-coding genes is a highly coordinated process mediated, in eukaryotes, by RNA polymerase II (Pol II), which is aided in its function by other factors, termed general transcription factors (GTFs), including TFIIA, TFIIB, TFIID, TFIIE, TFIIF, and TFIIH (Table 1). For most genes, transcription is initiated once the preinitiation complex (PIC) is formed. The sequential PIC assembly process begins with the recruitment of TFIID to the core promoter, followed by the entry of TFIIA and TFIIB that help stabilize promoter-bound TFIID, and then the recruitment of Pol II/TFIIF. After formation of a stable TFIID-TFIIA-TFIIB-Pol II/TFIIF-promoter complex, TFIIE is then recruited, followed by TFIIH (Orphanides et al. 1996). In addition to this sequential assembly pathway, the PIC can also be formed by the Pol II holoenzyme pathway, whereby the Pol II holoenzyme associates with TFIID and TFIIA. The human Pol II holoenzyme complex contains Pol II, TFIIB, TFIIE, TFIIF, TFIIH, GCN5 histone acetyltransferase, SWI/SNF chromatin remodeling factor, and SRBs (suppressors of RNA polymerase B mutations) (Kim et al. 1994; Koleske and Young 1994), but is devoid of TFIID and TFIIA (Wu and Chiang 1998; Wu et al. 1999a). As soon as the nascent RNA is transcribed, it is modified by the addition of a “cap” structure at its 5’ end. The capping process protects the new transcript from attack by nucleases as well as serves as a platform for binding proteins that will export the mature mRNA. During transcription elongation, Pol II moves 5’ to 3’ along the gene sequence and extends the transcript. Both coding sequences (exons) and non-coding sequences (introns) of the gene are transcribed into pre-mRNA. Introns are then removed from pre-mRNA via splicing. Upon reaching the end of a gene, Pol II stops transcription (“termination”), the newly synthesized RNA is cleaved (“cleavage”), and a polyadenosine [poly (A)] tail is added to the 3’ end of the transcript (“polyadenylation”). The diverse steps of gene

expression are considered to be physically and functionally connected to each other (Orphanides and Reinberg 2002).

Table 1: Human general transcription factors (GTFs) (Thomas and Chiang 2006)

Factor	Protein composition	Function
TFIIA	p35 (*α*), p19 (*β*), and p12 (*γ*)	Antirepressor; stabilizes TBP-TATA complex; coactivator
TFIIB	p33	Start site selection; stabilizes TBP-TATA complex; Pol II/TFIIF recruitment
TFIID	TBP+TAFs (TAF1-TAF14)	Core promoter-binding factor Coactivator Protein kinase Ubiquitin-activating/conjugating activity Histone acetyltransferase
TFIIE	p56 (*α*) and p34 (*β*)	Recruits TFIIH Facilitates formation of an initiation-competent Pol II Involved in promoter clearance
TFIIF	RAP30 and RAP74	Binds Pol II and facilitates Pol II recruitment to the promoter Recruits TFIIE and TFIIH Functions with TFIIB and Pol II in start site selection Facilitates Pol II promoter escape Enhances the efficiency of Pol II elongation
TFIIH	P89/XPB, p80/XPD, p62, p52, p44, p40/CDK7, p38/Cyclin H, p34, p32/MAT1, and p8/TFB5	ATPase activity for transcription initiation and promoter clearance Helicase activity for promoter opening Transcription-coupled nucleotide excision repair Kinase activity for phosphorylating Pol II CTD E3 ubiquitin ligase activity

1.1.1 Promoter structure of protein-coding genes

Protein-coding genes contain DNA elements that are recognized by transcription factors and the transcription machinery. Promoters harbor core promoter elements and distal regulatory elements. Core promoter elements define the site for proper assembly and orientation of the PIC, and include the TATA box, the initiator (Inr), the downstream promoter element (DPE), the motif ten element (MTE), the downstream core element (DCE), the upstream TFIIB-recognition element (BRE^u), and the downstream TFIIB-recognition element (BRE^d) (Figure 1). The TATA box is an A/T-rich

sequence located approximately 25 to 30 nucleotides upstream of the transcription start site, and is recognized by the TATA-binding protein (TBP). The Inr contains a pyrimidine-rich sequence surrounding the transcription start site (Smale and Kadonaga 2003), and is capable of directing accurate transcription initiation. The third core element, DPE, is located about 28 to 34 nucleotides downstream of the start site and functions together with Inr as a binding site for the general transcription factor TFIID at TATA-less promoters. Alternatively, DPE can restore the core promoter activity if a TATA-dependent promoter is inactivated. The MTE and DCE are also situated, along with the DPE, downstream of the transcription start site. MTE functions in conjunction with the Inr to enhance Pol II-mediated transcription, whereas DCE binds the TAF1 component of TFIID to establish downstream promoter-regulated transcription. Furthermore, BRE^{u} (Lagrange et al. 1998; Qureshi and Jackson 1998), located immediately upstream of the TATA element, and BRE^{d}, located downstream of the TATA box (Deng and Roberts 2005), help orient the directionality of the PIC.

Distal regulatory elements are gene-specific sequences that control the rate of transcription initiation by binding the transcription factor to affect the basic apparatus, which includes the upstream activation sequence (UAS), enhancer, locus control region (LCR), upstream repression sequence (URS), silencer, insulator, and S/MAR. The UAS is recognized by activators to influence transcription from nearby start sites. Similarly, enhancers can regulate transcription, but this influence is independent of their orientation and distance from the core promoter. The LCR enhances the expression of linked genes to physiological levels in a tissue-specific manner (e.g., *cis*-independent) at the gene's integration site. LCR activation results in chromatin opening, suppression of position effects, and large distance gene activation. The URS is bound by sequence-specific repressors to inhibit transcription by interfering with activator binding, preventing recruitment of the transcription apparatus, and modifying chromatin structure. Silencers are sequence elements that can repress promoter activity in an orientation- and position-independent manner. Insulators are regulatory elements that can shelter genes from inappropriate regulatory interaction (Brasset and Vaury 2005). They are able to block interaction of enhancer to promoter and prevent the spread of repressive chromatin, like barriers. S/MARs are sequences by which chromatin loops attach to the nuclear scaffold and matrix. The S/MARs remodel the chromatin loop domains to move the gene near to the nuclear matrix so as to access the transcription machinery, thereby initiating transcription and replication (Heng et al. 2004).

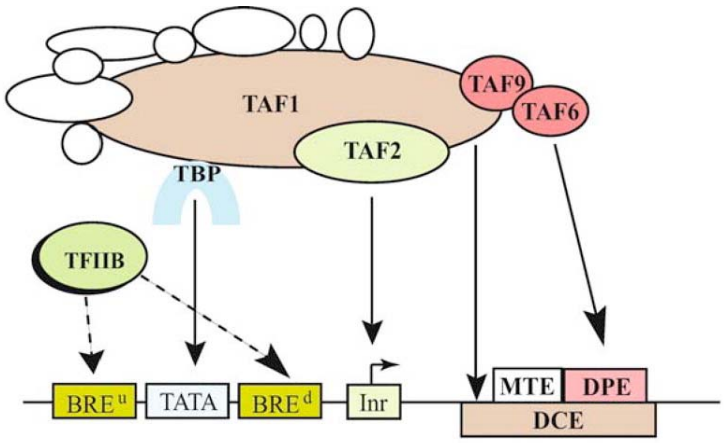

Core Promoter Element	Position	Consensus Sequence (5' to 3')	Bound Protein
BRE^u	-38 to -32	(G/C)(G/C)(G/A)CGCC	TFIIB
TATA	-31 to -24	TATA(A/T)A(A/T)(A/G)	TBP
BRE^d	-23 to -17	(G/A)T(T/G/A)(T/G)(G/T)(T/G)(T/G)	TFIIB
Inr	-2 to +5	PyPyAN(T/A)PyPy	TAF1/TAF2
MTE	+18 to +29	C(G/C)A(A/G)C(G/C)(G/C)AACG(G/C)	n.a.
DPE	+28 to +34	(A/G)G(A/T)CGTG	TAF6/TAF9
DCE	3 subelements +6 to +11 +16 to +21 +30 to +34	core sequence: S_I CTTC S_{II} CTGT S_{III} AGC	TAF1

Figure 1: Core promoter elements and their recognition by TFIID (TBP and TAFs) and TFIIB (Thomas and Chiang 2006).

1.1.2 Eukaryotic RNA polymerases

Three eukaryotic RNA polymerases (Pol I, II, and III, respectively) were first identified by Roeder and Rutter (Roeder and Rutter 1969), based on the chromatographic fractionation of sea urchin embryo nuclei on a DEAE-Sephadex column. Pol I came off the column first at the lowest salt concentration, whereas Pol III eluted at the highest salt concentration. Moreover, these polymerases are also responsible for the transcription of different classes of RNA, and they can be distinguished biochemically according to their sensitivity to α-amanitin (Table 2). In rapidly growing cells, Pol I and III can contribute up to 80% of all nuclear transcription.

Pol II comprises 12 subunits (Rpb1-12) that are highly conserved among eukaryotes, while Pol I and III possess 14 and 17 subunits, respectively. Five subunits, Rpb5, 6, 8, 10, and 12, are common to all three RNA polymerases, whereas the Rpb1, 2, 3, and 11 subunits of Pol II are homologous to subunits of Pol I and Pol III (Cramer et al. 2000; Asturias 2004; Cramer 2004). A unique feature of the largest Pol II subunit is the

presence of tandem repeats of a heptapeptide sequence at its carboxy-terminus, known as the carboxy-terminal domain (CTD). The CTD has the consensus sequence Tyr-Ser-Pro-Thr-Ser-Pro-Ser that is highly conserved among eukaryotic organisms. Moreover, it contains binding sites for proteins that regulate processes such as transcriptional initiation, elongation, termination, and mRNA processing (Palancade and Bensaude 2003). Phosphorylation of the CTD regulates the activity of Pol II. During initiation, Pol II carries an unphosphorylated CTD, while elongating polymerase molecules contain phosphorylated CTDs. The switch in CTD phosphorylation between initiation and elongation seems to cause Pol II to switch cofactors (Meinhart et al. 2005). Several kinases have the potential to phosphorylate the CTD of Pol II *in vitro*. Most CTD kinases belong to the class of cell-cycle-dependent kinases (CDKs) and require a cyclin as cofactor for full activation; they include the cyclin-dependent kinase 7 (CDK7) associated with TFIIH (Feaver et al. 1991); CDK8 found in the general cofactor, Mediator; and CDK9 present in the positive transcription elongation factor b (P-TEFb). There are five potential phosphorylation sites in the CTD consensus sequence. It has also been established that Pol II can be phosphorylated at Ser2, -5 and -7 of the heptarepeat. Ser5 phosphorylation occurs in promoter-proximal regions, and leads to recruitment of the capping enzyme. Ser2 phosphorylation predominates in regions that are more distal from the promoter, and triggers binding of the 3'-RNA processing machinery. Phosphorylation of Ser7 facilitates snRNA gene expression (Egloff et al. 2007), but the restriction of Ser7 epitopes to the Linker-proximal region limits CTD phosphorylation patterns and is a requirement for optimal gene expression (Chapman et al. 2007).

Table 2: Eukaryotic RNA polymerases

Type	Genes	Transcripts	Localization	Response to α-amanitin
Pol I	class I	18S-, 5.8S- 28S-rRNA	nucleoli	none
Pol II	class II	pre-mRNA, snRNA	nucleoplasm	strong, $K_D=10^{-8}$ M
Pol III	class III	tRNA, 5S-rRNA, snRNA	nucleoplasm	weak, $K_D=10^{-6}$ M

Pol I, Pol II, and Pol III: the three DNA-dependent RNA polymerases; rRNA: ribosomal RNA; mRNA: messenger RNA; snRNA: small nuclear RNA, tRNA: transfer RNA.

1.1.3 Transcription coactivators

The transcription coactivators are distinct from the GTFs in that they are dispensable for basal-level transcription and distinct from activators in that most do not directly bind DNA and none appears to bind DNA in a sequence-dependent manner. They are required for transcription activation and some act as a bridge to accumulate the gene-specific activators to their target sequence [TFIIA, TAFs found in TFIID, USA factors, and SRB/Mediator (Myers and Kornberg 2000; Kornberg and Lorch 2002; Bjorklund and Gustafsson 2004; Blazek et al. 2005)], while some interact with nucleosomes, promoting chromatin modification (histone acetyltransferases), or chromatin remodeling (SWI/SNF remodeling complex).

USA factors include both positive and negative effectors of transcription, and interact with the PIC to repress transcription in the absence of activators or to stimulate transcription in the presence of activators (Meisterernst et al. 1991). At least six positive cofactors were discovered in the human USA fraction: PC1 [later identified as the poly(ADPribose) polymerase, PARP] (Meisterernst et al. 1997); PC2 (the smaller form of human Mediator complexes) (Malik et al. 2000); PC3/Dr2, which is the topoisomerase I and functions in both repression of basal transcription and stimulation of activated transcription (Kretzschmar et al. 1993; Merino et al. 1993); PC4; PC5, which coactivates the transcription regulated by upstream stimulatory factor 1 (USF1) in a reconstituted, class II gene transcription system (Halle et al. 1995); and PC6 (Mittler et al. 2003). Among all the positive cofactors, PC4 was the first to be cloned, and it will be discussed below in detail. The negative cofactors include NC1/HMG1 and NC2. NC1 represses basal transcription via binding to the TBP-DNA complex, and is competed by binding of TFIIA to the same complex (Meisterernst and Roeder 1991). NC2 is a heterodimer consisting of two subunits, NC2α and NC2β, also called DRAP1 and DR1, respectively, (Goppelt and Meisterernst 1996; Goppelt et al. 1996; Mermelstein et al. 1996) and inhibits transcription initiation by Pol II (Meisterernst and Roeder 1991; Inostroza et al. 1992; Albert et al. 2007; Schluesche et al. 2007).

1.2 Transcription cofactor PC4

PC4 was originally purified from the USA fraction as a positive general transcription cofactor that could increase GAL4-AH dependent transcription in conjunction with other general transcription factors (Kretzschmar et al. 1994). PC4 is composed of 127 residues, with a so-called SEAC domain (serine/acidic residue-rich, spanning amino acids 7 to 22, aa 7-22) followed by a lysine-rich motif (aa 23-41) in the N-terminal

region and a DNA-binding region at the C-terminal domain (PC4-CTD, aa 63-127). A comparison of human, mouse, and rat homologues indicate that full-length PC4 is highly conserved (Figure 2). The yeast homolog SUB1 and PC4 are conserved in the PC4-CTD (Henry et al. 1996). PC4 not only facilitates Pol II-regulated transcription by interacting with the acidic activation domain of different activators and GTFs, but also plays a role in mRNA processing, viral DNA replication, DNA repair, and tumor repression (Kannan and Tainsky 1999). Apart from its role in Pol II transcription, SUB1 was implicated in Pol III transcription by its interactions with components of the Pol III transcription system, and presence on Pol III-transcribed genes.

1.2.1 Purification and cloning of PC4 (p15) and SUB1

In 1994, the laboratories of Meisterernst and Roeder simultaneously purified a new transcription factor from the P11 0.85 M KCl (USA) fraction of HeLa cell nuclear extracts, called PC4 or p15, which is able to enhance activator-dependent transcription (Ge and Roeder 1994; Kretzschmar et al. 1994). PC4 (p15) turned out to be a novel cofactor with a smaller native size of 50-100 kDa on sizing columns. In contrast to TAFs, PC4 does not tightly associate with TFIID, and can be separated from it at moderate ionic strength. Subsequent to the purification of PC4,
SUB1, the yeast homolog, was isolated as a suppressor of the cold sensitive TFIIB mutant and as a transcription stimulator by two different groups in 1996 (Henry et al. 1996; Knaus et al. 1996). Its N-terminal third shows strong similarity to a 73-residue region encompassing the majority of the 127-amino acid mammalian co-activator PC4 (48% identity, 70% similarity) (Figure 2).

1.2.2 PC4 stimulates activator-dependent transcription and functions as a general repressor

1.2.2.1 PC4 stimulates and represses basal transcription

In the absence of a transcriptional activator, high concentrations of PC4 were demonstrated to inhibit basal transcription in a system reconstituted with only TBP, TFIIB, TFIIF and Pol II (Malik et al. 1998), while low concentrations stimulated transcription. When TFIID (TBP + TAF_{II}s) was substituted for TBP, or when the amounts of TFIID, TAF_{II}s, TFIIH, and a preassembled Pol II holoenzyme were increased, PC4 repression was alleviated (Malik et al. 1998; Wu and Chiang 1998; Wu et al. 1998). Kornberg and colleagues suggested that the yeast PC4 (SUB1/TSP1)

exerts positive effects on basal transcription in the presence of Mediator and TFIIH (Henry et al. 1996). In *Schizosaccharomyces pombe*, PC4 was shown to stimulate

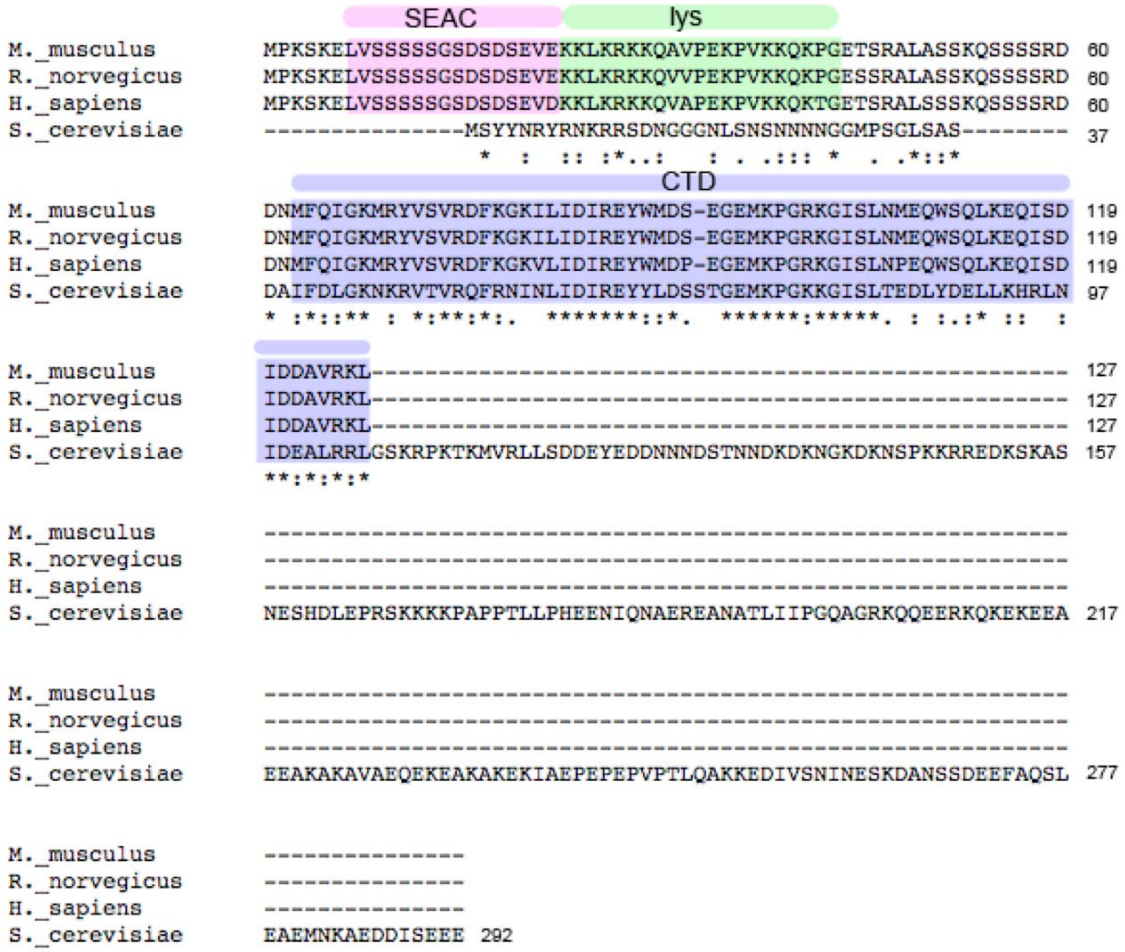

Figure 2: PC4-CTD is highly conserved from yeast to human.
Homologs of PC4 are aligned using ClustalW. Organism names are indicated at left, and amino acid residues are indicated at right. Identical (*) and similar (.) residues are identified below.

basal transcription from both TATA-containing and TATA-less promoters. The stimulation of basal transcription with TATA-containing templates is dependent on Mediator and TFIIA, but not TAFs (Contreras-Levicoy et al. 2008). Because human PC4 was observed to interact with multiple components of PIC, including TFIIA, TFIID,TFIIH, and Pol II (Ge and Roeder 1994; Kretzschmar et al. 1994; Kaiser et al. 1995; Malik et al. 1998; Fukuda et al. 2004), the *Sc. pombe* PC4 was also tested for its interaction with GTFs and found to interact with TFIIA, TFIIB, TBP, TFIIH, and the Pol II holoenzyme (Contreras-Levicoy et al. 2008). The highly conserved interaction of PC4 and components of the transcription machinery play a critical role in regulating promoter activity.

1.2.2.2 PC4 functions as a coactivator

1.2.2.2.1 PC4 stimulates activator-dependent transcription

To elucidate the relationship between the various PC4 domains and their coactivator activities, many PC4-deletion mutants, including both N-terminal (p15[1-87], p15[22-127]), and C-terminal (p15[88-127], p15[62-127]) mutants (Kretzschmar et al. 1994). These studies demonstrated that the amino-terminal portion is critical for PC4 cofactor activity and double-stranded DNA (dsDNA) binding, the C-terminal domain is important for single-stranded DNA (ssDNA) binding, and amino acids 61-87 are critical for interaction with both dsDNA and ssDNA (Kretzschmar et al. 1994). The relevance of dsDNA binding activity for cofactor activity was tested in a promoter-competent assay, which showed that PC4 binds to the promoter, thereby stabilizing the TFIID-TFIIA (DA) complex during PIC formation (Kaiser et al. 1995). Consequently, the activator and PC4 initiate stimulation of transcription during DA complex formation. Moreover, Roeder et al. (Malik et al. 1998) provided another dynamic model for PC4 coactivator function. In this model, activator-mediated recruitment of TFIIH to a TAF-containing PIC is stabilized by PC4 via its interaction with components of the transcription machinery. However, the resulting complex cannot initiate transcription unless a mechanism such as phosphorylation of PC4 by $TAF_{II}250$ or TFIIH dislodges PC4 and/or an ATP-hydrolysis-dependent TFIIH helicase activity frees the Pol II.

1.2.2.2.2 Activators require PC4 to activate transcription

In addition to its role as a coactivator with GAL-VP16 (Ge and Roeder 1994; Kretzschmar et al. 1994), PC4 was also shown to stimulate transcription *in vitro* with diverse other activators, including NF-κB, Sp1 (Guermah et al. 1998), thyroid hormone receptor (Fondell et al. 1999), octamer transcription factor A-B (Luo et al. 1998), and BRCA-1 (Haile and Parvin 1999), presumably by facilitating assembly of the preinitiation complex through bridging between activators and the general transcriptional machinery (Ge and Roeder 1994; Kaiser et al. 1995).

Alternatively, it was demonstrated that human PC4 stimulates activated transcription by GAL4-VP16 at the level of preinitiation complex assembly, promoter opening, promoter escape, elongation, and reinitiation (Fukuda et al. 2004). Further studies also demonstrated the importance of PC4 for transcriptional activation by AP-2 (Kannan and Tainsky 1999), hepatocyte nuclear factor IV-α (HNF-4α) (Guo et al. 2007), and the HIV transcriptional transactivator (Tat) (Holloway et al. 2000) *in vivo*. Among these

factors, PC4 was found to physically interact with Tat and AP-2 via its C-terminal domain (Zhong et al. 2003). All the activators regulated by PC4 were summarized in table 3.

Table 3: Coactivators that cooperate with PC4

Activators	Physical interaction with the following domains of PC4	Functional consequences	References
Ap-2α	CTD domain	PC4 is critical for AP-2α transcriptional interference by which *ras* transform cells, and PC4-expression *ras* cells were highly growth suppressed.	(Kannan and Tainsky 1999; Zhong et al. 2003)
BRCA1	N/A	PC4 facilitates transcriptional activation by GAL4-BRCA1.	(Haile and Parvin 1999)
GAL4-AH	N/A	PC4 enhances transcription activated by GAL4-AH.	(Kretzschmar et al. 1994)
GAL-VP16	Coactivator domain (aa 22-91)	PC4 facilitates the assembly of the preinitiation complex (PIC) and stimulates promoter escape in response to GAL-VP16.	(Ge and Roeder 1994; Kretzschmar et al. 1994; Fukuda et al. 2004)
HNF4α	CTD domain	The presence of the inflammatory-redox state enhances PC4-HNF4α binding to upregulate transcription of target hepatocyte genes, such as iNOS.	(Guo et al. 2007)
OCA-B	Full length	PC4 as an essential component of USA acts synergistically with PC2, to support the function of Oct1/ OCA-B in a reconstituted transcription system.	(Luo et al. 1998)
Rel/NF-κB and Sp1	N/A	PC4 together with PC2 could synergistically facilitate activation by both activators.	(Guermah et al. 1998)
Tat	Lysine-rich motif	PC4 is involved in linking Tat to the basal transcription machinery and enhances Tat-mediated activation.	(Holloway et al. 2000)
Thyroid hormone receptor	N/A	PC4 and PC2 synergistically mediate thyroid receptor-dependent transcription activation *in vitro* system.	(Fondell et al. 1999)
VP16	Full length	PC4 markedly enhances activation by acidic activation domain of VP16.	(Ge and Roeder 1994)

1.2.2.3 Structure analysis of PC4

X-ray crystallography identified a novel dimeric fold located within the PC4-CTD (Figure 3), spanning aa 63-127 (Brandsen et al. 1997) that provides a novel binding motif for two antiparallel ssDNA strands and heteroduplex nucleotides. The affinity for ssDNA that can fold into two antiparallel strands is indeed very high, exceeding that for dsDNA at least 100 times (Werten et al. 1998a). The β-sheets and loops that form the two quarterpipe structures are flexible in the absence of ssDNA, which is significantly reduced upon ssDNA binding (Werten et al. 1999). The evolutionary conservation suggests a critical role of the ssDNA fold in the cellular function of PC4. The ssDNA fold is composed of a ß-ridge region, two flanking antiparallel channels formed by the ß2 and ß3 strands, and a ß2-ß3 loop (Figure 3). It was expected that both Trp89

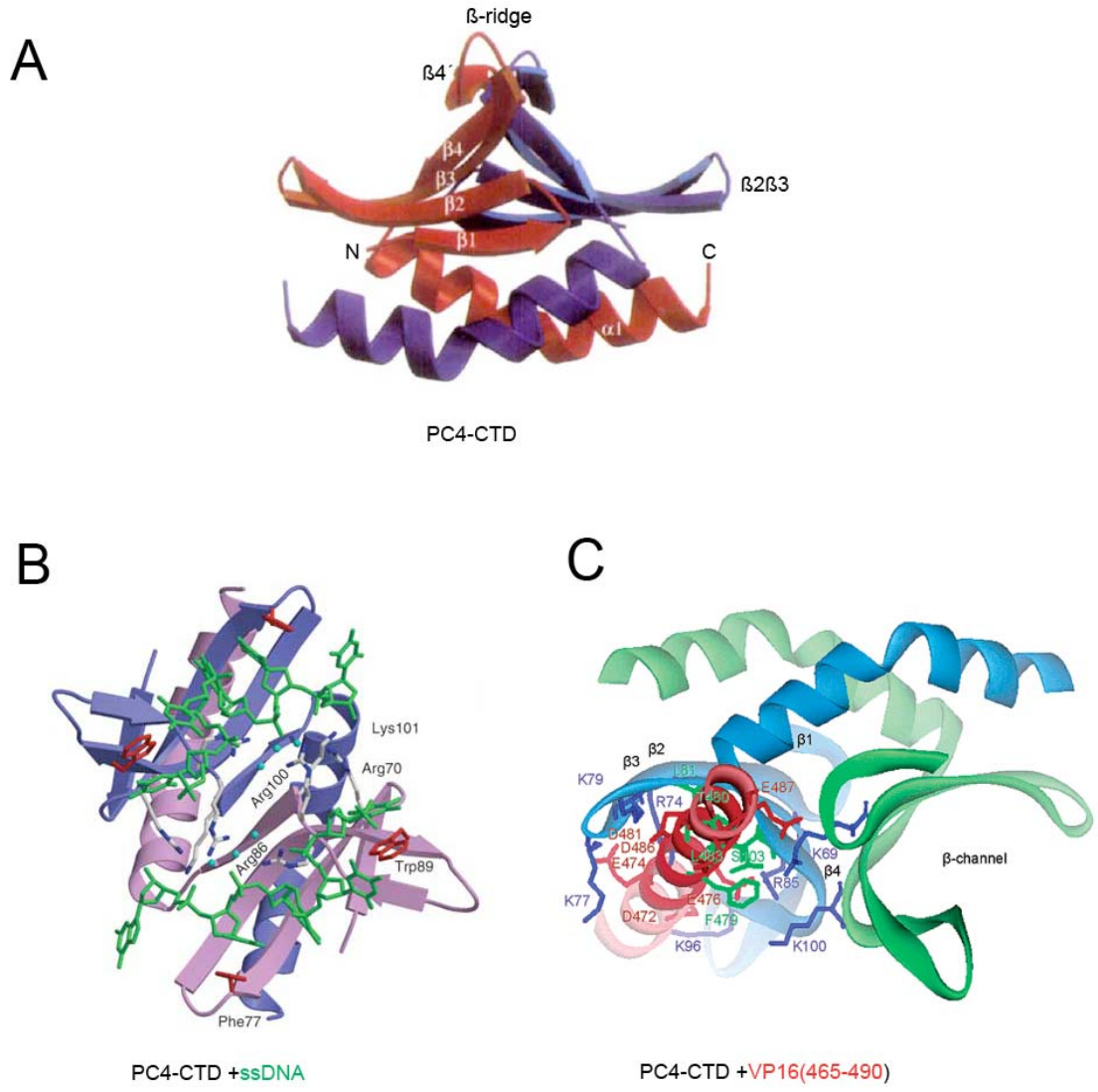

Figure 3: Structure of PC4-CTD dimer.
(A) Fold of the PC4-CTD dimer. Monomers of the PC4-CTD dimer were shown blue and pink. Indicated are the ß-ridge formed by residues 87-101(Brandsen et al. 1997). (B) Interaction

model of PC4-CTD with ssDNA (Werten and Moras 2006). (C) Interaction model of PC4-CTD with VP16 (an activator) (Jonker et al. 2005).

(located in the β-ridge) and the β2-β3 loop (connecting β-strands 2 and 3) would be particularly important for the interaction with ssDNA (Figure 3). A PC4 mutant, in which Trp89 was replaced by Ala (W89A), and a triple mutant, in which the Phe residue and both of the Lys residues of the β2-β3-loop were replaced by Ala and Gly, respectively (F77A/K78G/K80G, β2-β3), were constructed to study PC4 coactivator and repressor activity (Werten et al. 1998b). These mutants lost the ability to repress transcription. Combining these results with those of the N-terminal mutants depleted of PC4 cofactor function, leads to the conclusion that PC4 interaction with unpaired DNA during opening of the promoter is not required for its co-activator function *in vitro.* Its interaction with dsDNA may also provide a second mode of repression. Furthermore, PC4 at very low concentrations can antagonize binding of heteroduplex by Pol II.

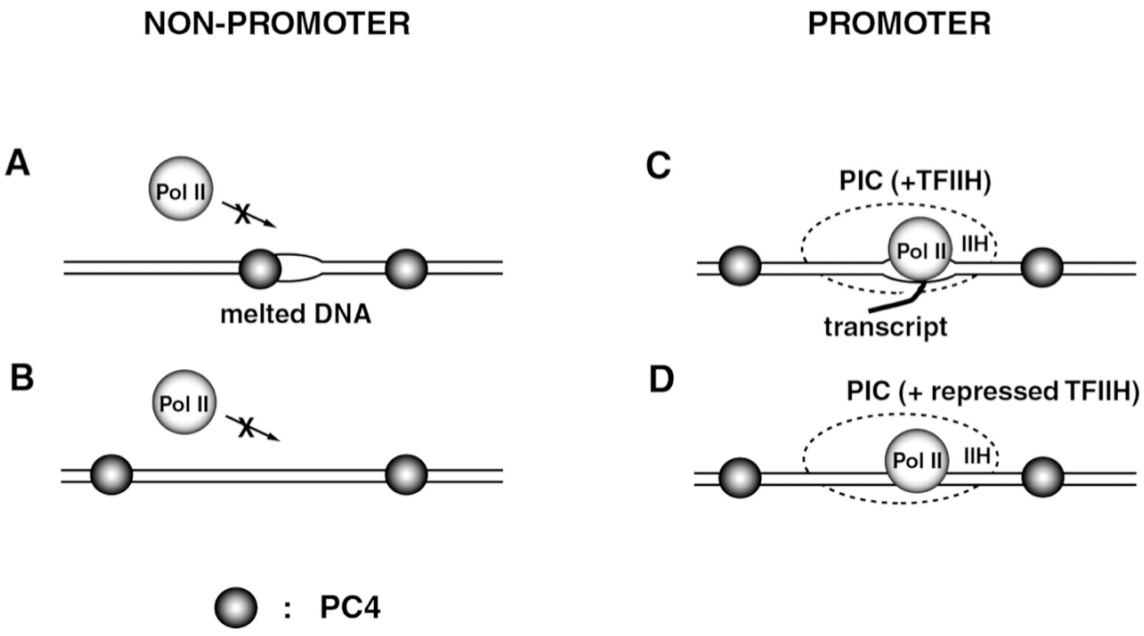

Figure 4: Model for the roles of PC4 in the regulation of transcription from non-promoter and promoter regions.
(A) PC4 binds to dsDNA and ssDNA regions and prevents the binding of Pol II to ssDNA regions by direct competition. PC4 bound to dsDNA regions may also serve as a reservoir for PC4 recruited to ssDNA regions. (B) PC4 binds dsDNA regions and prevents the binding of Pol II to DNA by restricting the formation of transient ssDNA regions. (C) The PIC (dotted line) containing TFIIH can initiate transcription from the promoter DNA that is bound by PC4. (D) The PIC, whose TFIIH activity is repressed, fails to initiate transcription from the promoter DNA that is bound by PC4 (Fukuda et al. 2003).

This novel role of PC4 reveals a mechanism for repressing non-promoter regions and unpaired DNA generated by DNA damage. TFIIH-binding and PC4-CTD

phosphorylation might attenuate this inhibitory activity (Werten et al. 1998b). The mechanism for alleviating PC4-mediated transcription repression was investigated in more detail with purified recombinant protein (Fukuda et al. 2003). A transcription assay showed that PC4-repression was restored by adding TFIIH and ATP, which is required for ß-γ bond hydrolysis. The ERCC3 helicase activity, but not CDK7 kinase, counteracted PC4-regulated repression. In light of these studies, PC4 represses promoter-independent transcription in both 'direct' and 'indirect' ways (Figure 4).

1.2.2.4 Phosphorylation of PC4 negatively regulates its coactivation function and DNA binding activities

In the N-terminus region of PC4 there are two SEAC motifs (one major motif aa 7 to 21 and one minor motif aa 50 to 63) flanking a lysine-rich region (aa 23-41). Phosphorylation of the SEAC domain inhibits the PC4-coactivation function (Ge et al. 1994; Kretzschmar et al. 1994). Protein interaction studies (Ge et al. 1994) and *in vitro* transcription assays (Kretzschmar et al. 1994) demonstrated that only the nonphosphorylated form of PC4 stimulates TAF-dependent activator functions. Casein kinase II (CKII) and protein kinases phosphorylate PC4 *in vitro*, but *in vivo,* hyperphosphoration of PC4 is meditated mainly by CKII (Ge et al. 1994). Phosphorylated PC4 was also detected in PIC, and both TFIIH and $TAF_{II}250$, the largest subunit of TFIID, can phosphorylate PC4 (Malik et al. 1998). PC4 also competitively inhibits the TFIIH-Cdk7 enzyme subcomplex-mediated phosphorylation of the Pol II CTD, but does not inhibit phosphorylation of other substrates of the same kinases. Phosphorylated PC4 is devoid of kinase inhibitory activity, and mutations in its lysine-rich domain abolish its inhibitory ability (Schang et al. 2000).

As there are many serines in the N-terminal region to act as potential phosphorylation sites, gradual phosphorylation occurs and phosphorylation status differentially influences the various biochemical functions (Jonker et al. 2006). For example, ssDNA binding activity is slightly enhanced by phosphorylation of one serine residue without augmentation by further phosphorylation, whereas, dsDNA binding decreases with gradual phosphorylation, and the presence of at least two phosphoserines decreases DNA-unwinding activity and abrogates binding to the activator. Compared with negative regulation of PC4 activity by phosphorylation, acetylation positively stimulates PC4 DNA binding activity. It is reported that p300 can acetylate PC4 specifically, and that phosphorylation of PC4 by CKII inhibits the p300-mediated acetylation (Kumar et al. 2001).

1.2.3 PC4 and DPE, promoter escape

A study of downstream promoter element (DPE)-dependent transcription demonstrated that PC4 and CKII were required to establish DPE-specific transcription (Lewis et al. 2005). However, in the same study, depletion of PC4 with an anti-PC4 antibody in nuclear extracts increased spurious initiation rather than specific promoter-dependent transcription. And a chromatin immunoprecipitation (ChIP) assay showed that PC4 and CKII were present in *IRF-1* and *TAF7* promoters. CKII was shown by the same group to eliminate DCE-dependent transcription and to phosphorylate the HMG box of TAF1, thereby converting TFIID from DCE-specific recognition to a DPE-specific recognition function. However, as PC4 is also a popular target of CKII *in vivo*, does phosphorylated PC4 repress DPE-specific transcription?

1.2.4 PC4 has a role in viral replication

The trimeric, ssDNA-binding protein HSSB plays important roles in the replication of simian virus 40 (SV40) DNA (Matsumoto et al. 1990; Murakami et al. 1992). Because PC4 harbors ssDNA-binding activity, it can form a PC4-HSSB-ssDNA complex and replace HSSB for unwinding of the SV40 origin by T-antigen. PC4 has been shown to inhibit RNA primer synthesis and DNA elongation carried out by pol δ. By contrast, PC4 inhibits SV40 DNA replication in the presence of low concentrations of HSSB, but activates it under high HSSB concentrations (Pan et al. 1996). Another report also showed that PC4 functionally interacts with Rep in 293-31 cells to regulate adeno-associated virus replication (Weger et al. 1999).

1.2.5 PC4 participates in DNA repair process

A study from Michael Volkert's lab demonstrated that PC4 was also a suppressor of oxidative mutagenesis in *E. coli* and yeast, and that it could revert an oxidative mutate phenotype in a DNA repair-deficient *E. coli* strain, possibly by physically interacting with Rad2, the homolog of human endonuclease XPG that functions in multiple DNA repair pathways in mammals (Wang et al. 2004). This report implies that apart from the many different roles of PC4 described so far, PC4 may take part in the DNA repair process. Work on human and mouse cells in our laboratory showed that endogenous PC4 accumulates at DNA damage sites introduced by either chemical agents or laser microirradiation (Mortusewicz et al. 2008). In addition, rapid recruitment of PC4 to laser-induced DNA damage sites was independent of poly (ADP-ribosylation) and γH2AX, but dependent on its single strand binding capacity. Therefore, PC4 might play

a role in the early response to DNA damage by recognizing ssDNA to facilitate or repress subsequent DNA repair steps. This repair role of PC4 was also confirmed by data showing that PC4 can activate nonhomologous end joining and double-strand break repair (Batta et al. 2009).

1.2.6 PC4 and p53

The highly abundant, non-histone, chromatin protein, HMGB-1, is reported to be a unique activator of p53-mediated DNA binding and transcription activation (Jayaraman et al. 1998). Likewise, it was shown that PC4, which displays significant functional homology to HMGB-1, enhanced the DNA binding of p53 to its cognate sites by direct interaction with p53 *in vitro* and *in vivo* (Banerjee et al. 2004). Furthermore, the same study showed that p53-dependent apoptosis was enhanced by PC4; thereby, establishing the first physiological role of PC4. On the other hand, they also reported that p53 regulated PC4 expression by directly binding to the PC4 promoter region. Further evidence of the relationship between p53 and PC4 was provided by showing that PC4 was over expressed in a p53-dependent way upon genotoxic insult (Kishore et al. 2007). The interaction of different PC4 truncation mutants with p53 implied that aa 62 to 87 of the PC4 DNA-binding domain were essential for p53 interaction and activation. Furthermore, this protein-protein interaction, together with PC4 DNA bending activity, is responsible for p53 activation. Phosphorylation of PC4 abolishes its ability to activate p53 binding to its cognate sites, whereas acetylation of PC4 facilitates this function (Batta and Kundu 2007). Recently, it was shown by NMR spectroscopy that the p53 TAD domain interacts with the PC4 C-terminal DNA-binding domain, confirming that PC4 directly interacts with p53 (Rajagopalan et al. 2009). Taken together, these data suggest that p53 is a potential target gene of PC4; of note, however, these data were not confirmed independently, and they were not proven in mammalian model.

1.2.7 Yeast SUB1

1.2.7.1 Transcription functions of SUB1

The yeast homologue of PC4, SUB1/TSP1, is not essential for cell growth on medium containing galactose or lactate when it's coding sequence is entirely deleted, however, it is essential for viability in the presence of TFIIB mutations (Knaus et al. 1996). SUB1 also functions as a coactivator for the GCN4 and HAP proteins *in vivo* and specifically inhibits the formation of TBP-TFIIB-promoter complexes *in vitro* (Knaus et al. 1996).

Phosphorylated form of SUB1/TSP1 does not bind to TFIIB and interacts less tightly with GAL4-VP16, and dephosphorylated recombinant SUB1/TSP1 binds strongly to single-strand DNA (Henry et al. 1996). Additionally, SUB1 was found to interact physically and genetically with the polyadenylation factor CstF64/Rna15p (in yeast) (Calvo and Manley 2001). Deletion and over-expression of SUB1 in yeast suppressed or enhanced, respectively, growth and termination defects in an Rna15 mutant strain, suggesting that transcription is linked to RNA polyadenylation and termination, and that PC4 has anti-termination activity. In yeast, in the presence of SSU72, another component of the cleavage/polyadenylation factor (CPF), SUB1 did not bind to the Pta1 of CPF, indicating that SUB1 plays a role in the 3'-end processing of RNA (Wu et al. 1999b; He et al. 2003). Furthermore, SUB1 and Rna15 are recruited to promoters and remain chromatin-associated during transcription elongation. Additionally, SUB1 function is connected to Pol II CTD phosphorylation. By accumulating FCP1 (phosphatase in yeast) to the CTD, PC4 dephosphorylates Pol II and facilitates elongation (Calvo and Manley 2005).

1.2.7.2 SUB1 functions in Pol III transcription

Apart from its role in Pol II transcription regulation, PC4 is also involved in Pol III transcription both *in vitro* and *in vivo*. In 1998, PC4 was found in the holo TFIIIC complex and to enhance interaction of TFIIIC with downstream promoters and termination sequences. Additionally, PC4 promoted multiple-round transcriptions by Pol III from preformed preinitiation complexes (Wang and Roeder 1998). Eleven years later, Manley's group not only confirmed the function of PC4 (SUB1) in Pol III-dependent transcription, but also showed the underlying mechanism (Rosonina et al. 2009). They found that SUB1 rapidly associated with osmoresponse gene promoters upon osmotic shock. SUB1 was present at Pol III-transcribed genes, such as *SNR52* (snoRNA), *SNR6* (U6 snRNA), *SUP56* (tRNA), and *5S* (rDNA) and at constitutively expressed Pol II-transcribed genes, such as *RPP2B* (ribosomal protein gene) and *HHT1* (histone H3 gene), but was not detected at inactive genes. *SUB1* deletion suppressed Pol II and Pol III recruitment to their transcribed genes without affecting TBP occupancy. During conditions of stress, such as exposure to NaCl, SUB1 was predominately recruited to stress response genes by temporarily evacuating constitutively transcribed Pol II and III genes due to reduced availability of the polymerases (Rosonina et al. 2009). Almost at the same time, Acker's group confirmed the presence of SUB1 on all Pol III-transcribed genes by genome-wide mapping (Tavenet et al. 2009). They also reported that in a reconstituted Pol III

transcription system, SUB1 stimulated Pol III transcription initiation by enhancing the assembly of TFIIIC-TFIIIB-DNA through protein-protein interactions with basal factors - Bdp1 (a component of TFIIIB) as well as with τ138 and τ95 (2 subunits of TFIIIC). Because Pol III transcription reinitiation accounts for a large number of noncoding RNAs, they tested the activity of SUB1 in transcription reinitiation. The data indicated that SUB1 played a critical role in stimulating transcription reinitiation. Although deletion of *SUB1* in yeast did not affect the growth rates of exponentially growing cells or of steady state levels of Pol III, Pol III transcription was decreased and TFIIIB occupancy was reduced in Pol III-transcribed genes (Tavenet et al. 2009). Together, these two reports present a consistent issue: SUB1 directly regulate Pol III transcription. However, these two studies also present a contradictory issue: does SUB1 deletion affect TFIIIB occupancy at Pol III-transcribed genes? Therefore, further investigations are necessary to determine by which molecular mechanisms Pol III transcription is regulated by SUB1 under different conditions and whether PC4 is important for Pol III transcription in mammalian cells.

1.3 Mouse embryonic stem cells: vehicles for creating mutant mice

Two laboratories first succeeded in isolating the cell lines from the cultured early mouse embryos, that proved pluripotent (Evans and Kaufman 1981; Martin 1981). These cells, derived from the inner cell mass (ICM) of blastocysts, named embryonic stem (ES) cells, are able to generate all tissues including the germ line after microinjection into blastocysts, initially giving birth to chimeras. ES cells can be genetically modified *in vitro* via transfection with target vector carrying a mutation. As a consequence, mutant mouse models could be constructed. It is helpful if the genetic background of ES cells is different from the host blastocysts. Male ES cells are preferred because of the efficient incorporation of XY cells into XX host embryos. This causes phenotypic sex conversion to yield male animals. Generally, ES cells can be derived from 129/sv, C57BL/6J, Balb/c and so on. However, the ES cells from 129/sv strain proved to be efficient in germ line transmission, and hence are often used to produce knockout mice. 129/sv ES cells encode brown coat color because they are A/A (A is the gene affecting hair color. An agouti mouse is described as ‘‘brownish-gray’’ with alleles A/A. Non-agouti mice contain the alleles a/a.). The C57BL/6J host embryos give rise to completely plain black coat color because they are non-agouti (a/a). Hence, if the chimeras are male and mostly brown, the chances are good that the ES cells also generated germ line cells. To test the percentage of germ line

transmission, chimeras are bread to non-agouti mice (C57BL/6J), and agouti offspring (A/a) must arise from ES cell-derived gametes.

ES cell-growth requires a monolayer of inactivated MEFs. These provide critical factors that promote self-renewal and suppress differentiation. In addition, Leukemia Inhibitory Factor (LIF) is needed to maintain mouse ES cells in a pluripotent state. LIF is a soluble glycoprotein of the interleukin (IL)-6 families of cytokines. It acts via a membrane bound gp130 signaling complex to regulate a variety of cell functions through signal transduction and activation of transcription (STAT) signaling.

ES cells are different from embryonic carcinoma (EC) cells, which originate from malignant teratocarcinomas. EC cells have extensive differentiation potential leading to formation of three germ layers. But they showed chromosomal aberrations and could not form viable mice. Moreover, mouse embryonic germ (EG) cell lines, which are originated from primordial germ cells, unlike ES cells, retain the capacity to erase gene imprinting. Some experiments suggest that ES cells closely resemble cells from the primitive ectoderm, which are known as epiblast or embryonic ectoderm (Brook and Gardner 1997).

1.3.1 Targeting constructs for the generation of knockout mice

Targeting constructs carry homologous isogenic DNA (ideally between 5-8kb split between upstream and downstream arms), a positive selectable marker whose expression is driven by a promoter active in ES cells and a negative selectable marker to screen for recombination and against random integration events of the vector.

1.3.1.1 Positive selection for vector incorporation

Neomycin phosphotransferase (*neo*) gene expression cassette, which mediates resistance to G418, is often used to select ES cell clones carrying the targeting vector. Alternatively, are the puromycin resistance gene (*puro*), the hygromycin resistance gene (*hygro*) and the hypoxanthine phosphor-ribosyltransferase (*hrpt*). Problems could arise from the fact that the selectable marker gene with its associated promoter may influence the expression of neighboring genes, especially in multigene cluster (Pham et al. 1996). Secondly, presence of the resistant gene could affect the level of the gene targeted resulting a hypomorphic phenotype (Zhou et al. 2008). Hypomorphic alleles in the extreme situation may be lethal for the mutant mice. On the other hand such a scenario may be used for the biological analysis. To avoid the negative effect, the selectable marker can be removed by using the Cre/LoxP or FLP/FRT technology.

1.3.1.2 Negative selection against random integration events

Random integration of the targeting vector usually occurs during positive selection. To select for the homologous recombination event, a negative selection is applied to remove ES cell clones that have randomly incorporated the targeting vector. The method of choice is expression of the herpes simplex virus (HSV) thymidine kinase (tk) gene. HSV-tk is usually positioned on the vector outside of the homology region. ES cells are then cultured with Ganciclovir. Cells expressing the tk gene become sensitive to drug treatment and will be eliminated. An alternative negative selection gene, diphtheria toxin A-chain (DT-A) which kills cells in the absence of drug addition can also be used.

1.3.1.3 Reporters

LacZ (ß-galactosidase gene from *E.coli*) and GFP (Green Fluorescent Protein gene) are used as reporters for gene expression and exon disruption. LacZ has been ideally used in gene trap construct as a tool to identify and disrupt active genes, for example via IRES (internal ribosome entry site) to be connected with a splice acceptor.

1.3.1.4 Site specific recombinases

Site-specific recombinases catalyze the recombination between two consensus DNA sequences. If these sites are designed in the target locus and the recombinases are expressed in the same cell, site-specific recombination may be induced resulting in gain function or loss of function. These strategies are standard tools for targeted mutations in cells and mice. For example, Cre recombinase of the bacteriophage P1 and FLP recombinase from yeast (*Saccharomyces cerevisia*) are popular instruments in recombinant mouse technology. Both belong to the λ integrase superfamily and share an overall structure of recognition sites in which an eight base pair (bp) asymmetric core sequence is flanked by two inverted or repeated 13bp palindromic sequences. The 34bp consensus recombination sites of Cre and FLP are called loxP and FRT respectively, and have a defined polarity. Consequently, the relative orientation of target sites with respect to one another determines the outcome of recombination: Cre and FLP recombinases excise the sequence between two directly repeated recombination sites. Two sites in opposing direction cause DNA inversion on chromosomes. Recombinase can also exchange chromosome area. Many variant targets sites for Cre and FLP were created, which include spacer variants and inverted-repeat variants. The mutation targeting sites for Cre and FLP could increase

the efficiency of recombination, and protect gene expression from excising by heterotypic target sites instead of homotypic. This strategy is the basis for RMCE (recombinase-mediated cassette exchange) and FLEx switch (invert the orientation of genes) (Bode et al. 2000; Schnutgen et al. 2003). Expression of recombinases may be regulated at the translation and transcription level. Furthermore, recombinase estrogen receptor fusion proteins have been created rendering the enzyme accessible to rapid induction by hormones. Relatedly, conditional expression of Cre under the Mx1 gene has been reported (Kuhn et al. 1995). And tetracycline response system could activate or repress recombinase expression to control the sites specific recombination.

1.3.2 Constitutive knockout versus conditional knockout

The conventional gene targeting strategy generates null allele in mice for the target gene. Usually, the genes as a whole or at least an essential part of it are removed. This procedure provides information about the earliest essential role of the target gene during development. To study the multiple roles of a target gene in different tissues at different development stages, conditionally switching on or off recombinase genes using tissue specific promoters has been employed. These methods provide means to bypass the early embryonic lethality. Conditional null alleles are usually generated by two loxP sites introduced in the same orientation into non-coding regions flanking the critical protein coding exons. Meanwhile, a conditional knockout can be converted to a constitutive knockout model, which is carried out by crossing with recombinase 'deleter' mice, a strain that expresses the relevant recombinase in whole tissues including germ cells (Schwenk et al. 1995; Rodriguez et al. 2000). Although the conditional knockout strategy is a better way to identify the gene function *in vivo*, a tissue-specifically expressed recombinase may not completely delete the target gene, which can compromise the analysis of the lose of function in the tissues.

1.4 Mouse development

1.4.1 Ovulation and fertilization

Luteinizing hormone stimulates oocytes to undergo nuclear maturation by setting first meiotic division. After finishing the first meiosis and polar body formation, the oocytes are arrested at the metaphase of second meiosis (MII) and released from the ovary into oviduct for fertilization. Completion of second meiotic division and extrusion second polar body are triggered by fertilization, then female and male pronuclei form. When both pronuclei migrate to the center of zygote, visible nucleoli form and DNA

duplication starts. Fertilization also induces demethylation of DNA to erase epigenetic information for establishing a pluripotent state.

1.4.2 Embryonic development

Mouse embryogenesis is a coordinated process. Cleavage and blastulation is the first event, which is followed by implantation, gastrulation, organogenesis, and fetal growth. During this process, the embryo development can be staged according to the days post coitum (dpc). Since mating usually takes place around midnight during the dark cycle (7 pm to 5 am) (vaginal plugs were checked in the morning), at this point, the embryos are staged as half-day post coitum [(0.5 dpc, embryo stage (E0.5)]. There are further criteria to distinguish stages of embryo development. For example, cell and somite number are commonly used to classify stages. Different stages have specific characters. Briefly, at the 2-cell stage (1.5 dpc, E1.5), the zygotic genome is activated. Up to the early 8-cell stage (uncompacted morula, 2.5 dpc, E2.5), the blastomeres in an embryo are regarded as equipotent; as the compaction and cavitation proceed, a blastocyst is formed (3.5 dpc, E3.5, 16-40 cells); after hatching from the zona pellucida, the blastocyst is ready for implantation in the uterus (4.5 dpc, E4.5); with the implantation proceeding, trophoblast, primitive endoderm and ectoderm (epiblast) are formed (5.5 dpc, E5.5); at 6.5 dpc, gastrulation begins and results in the formation of a multilayered, three-chambered conceptus; amnion is formed at 7.5 dpc (E7.5); at 8.0 dpc (E8.0), somites begin to develop until 11 dpc (E11.0); most organs are generated till 14 dpc (E14.0); from 14 dpc to 19 dpc (E19.0), fetal growth is increased twice in size.

During the early mouse embryo development, the cell growth in different stages is fast and not uniform. Prior to E6.5, the mean cell cycle time of mouse embryo is 11.5 and 9.1 hours in E5.5 and E6.0, respectively. Once gastrulation starts at E6.5, the primitive streak is formed and the cell cycle is decreased to 4.4 hours. A region called ‘proliferative zone’, constituting 10% of the whole epiblast, proliferates fast and the average cell cycle time is only 2 hours versus 6.5 hours for other epiblast regions. This short cell cycle time facilitates rapid increase of cell numbers during embryo gastrulation.

1.4.3 Differentiation of tissue lineages in early embryo

In the blastocyst stage, two distinct lineages are generated: the outer epithelial trophectoderm (TE) and inside inner cell mass (ICM) (Figure 5). After implantation, TE can develop into the mural trophectoderm and the polar trophectoderm. The mural

trophectoderm is derived from the cells surround the blastocyst cavity without contacting the ICM, while the polar trophectoderm is derived from cells in close proximity to the ICM. The mural trophectoderm differentiates into the post-mitotic primary trophoblast giant cells (TGCs), which carry up to a thousand copies haploid of DNA in one cell. Some TGCs migrate into the antimesometrial portion of the implantation chamber and surround the future parietal yolk sac. On the other hand, the polar trophectoderm spreads in several directions, and finally forms the extraembryonic ectoderm of pregastrula and ectoplacental cone. Cdx2, a homeobox transcription factor, is essential for maintaining trophectoderm identity, which is the precursor to all trophoblast cell subtypes (Kunath et al. 2004). FGF4 produced by ICM interacts with Fgfr2, which is the receptor of FGF4 and is specifically expressed in trophectoderm and extraembryonic ectoderm, to promote the trophoblast proliferation. This conclusion is based on FGF4 requirement for the establishment of trophoblast stem cells (TSCs) (Tanaka et al. 1998) from blastocysts or E6.5 extraembryonic ectoderm (Simmons and Cross 2005). At E6.5, TSCs potential is maintained in the extraembryonic ectoderm by FGF4 signaling pathway through Fgfr2 to sustain Err2, Eomes, and Cdx2 expression and suppress Mash2 expression. However, the TSCs potential will lose at approximately E8.5-E8.75, because of occlusion of the ectoplacental cavity.

After formation of the trophectoderm lineage, another epithelial layer, primitive endoderm, appears on the free surface of ICM, which contacts with blastocyst cavity. In parallel, the remaining core of ICM organizes into primitive ectoderm, which is also known as the epiblast. Primitive endoderm gives rise to visceral endoderm and parietal endoderm during differentiation. The epiblast is pluripotent and gives rise to the embryonic ectoderm, definitive endoderm, embryonic mesoderm, and extraembryonic mesoderm (Figure 6). Oct4 is expressed in the epiblast cells in the blastocyst and in early gastrulation stages, but disappears as the definitive germ layers form. A tight control of Oct4 levels is important for cell fate allocation in blastocysts. For example, it was reported that depletion of Oct4 in ES cells resulted in differentiation of ES cells into trophectoderm, while two-fold increase in Oct4 expression causes ES cells to adopt a visceral endoderm and mesoderm fate (Niwa et al. 2000).

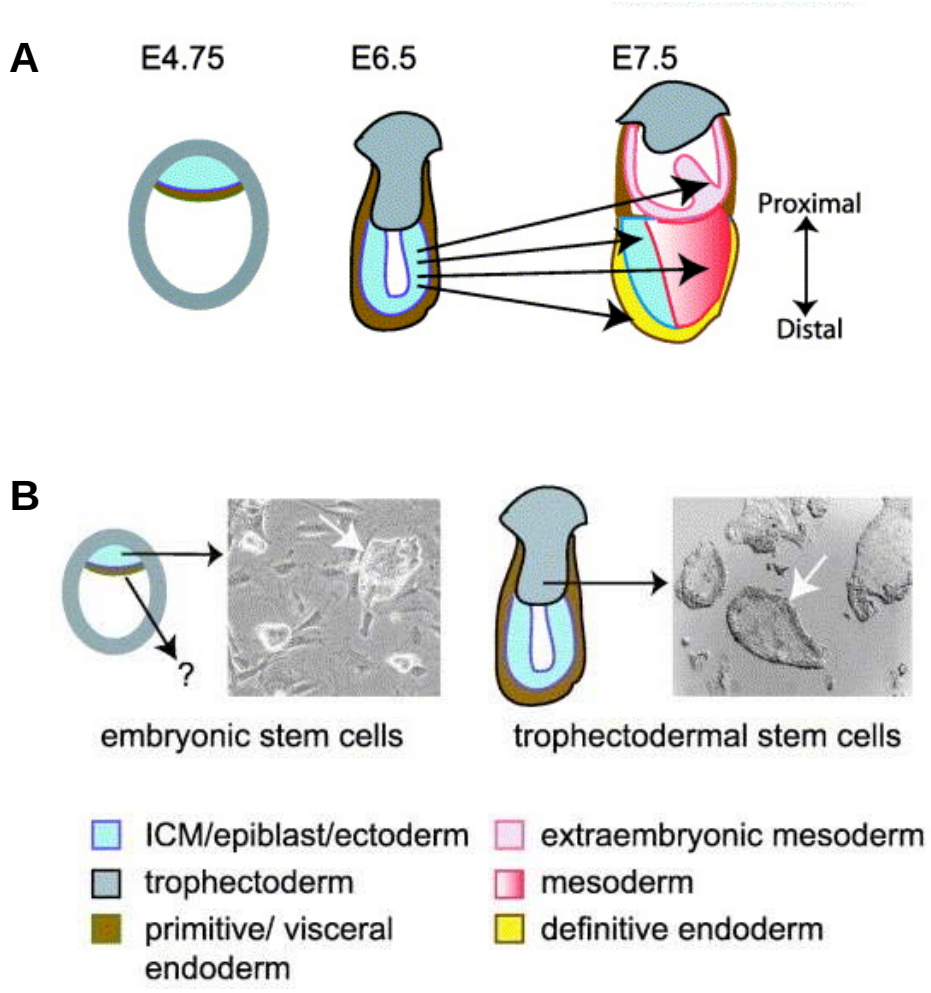

Figure 5: Differentiation of tissue lineage from early embryos.
(A) The differentiation of trophectoderm (gray), ICM (blue), and primitive endoderm (brown) of E4.75 embryo to the extraembryonic and embryonic tissues of E7.5 embryo (germ layer tissues are color-coded, see key). (B) Colonies of embryonic and trophectodermal stem cells (white arrows) derived from the ICM and extraembryonic ectoderm, respectively (Loebel et al. 2003).

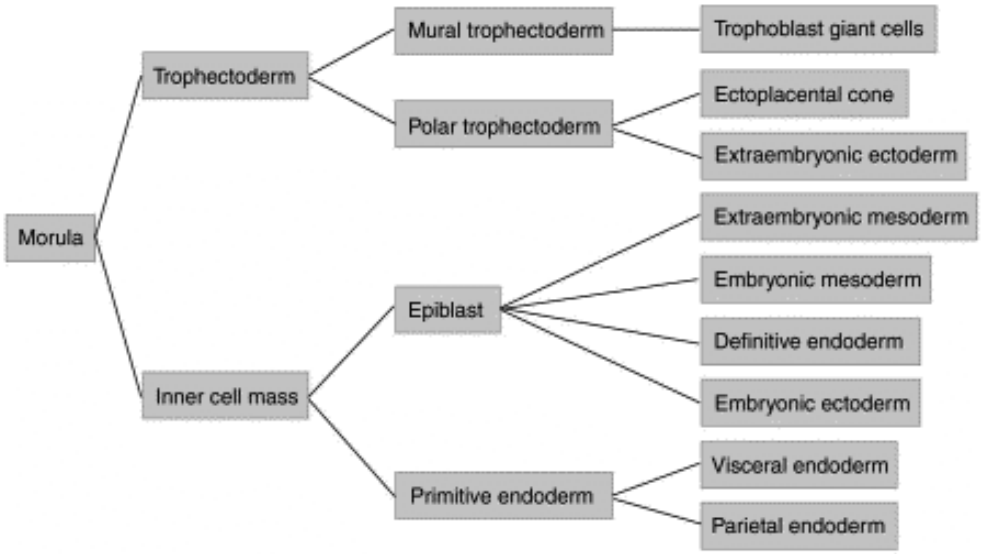

Figure 6: Cell lineage relationships in the early mouse embryo (Lu et al. 2001).

1.4.4 Gastrulation

Gastrulation is a pivotal step to generate a blueprint for the subsequent morphogenesis of the embryo. The characterization of gastrulation includes formation of the primitive streak, allocation of germ-layer precursors, and morphogenetic cells and tissue movement. The primitive streak is a prerequisite to set anterior-posterior axis for directing future embryo development. The formation of the germ layers requires movement of the progenitor cells from the epiblast through the primitive streak, to either emerge as a new mesoderm layer or be incorporated as definitive endoderm into the pre-existing visceral-endoderm layer. It has been reported that the deployment of different levels of nodal and WNT signaling in the primitive streak determine the formation of different population for mesoderm and endoderm cells (Tam and Loebel 2007). In addition, TGFB-related factor, activin A, can also support endodermal marker gene activation. It is further demonstrated that interactions between extra-embryonic and embryonic tissues are crucial for lineage specification and embryonic patterning to build the mouse gastrula, and these interactions are mediated by WNT and TGF signaling (Tam et al. 2006).

1.5 Aims and scope of this work

The objective of this work was to characterize the *in vivo* function of transcription cofactor PC4. To address this question, a conditional PC4 mouse model was generated. From this mouse strain, a null functional PC4 mouse strain was derived to investigate its generic role in all tissues. Furthermore, in order to disclose the underlying mechanism of the phenotype, PC4 knockout embryonic stem cell lines were derived as a cellular model.

2. MATERIALS AND METHODS

2.1 Materials

2.1.1 Chemicals and biochemicals

Acetic Acid (analytical grade, 100%)	Roth
Acrylamide solution 30% (Rotiphorese Gel A)	Roth
Agarose	Roth
Ammonium persulfate (APS)	Merck, Roth
Ammonium sulphate	Merck
Aprotinin	Sigma
Ampicillin	Roth
Bacto Agar	Difco
Bacto Trypton	Difco
Bacto Yeast Extract	Difco
Benzamidin	Sigma
Bisacrylamide solution 2% (Rotiphorese Gel B)	Roth
Boric Acid	Roth
Bradford reagent	Bio-Rad
Bromophenol Blue	Sigma
Bovine Serum Albumin (BSA) (10 mg/ml)	NEB
Colcemid	Sigma
Coomassie brilliant blue R-250	Sigma
DAPI (4',6-diamidino-2-phenylindole)	Sigma
Denhardt's	Invitrogen
Dextransulphate	Amersham
Diethylpyrocarbonate (DEPC)	Sigma
Dimethylsulfoxide (DMSO) (cell culture grade, 99.7%)	Sigma
Dithiothreitol (DTT)	Roth
DMEM medium	Gibco

dNTPs	MBI, Roche
Ethanol (EtOH, analytical grade, 99.8%)	Merck
Ethidium bromide (10 mg/mL)	Sigma
Ethylendiamintetraacetate disodium salt (EDTA)	Merck
Ethylene Glycol Tetraacetic acid (EGTA)	Merck
Fetal Bovine Serum (FBS)	Invitrogen
Formamide	Fluka
Gancyclovir	Sigma
Gelatin solution	Sigma
Geneticin G-418 sulphate	PAA
Glucose	Merck
Glycerol (analytical grade, 99.5%)	Roth
Glycine	Roth
Hepes	Biomol
Histogel mounting medium	Linaris
Isopropanol	Merck
Leupeptin	Roche
Leukaemia inhibitory factor (LIF)	ESGRO Chemicon International
Mineral oil	Sigma
Mitomycin C	Sigma
Magnesiumchloride	Merck
2-Mercaptoethanol	Invitrogen
Methanol (analytical grade, 99.9%)	Merck, Roth
Milk powder	Roth
N-Lauroylsarcosine	Sigma
Nocodazole	Sigma
NP40 (IGEPAL CA630)	Sigma
Paraffin	Fisher Scientific
Paraformaldehyde (PFA)	Fluka
Penicillin-Streptomycin	Invitrogen

Pepstatin	Sigma
Phenol Clorophorm Isoamyl alcohol 25/24/1	Roth
Phenylmethylsulphonylfluoride (PMSF) (biochemistry grade, 99%)	Roth
Polyvinylpyrrolidone	Sigma
Ponceau S	Sigma
Potassium chloride	Sigma
Potassium hydroxide	Roth
Sodium azide	Sigma
Sodium carbonate	Merck
Sodium chloride	Merck, Roth
Sodium citrate	Merck
Sodiumdodecylsulphate (SDS)	Merck, Roth
Sodium hydroxide	Merck
Spermidine	Sigma
Sucrose	Roth
Tetramethylethylendiamine (TEMED)	Sigma, Roth
Top agar	Sigma
Tris(hydroxidmethyl)-aminomethan (Tris)	Sigma
Triton X-100	Sigma
Trypsin-EDTA (0.05%)	Invitrogen
Trypsin (0.25%)	Invitrogen
TWEEN 20	Sigma
Xylene	Merck

2.1.2 Additional material

Disposable plastic material	Greiner, Nunc,Falcon
DNA maxi and midi preps kit	Qiagen, NucleoBond
ECL detection system	Perkin Elmer
Film X-OMAT	BioMax Kodak

Megaprime DNA labelling system Kit	Amersham
Membrane Hybond-N	Amersham
MicroSpin colums G25	Amersham
Miniprep Kit	Amersham
Nitrocellulose membrane	Bio-Rad
Power SYBR Green PCR Kit	Applied Biosystem
RNeasy Kit	Qiagen
Sterile flter (0.22/0.45 µm)	Roth
ThermoScript™ RT-PCR system Kit	Invitrogen
Whatman 3MM Paper	Whatman

2.1.3 Instruments

Acrylamide gel electrophoresis	Bio-Rad
Agarose gel electrophoresis	Bio-Rad
Autoradiography cassette	Amersham, Kodak
Camera	C-5060, wide zooms, Olympus
Centrifuges	Avanti, Beckman; Multifuge 3SR+, Heraeus; Centrifuge 5418, 5415R, Eppendorf
Confocal light microscope TCS SP2	Leica
Developing machine Curix60	Agfa
Electroblot, semi-dry	Bio-Rad
Electroporator Gene Pulser II	Bio-Rad
Geiger counter LB122	Berthold
Heating block	Eppendorf
Homogenizer Douncer,	Wheaton
Incubator	WJ311, Forma Scientific; Unequip, Unitherm; B6200, Heraeus; MCO-18AIC, SANYO

Inverted microscope	SZ61, Olympus; ECLIPSE TE-2000U, Nikon; Axiovert 200 M, Zeiss; Light microscope Axiovert 25, Zeiss
NanoDrop spetrophotometer	Thermo Fisher Scientific
PCR-Thermocycler GeneAmp 5700	Applied Biosystem
StepOnePlus™ Real-Time PCR System	Applied Biosystem
Thermomixer compact	Eppendorf
pH-Meter	Calimatic 760, Knick
Photometer GeneQuant Pro	Amersham
Rotors	JA10, JA25-50, SW41, SW28,Beckman
UV–Illuminator	Bachofer (254 nm, 366 nm)

2.1.4 General buffers

LB medium (for 1 L):
10 g Trypton
5 g Yeast extract
5 g NaCl
To prepare LB-agar plates add 15 g top agar to 1 L of LB medium. Autoclave.

6x SDS loading buffer:
0.35 M Tris/HCl pH 6.8
0.12 mg/ml Bromphenol blue
10% (w/v) SDS
30% (v/v) Glycerol
50 mM DTT

20x SSC (for 2 L):
350 g NaCl
176 g Sodium Citrate
Adjust to pH 7.0 with NaOH.

50x TAE (for 1 L):
242 g Tris
57.1 ml Glacial Acetic Acid
100 ml 0.5M EDTA, pH 8.0.

0.5 M EDTA (pH 8.0, for 1 L):
86.1 g EDTA
Adjust to pH 8.0 with NaOH before adding dH_2O to 1 L.

10x TBE (for 5 L):
275 g Boric Acid
46.5 g EDTA
540 g Tris.

10x TBS (for 1 L):

24.2 g Tris
80 g NaCl
2 g KCl. Adjust pH to 7.6 with HCl.

1x TBST (for 1 L):
100 ml 10x TBS
2 ml 10% (v/v) Tween-20

10% (v/v) Tween 20 (for 50 ml):
5 ml Tween 20
45 ml H_2O
50 µl 0.5 M EDTA, pH 8.0

1x TE:
10 mM Tris/HCl pH 7.5
1 mM EDTA pH 8.0

5x Western blot transfer buffer (for 1 L):
72 g Glycine
15 g Tris

1x Western blot transfer buffer (for 1 L):
200 ml 5x Western blot transfer buffer
200 ml Methanol
600 ml dH_2O

10x TGS (for 1 L):
30.2 g Tris
148 g Glycine
10 g SDS

PBS (phosphate-buffered saline):
137 mM NaCl
2.7 mM KCl
4.3 mM $Na_2HPO_2 \cdot 2H_2O$
1.4 mM KH_2PO_4

20x SSC (for 2 L):
350 g NaCl
176 g Sodium Citrate
Adjust to pH 7.0 with NaOH.

Denaturation buffer for Southern blot:
0.5 M NaOH
1.5 M NaCl

Neutralization buffer for Southern blot:
0.5 M Tris/HCl, pH 7.4
1.5 M NaCl

Hybridization buffer for Southern blot (for 150 ml):
15 g Dextransulphate (Amersham Biosciences, Cat. No. 17-0340-01)
resolve Dextransulphate in dH_2O in a final volume of 30 ml at 80°C on a stirrer
72 ml Formamide (Fluka, Cat. No. 47670)
36 ml 20x SSC
1.5 ml 1 M Tris/HCl, pH 7.5
15 ml 10% (w/v) SDS
3 ml 50x Denhardt's solution (Invitrogen, Cat. No. 750018)

Proteinase K lysis buffer:

10 mM NaCl
10 mM Tris/HCl pH 7.5
10 mM EDTA
0.5% (w/v) N-Lauroylsarcosine
0.2 mg/ml Proteinase K freshly added.

ES cells lysis buffer:
10 mM NaCl
10 mM Tris/HCl pH 7.5
10 mM EDTA pH 8.0
1 mg/ml Proteinase K freshly added.

Tail lysis buffer:
100 mM Tris/HCl pH 8.5
5 mM EDTA
0.2% (w/v) SDS
200 mM NaCl
200 µg/ml Proteinase K and 0.5 mg/ml RNase A (Fluka, Cat. No. 83832) freshly added.

Oocyte lysis buffer:

10 mM Tris/HCl pH7.8
17 µM SDS
150 µg/ml Proteinase K freshly added.

2.1.5 Enzymes

DNase (RNase-free)	Qiagen
Proteinase K (PCR grade)	Roche
Restriction enzymes	NEB or Fermentas
RNase A (molecular biology grade)	Sigma
Taq polymerase	Fermentas, Invitrogen

2.1.6 Antibodies

Table 4: Primary antibodies used in this work

PRIMARY ANTIBODY	ORIGIN	PROVIDER	DILUTION WB	DILUTION IF
PC4 (SA2249)	Rabbit	Eurogentec	1:500	1:400
α-tubulin	Mouse	Sigma	1:20000	

Polymerase II (N-20,sc-899)	Rabbit	Santa Cruz	1:1000	
p53 (sc-6243)	Rabbit	Santa Cruz	1:1000	
p53 (phosphoS15) (ab1431)	Rabbit	abcam	1:1000	
NC2 (4G7)	Rat	E. Kremmer	1:10	

Table 5: Secondary antibodies used in this work

SECONDARY ANTIBODY	PROVIDER	DILUTION WB	DILUTION IF
Anti Rabbit	Promega	1:5000	
Anti Rat	Promega	1:4000	
Anti Mouse	Promega	1:5000	
Anti-Rabbit-Cy3	Dianova		1:500
Anti-rabbit Rhodamine Red-X	Jackson ImmunoResearch		1:100

2.1.7 List of plasmids

Table 6: Plasmids used in this work

PLASMID ID	PARENTAL PLASMID	DESCRIPTION	CLONED BY	USED FOR
pWR1	pBluescriptSKII	mPC4 exon 1-intron 1 (587bp)	Wera Roth	Preparation for probe A used for Southern blot
pWR3	pBluescriptSKII	mPC4 intron 3 (541bp)	Wera Roth	Preparation for probe C used for Southern blot
pWR5	pBluescriptSKII	mPC4 intron 5 downstream (500bp)	Wera Roth	Preparation for probe B used for Southern blot
pWR11	pBluescriptSKII+	PC4 conditional targeting construct	Gene Bridges	Generation of PC4 conditional knockout mice
pWR-12	pEGFP-C1	EGFP vector	Clonetech	Rescue of PC4 knockout in

				mouse ES cells
pWR-23	pEGFP-C1	human PC4 1-127	Wera Roth	Rescue of PC4 knockout in mouse ES cells
pNL-4	pMSCV	Cassette A	Vigo Heissmeyer	Knockdown of PC4 in MEFs
pNL-5	pMSCV	Cre recombinase gene	Vigo Heissmeyer	Knockdown of PC4 in MEFs
pNL-6	pEco-pac	gag/pol/env insertion	Vigo Heissmeyer	Knockdown of PC4 in MEFs

2.1.8 List of oligonucleotides

Table 7: Oligonucleotides used in this work

OLIGO ID	SEQUENCE 5'–> 3'	GENERAL USE
oWR1	CGGGATCCATCACATTGAATGCCAGTTTGG	PCR cloning for generation of Southern blot probe A
oWR2	CGGAATTCTAACTCACATTGAGGGGACCAG	PCR cloning for generation of Southern blot probe A
oWR5	CGGGATCCATTCCTCAAGAGCAGAGGCTGT	PCR cloning for generation of Southern blot probe C
oWR6	CCATCGATGGTTAGGACACCTGGCCTTGTC	PCR cloning for generation of Southern blot probe C
oWR9	CGGGATCCATGAGATCTGCCGTCTGCTACC	PCR cloning for generation of Southern blot probe B
oWR10	CGGAATTCTAGGAGAATCATCTTGCCTGCT	PCR cloning for generation of Southern blot probe B
siRNA-PC4-NL	AAGACAGGUGAGACUUCGAGA (target sequence)	Knockdown of human PC4 in HeLa and A549 cells
siRNA-PC4-WR	GCAAAGUGCUAAUUGAUAUU (target sequence)	Knockdown of human PC4 in HeLa cells
siRNA-PC4-TK	ACAGAGCAGCAGCAGCAGA (target sequence)	Knockdown of human PC4 in HeLa and A549 cells
mouse scrambled siPC4	AAGCCUGGUGAGACUUCUAGA (target sequence)	"scrambled" non-silencing control siRNA for knocking down PC4 in human cells
scrambled siPC4	GCATAGTAGCAATAGAGTT	"scrambled" non-silencing control siRNA for knocking down PC4 in human cells
oWR77	TGTCAGTGTTCGGGACTTCA	Genotyping conditional PC4 knockout mice offspring with PCR
oWR78	TGACTAGGGGAGGAGTGGAA	Genotyping conditional PC4 knockout mice offspring with PCR

oWR79	CAACCAAGTAAGGCCAATCC	Genotyping conditional PC4 knockout mice offspring
oWR80	GCCGCATAACTTCGTATAGCA	Genotyping conditional PC4 knockout mice offspring with PCR
oWR81	GCTTTTGCTGCCTTCAGATT	Genotyping conditional PC4 knockout mice offspring with PCR
oWR82	TTTGGGCTGCATTCTTAATTC	Genotyping conditional PC4 knockout mice offspring with PCR
oWR83	TGTGGCTTGAGCTTCTGAAA	Genotyping conditional PC4 knockout mice offspring with PCR
oNL1	GCCTAATCTGCCTAGGAACTAG	Genotyping conditional PC4 knockout mice offspring with PCR
oNL2	CGCATAACCAGTGAAACAGCAT	Genotyping Cre transgene
oNL3	GAAAGTCGAGTAGGCGTGTACG	Genotyping Cre transgene
oNL7	GACAAGCGTTAGTAGGCACAT	Genotyping FLP transgene
oNL8	GAGAAGAACGGCATAGTGCGT	Genotyping FLP transgene
oNL36	TTCAAGGCAAGGCAGAGAAT	Genotyping of $PC4^{+/-}$ mice embryos with nested PCR
oNL37	CCCCCTGAGGTAGTTGGATT	Genotyping of $PC4^{+/-}$ mice embryos with nested PCR
oNL38	ACTGGGCAAAGCACCAATAC	Genotyping of $PC4^{+/-}$ mice embryos with nested PCR
mPC4F-101	TGATTCGGACAGCGAAGTTG	Mouse qRT-PCR (for gene PC4)
mPC4R-289	TTGAAGTCCCGAACACTGAC	Mouse qRT-PCR (for gene PC4)
mP53F1	GTCACAGCACATGACGGAGG	Mouse qRT-PCR (for gene p53)
mp53R1	TCTTCCAGATGCTCGGGATAC	Mouse qRT-PCR (for gene p53)
mP21F1	CCTGGTGATGTCCGACCTG	Mouse qRT-PCR (for gene p21)
mP21R1	CCATGAGCGCATCGCAATC	Mouse qRT-PCR (for gene p21)
mBaxF1	TGAAGACAGGGGCCTTTTTG	Mouse qRT-PCR (for gene Bax)
mBaxR1	AATTCGCCGGAGACACTCG	Mouse qRT-PCR (for gene Bax)
mβ-Actin-F	GACGGCCAGGTCATCACTATTG	Mouse qRT-PCR (for gene β-Actin)
m β-Actin-R	TACGGATGTCAACGTCACACTTCA	Mouse qRT-PCR (for gene β-Actin)
m18s-R	GCAGCAACTTTAATATACGCTATTGG	Mouse qRT-PCR (for gene 18S)
m18s-F	GAGGCCCCGTAATTGGAATGAG	Mouse qRT-PCR (for gene 18S)
m5S-F	GCCATACCACCCTGAACG	Mouse qRT-PCR (for gene 5S)
m5S-R	AGCCTACAGCACCCGGTATT	Mouse qRT-PCR (for gene 5S)
m5.8s-F	CTCTTAGCGGTGGATCACTC	Mouse qRT-PCR (for gene 5.8S)

m5.8s-R	GATGATCAATGTGTCCTGCAA	Mouse qRT-PCR (for gene 5.8S)
m28s-F2	CAGGGGAATCCGACTGTTTA	Mouse qRT-PCR (for gene 28S)
m28s-R2	ATGACGAGGCATTTGGCTAC	Mouse qRT-PCR (for gene 28S)
U6 snRNA-F	GCTCGCTTCGGCAGCACATATAC	Mouse qRT-PCR (for gene U6 snRNA)
U6 snRNA-R	TATCGAACGCTTCACGAATTTGCG	Mouse qRT-PCR (for gene U6 snRNA)
7SKRNA-F	GACATCTGTCACCCCATTGA	Mouse qRT-PCR (for gene 7SK)
7SKRNA-R	GCGCAGCTACTCGTATACCC	Mouse qRT-PCR (for gene 7SK)
mCcne1-F	GTGGCTCCGACCTTTCAGTC	Mouse qRT-PCR (for gene Ccne1)
mCcne1-R	CACAGTCTTGTCAATCTTGGCA	Mouse qRT-PCR (for gene Ccne1)
mCcna2-F	GCCTTCACCATTCATGTGGAT	Mouse qRT-PCR (for gene Ccna2)
mCcna2-R	TTGCTGCGGGTAAAGAGACAG	Mouse qRT-PCR (for gene Ccna2)
mCcnb1-F	AAGGTGCCTGTGTGTGAACC	Mouse qRT-PCR (for gene Ccnb1)
mCcnb1-R	GTCAGCCCCATCATCTGCG	Mouse qRT-PCR (for gene Ccnb1)
mCcnd1-F	GCGTACCCTGACACCAATCTC	Mouse qRT-PCR (for gene Ccnd1)
mCcnd1-R	CTCCTCTTCGCACTTCTGCTC	Mouse qRT-PCR (for gene Ccnd1)
mCDK2-F	CCTGCTTATCAATGCAGAGGG	Mouse qRT-PCR (for gene CDK2)
mCDK2-R	TGCGGGTCACCATTTCAGC	Mouse qRT-PCR (for gene CDK2)
mOct4-F	TGAGAACCTTCAGGAGATATGCAA	Mouse qRT-PCR (for gene Oct4)
mOct4-R	CTCAATGCTAGTTCGCTTTCTCTTC	Mouse qRT-PCR (for gene Oct4)
mNanog-F	TCTTCCTGGTCCCCACAGTTT	Mouse qRT-PCR (for gene Nanog)
mNanog-R	GCAAGAATAGTTCTCGGGATGAA	Mouse qRT-PCR (for gene Nanog)
mDppa3-F	GACCCAATGAAGGACCCTGAA	Mouse qRT-PCR (for gene Dppa3)
mDppa3-R	GCTTGACACCGGGGTTTAG	Mouse qRT-PCR (for gene Dppa3)
mFgf17-F	GCTGCCTAACCTTACCCTGTG	Mouse qRT-PCR (for gene Fgf17)
mFgf17-R	CCTGGTCCCTCACGTACTG	Mouse qRT-PCR (for gene Fgf17)
mRbp1-F	CTGAGCAATGAGAATTTCGAGGA	Mouse qRT-PCR (for gene Rbp1)
mRbp1-R	GCGGTCGTCTATGCCTGTC	Mouse qRT-PCR (for gene Rbp1)
mGng3-F	GCACTATGAGTATTGGTCAAGCA	Mouse qRT-PCR (for gene Gng3)
mGng3-R	GTGGGCATCACAGTATGTCATC	Mouse qRT-PCR (for gene Gng3)
mSfmbt2-F	AAGATAACCGGCTCAGCAAATG	Mouse qRT-PCR (for gene Sfmbt2)
mSfmbt2-R	TCTCTTCCAAATAGTCTCCCCAG	Mouse qRT-PCR (for gene Sfmbt2)
mRragd-F	CTGTTTGACGTGGTCAGTAAGAT	Mouse qRT-PCR (for gene Rragd)
mRragd-R	GTTGAGTCCTTGTCATACGGG	Mouse qRT-PCR (for gene Rragd)

mTdrd12-F	GGTGCTGAAGATTGAAGATCCA	Mouse qRT-PCR (for gene Tdrd12)
mTdrd12-R	CGTCCTGACACATGCTGTTATAG	Mouse qRT-PCR (for gene Tdrd12)
mNeurod1-F	ATGACCAAATCATACAGCGAGAG	Mouse qRT-PCR (for gene Neurod1)
mNeurod1-R	TCTGCCTCGTGTTCCTCGT	Mouse qRT-PCR (for gene Neurod1)
mDdit4l-F	CGGCCAGCATTTCAGAGTTG	Mouse qRT-PCR (for gene Ddit4l)
mDdit4l-R	CAGGGACCAAGACCTTAGAGC	Mouse qRT-PCR (for gene Ddit4l)
mRb1-F	TGCATCTTTATCGCAGCAGTT	Mouse qRT-PCR (for gene Rb1)
mRb1-R	GTTCACACGTCCGTTCTAATTTG	Mouse qRT-PCR (for gene Rb1)
mPerp-F	ATCGCCTTCGACATCATCGC	Mouse qRT-PCR (for gene Perp)
mPerp-R	CCCCATGCGTACTCCATGAG	Mouse qRT-PCR (for gene Perp)
mPlk2-F	CCTGCGGACTATCACCTACCA	Mouse qRT-PCR (for gene Plk2)
mPlk2-R	CTGCCCATCTTCAGAAGGCT	Mouse qRT-PCR (for gene Plk2)
mPhlda1-F	GGGCTACTGCTCATACCGC	Mouse qRT-PCR (for gene Phlda1)
mPhlda1-R	AAAAGTGCAATTCCTTCAGCTTG	Mouse qRT-PCR (for gene Phlda1)
mFgf5-F	CAGATCTACCCGGATGGCAAAG	Mouse qRT-PCR for EBs (for gene Fgf5)
mFgf5-R	GCGGACGCATAGGTATTATAGCTG	Mouse qRT-PCR for EBs (for gene Fgf5)
mOtx2-F	AGGAGCTGATGCGCCACCTC	Mouse qRT-PCR for EBs (for gene Otx2)
mOtx2-R	GTAGCCCAGGGAGGGATGCA	Mouse qRT-PCR for EBs (for gene Otx2)
mNestin-F	ACCTCAAGATGTCCCTTAGTCTGG	Mouse qRT-PCR for EBs (for gene Nestin)
mNestin-R	GGTGCTGGTCCTCTGGTATCC	Mouse qRT-PCR for EBs (for gene Nestin)
mT-F	TGAGGAGATTACAGCCCTTAAA	Mouse qRT-PCR for EBs (for gene T)
mT-R	GGTTCCTTAGAGCTGGGTAC	Mouse qRT-PCR for EBs (for gene T)
mFgf8-F	TCATTGTGGAGACCGATACTT	Mouse qRT-PCR for EBs (for gene Fgf8)
mFgf8-R	CAGCACGATCTCTGTGAATAC	Mouse qRT-PCR for EBs (for gene Fgf8)
mEvx1-F	ACAGGGAGAACTACGTTTCAA	Mouse qRT-PCR for EBs (for gene Evx1)
mEvx1-R	GTGGCTCATCATGTAGGTGTA	Mouse qRT-PCR for EBs (for gene Evx1)
mWnt3-F	GGGGCGTATTCAAGTAGCTG	Mouse qRT-PCR for EBs (for gene Wnt3)
mWnt3-R	GTAGGGACCTCCCATTGGAT	Mouse qRT-PCR for EBs (for gene Wnt3)
mHnf4α-F	TGACAATGAATATGCCTGCCTCAA	Mouse qRT-PCR for EBs (for gene

		Hnf4α)
mHnf4α-R	CAAAGCGGCCCCGAGAGT	Mouse qRT-PCR for EBs (for gene Hnf4α)
mSox17-F	CCATTTAGTGAAGAAACTGAAATATGGC	Mouse qRT-PCR for EBs (for gene Sox17)
mSox17-R	ATTCTCTTGATAGATACTTTGGGAGGAGT	Mouse qRT-PCR for EBs (for gene Sox17)
mGata4-F	CCTGGAAGACACCCCAATCTC	Mouse qRT-PCR for EBs (for gene Gata4)
mGata4-R	AGGTAGTGTCCCGTCCCATCT	Mouse qRT-PCR for EBs (for gene Gata4)
mGluR6-F	GCTGTTCAGTCCATCTGCAA	Mouse RT-PCR for EBs (for gene GluR6)
mGluR6-R	TCCACATCAAGAGCGAAGAG	Mouse RT-PCR for EBs (for gene GluR6)
mHNF3β-F	AGAAGCAACTGGCACTGAAGGA	Mouse RT-PCR for EBs (for gene HNF3β)
mHNF3β-R	GTAGTGCATGACCTGTTCGTAG	Mouse RT-PCR for EBs (for gene HNF3β)
mα-Cardiac myosin-F	GGCACAGAAGATGCTGACAA	Mouse RT-PCR for EBs (for gene α-Cardiac myosin)
mα-Cardiac myosin-R	CGAACATGTGGTGGTTGAAG	Mouse RT-PCR for EBs (for gene α-Cardiac myosin)
mβH1-F	CTCAAGGAGACCTTTGCTCA	Mouse RT-PCR for EBs (for gene βH1)
mβH1-R	AGTCCCCATGGAGTCAAAGA	Mouse RT-PCR for EBs (for gene βH1)
mα-Fetoprotein-F	AGGAGGAGTGCTTCCAGACA	Mouse RT-PCR for EBs (for gene α-Fetoprotein)
mα-Fetoprotein-R	TGCGTGAATTATGCAGAAGC	Mouse RT-PCR for EBs (for gene α-Fetoprotein)

The oligos used as RT-PCR and qRT-PCR are described as “m (mouse) gene name-F or R (F: forward primer, R: reverse primer)”.

2.2 Methods

2.2.1 Molecular Biology

2.2.1.1 Genomic DNA extraction

From 96-well plates: Genomic DNA was extracted from 96-well plates on which transfected TBV2 ES cells were grown to confluency. Cells were washed twice with 100 µl PBS and incubated in 50 µl proteinase K lysis buffer overnight at 55°C in a

humid chamber. On the next day, 100 µl cold NaCl/EtOH mixture (150 µl of 5 M NaCl was added in 10 ml EtOH) was added drop-wise to each well. To remove the buffer, the plate was gently inverted and drained on a paper towel. The cells were washed three times with 200 µl of 70% (v/v) EtOH. The DNA was air-dried at room temperature and resuspended in 50 µl H_2O.

Genomic DNA was subjected to restriction enzyme digestion. For each reaction, 50 µl of genomic DNA was used in a 60 µl total volume with the following components:

1 mM	Spermidine
1 mM	DTT
100 µg/ml	BSA (NEB)
50 µg/ml	RNase A
1x	Reaction buffer (NEB)

50 U *XbaI* (20 U/µl, NEB), or *KpnI* (50 U/µl, NEB) or *EcoRV* (20 U/µl, NEB)

Digestion was carried out overnight at 37°C. The plates were stored at -20°C or directly used for Southern blot analysis.

From expanded candidate clone cells: Genomic DNA was extracted from expanded candidate ES clones to confirm their genotype. Cells were grown on gelatin-coated 6-cm cell culture dish until confluence was reached and then trypsinized and pelleted. The pellets were washed with PBS, and the cells were resuspended in 250 µl of ES cell lysis buffer and incubated overnight at 56°C. Lysates were mixed with 800 µl Phenol/Clorophorm/Isoamil alcohol (PCI, Roth). After centrifugation (Eppendorf 5418, 13000 rpm, room temperature, 5 minutes), the aqueous phase was collected and DNA was precipitated by adding 40 µl of a 3 M Sodium Acetate solution and 800 µl of 100% EtOH. DNA was then pelleted, washed with 70% EtOH and resuspended in 50 µl 1x TE buffer. 25 µl genomic DNA was used for Southern blot analysis.

From mouse tails: Genomic DNA was extracted from mouse tails collected from the offspring of PC4 conditional knockout chimeras. Tails (approximately 5-10 mm) were cut and placed in Eppendorf tubes and kept overnight at 56°C in 200 µl of tail lysis buffer (containing 200 µg/ml proteinase K and 0.5 mg/ml RNase A) with proper shaking (650-700 rpm in a thermomixer). Hair and cell debris were removed by centrifugation (Eppendorf 5418, 13000 rpm, room temperature, 5 minutes). The supernatant was transferred to a new Eppendorf tube and mixed with 160 µl of isopropanol to allow DNA precipitation. The precipitated DNA was collected by using a Pasteur Pipette, washed with of 70% EtOH, and air-dried at room temperature. The genomic DNA was dissolved in 100 µl to 200 µl H_2O, and incubated for one to two hours at 37°C for complete resuspension. From this preparation, 25 µl of genomic DNA was used for Southern blot analysis, or 1 µl was used for PCR genotyping analysis.

2.2.1.2 Southern blot

To identify the homologous recombinant ES cell clones for PC4 conditional knockout, and to confirm the genotype of mouse offspring (F1 generation), Southern blot analysis was applied. The genomic DNA from ES cells or tails was digested with restriction enzymes as above. DNA fragments were resolved on a 0.8% agarose gel in 1x TAE buffer at 60 V for 8-10 hours or overnight at 20-25 V at room temperature. The gel was denatured by seating in two times in denaturation buffer for 15 minutes at room temperature. Then, the gel was neutralized two times by incubation in neutralization buffer for 15 minutes at room temperature. Subsequently, the gel was equilibrated in 20x SSC for 5-20 minutes at room temperature.

Then DNA fragments were transferred from the gel to a nylon membrane (Hybond-N) (Amersham Biosciences, Cat. No. RPN 203N), was carried out for overnight as follows. Specifically, a glass pan was covered by a glass plate, which was “bridged” by one layer of cut-in-size Whatman paper (GB 002, gel blotting paper, Schleicher & Schüll, 580 x 600 mm, Ref. No. 10426694). Then the gel was placed upside down on the Whatman paper, and covered with a cut-in-size Hybond-N membrane together with four layers of Whatman paper, multiple layers of paper and an additional glass plate. Finally a weight of 1-1.5 kg was placed on (i.e. Sigma catalogue + 0.5L filled bottle) the top to facilitate the transferring.

After transfer, the membrane was dried with two layers of Whatman paper and the DNA was cross-linked by using a Stratagene Stratalinker UV crosslinker (program: “automatic crosslink”), and baked in an oven for another two hours at 80°C.

The cross-linked membrane was prehybridized for one to two hours at 42°C in 5-15 ml hybridization buffer with 100 µg/ml boiled Salmon sperm DNA (Sigma, Cat. No. D1626) in a hybridization oven with constant agitation. During this period, the specific hybridization probes were labeled with “Megaprime DNA Labeling System” from Amersham (Cat. No. RPN1606) according to the instructions. Usually, 20 ng of DNA were labeled with 50 µCi of [α^{32}P] dCTP for one hybridization reaction. The labeled probes were purified by using “MicroSpin G25 Columns” (Amersham, Cat. No. 27532501), and counted in a β-counter to determinate labeling efficiency. More specifically, three probes were used for the Southern blot experiments (the localization of these probes was shown in Figure 13A). The probe A and the probe B were obtained by digestion of the vector pWR1 and pWR5 with the restriction enzymes *BamHI* and *EcoRI*, respectively. In addition, the probe C was resulted from the digestion of the plasmid pWR3 with restriction enzymes *BamHI* and *ClaI*. The correct

fragments were gel-purified with gel extraction kit (Qiagen, Cat. No. 28704) and eluted in X µl H_2O.

For the hybridization step, the appropriate amount of fresh hybridization buffer with equal amounts of boiled salmon sperm DNA and labeled probe were added into the membrane. Hybridization was carried out at 42°C overnight in an oven. After hybridization, the membrane was washed two times for 15 minutes each with 2x SSC, 0.1% (w/v) SDS at 65°C in a water bath. Then the membrane was dried on a layer of Whatman paper, and autoradiography was performed using X-ray film (Kodak BioMax MR Film, 24x30 cm) and intensifying screens for one to three days at -80°C.

2.2.1.3 PCR for genotyping of mouse offspring

Since the mouse offspring is heterozygous for the target gene, the PCR for genotyping should separate wild-type allele and mutant allele by different products. Three primers were designed for genotyping every mouse strain. One primer is common for both wild-type and mutant alleles, and the other two primers are specific for each allele.

The PCR reaction as follows:

Genomic tail DNA	1 µl
dNTPs (2 mM)	1 µl
10x Buffer	1 µl
$MgCl_2$ (25 mM)	0.6 µl
Taq polymerase (5 U/µl)	0.1 µl
Common primer (10 pmol/µl)	0.75 µl
Specific primer 1 (10 pmol/µl)	0.5 µl
Specific primer 2 (10 pmol/µl)	0.5 µl
H_2O	4.75 µl

For $PC4^{+/-}$ mouse strain: the common primer is oWR83, and the specific primers are oWR79 and oWR81;

For $PC4^{Neo\ flox/+}$ (F1 generation of PC4 conditional KO mice) mouse strain:

1. Neo cassette checking strategy: the common primer is oWR77, and the specific primers are oWR78 and oWR79;
2. Single loxP site checking strategy: the common primer is oWR81, and the specific primers are oWR80 and oWR83;

For $PC4^{+/flox}$ mouse strain: the common primer is oWR77, and the specific primers are oWR78 and oWR79;

The localization of all the primers for genotyping is shown in Figure 7

PCR program:

1. 94°C 2 minutes
2. 94°C 45 seconds
3. 58°C 45 seconds

4. 72°C 1 minute go to step 2, 32 cycles
5. 72°C 10 minutes
6. 4°C ∞

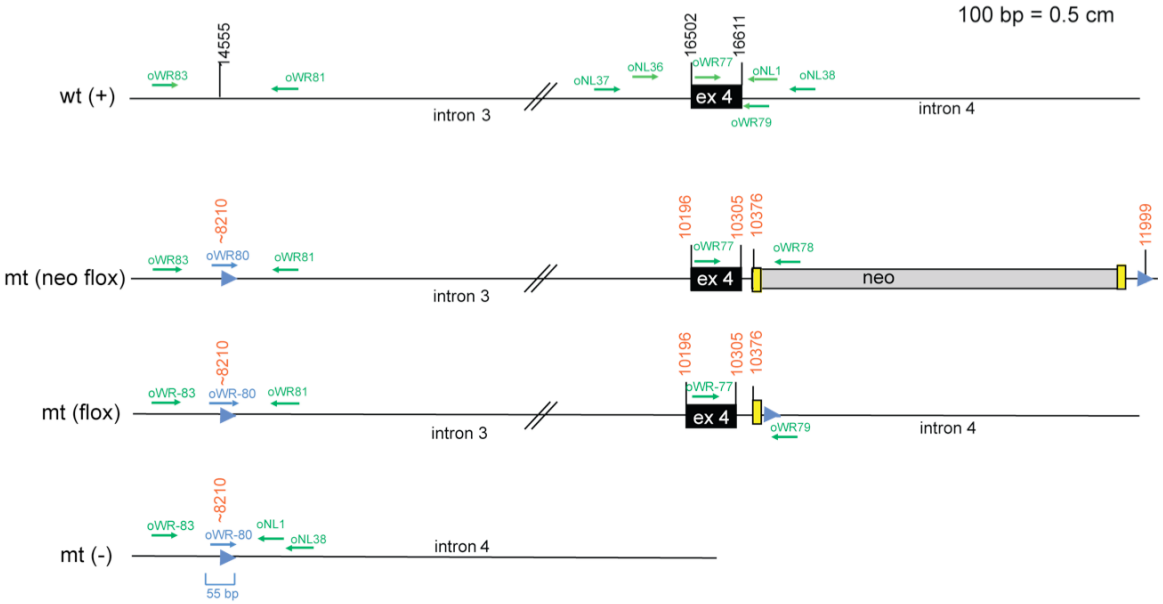

Figure 7: Localization of PCR primers in mouse genome for genotyping different mouse strains and embryonic stem cells.
Blue arrow indicates loxP sites. Yellow box indicates FRT sites.

2.2.1.4 Nested PCR for genotyping early embryos

To genotype the preimplantation or postimplantation embryos obtained from $PC4^{+/-}$ mice intercrosses, nested PCR was performed. The single blastomere or blastocyst or embryonic tissue from the sections was transferred into the PCR tube, in which 3 µl of oocyte lysis buffer was added and covered by one drop of mineral oil. The samples were incubate at 37°C overnight, and heated at 95°C for 15 minutes to inactivate Proteinase K (Roche, Cat. No. 03115828001), then directly used for the first PCR reaction.

The first round of PCR reaction was as following:

Embryo lysis mixture	3 µl
dNTPs (25 mM)	1.5 µl
10x Buffer	1.5 µl
$MgCl_2$ (25 mM)	0.9 µl
Taq polymerase (5 U/µl)	0.045 µl
oWR83 (10 pmol/µl)	0.3 µl
oNL37 (10 pmol/µl)	0.45 µl
oNL38 (10 pmol/µl)	0.6 µl
H_2O	6.7 µl

The second round of PCR reaction was as following:

DNA product from the first round PCR	1 µl
dNTPs (25 mM)	1.2 µl
10x Buffer	1.2 µl
$MgCl_2$ (25 mM)	0.72 µl
Taq polymerase (5 U/µl)	0.05 µl
oWR80 (10 pmol/µl)	0.5 µl
oNL1 (10 pmol/µl)	1 µl
oNL36 (10 pmol/µl)	0.5 µl
H_2O	5.83 µl

PCR program:

1. 95°C 2 minutes
2. 94°C 30 seconds
3. 58°C 30 seconds
4. 72°C 1 minute go to step 2, 25 cycles for the first round PCR or 35 cycles for the second round PCR
5. 72°C 7 minutes
6. 4°C ∞

2.2.1.5 Quantitative Reverse-Transcription PCR (qRT-PCR) and Reverse-Transcription PCR (RT-PCR)

Reverse Transcription (RT): Total RNA was extracted from wild-type (WT) and PC4 knockout (KO) ES cell lines or from embryo bodies (EBs) using the Qiagen RNeasy Mini kit (Qiagen, Cat. No. 74106) according to the manufacturer's instruction. An on-column DNase I digestion was performed using the RNase-free DNase Set (Qiagen, Cat. No. 79254) to eliminate residual amounts of genomic DNA. Total RNA was eluted in 30-50 µl 0.1% (v/v) Diethylpyrocarbonate-treated H_2O (DEPC-H_2O) and RNA was stored at -80°C or directly used for RT. Two microgram of total RNA was subjected to reverse transcription using the ThermoScript™ RT-PCR System (Invitrogen, Cat. No. 11146-024). The random primers provided by the kit were used to synthesize the first cDNA strand. The reaction was carried out as following: samples were incubated at 25°C for 10 minutes to allow primers annealing, reverse transcription was carried out at 50°C for 1 hour followed by a denaturation step at 85°C for 5 minutes. The cDNA was diluted into 80 µl and stored at -20°C or immediately used it for quantitative Real-time PCR or normal PCR.

For Real-time PCR (qRT-PCR), the “Power SYBR GREEN PCR Master Mix” was used (Applied Biosystem, Cat. No. 4309155). Each reaction was carried out with 0.8 µl cDNA and 0.4 µM of forward and reverse primers (all the sequences are list in table 7). Primers were designed with a melting temperature (Tm) of 60°C. Primers of β-Actin gene were included as a reference control. Samples obtained from reverse transcription reactions carried out without reverse transcriptase were used as negative

control. PCR reactions were performed in a StepOne™ Real-Time PCR System from Applied Biosystem.

For standard PCR reaction (RT-PCR), 1.6 µl cDNA was used as a template, and 1 µM of the gene specific primer pairs was used in a total reaction volume of 15 µl. During PCR reaction, the annealing temperature was 56°C, and 35 cycles of amplification were run. Reaction products were subsequently maintained at 4°C until they were analyzed by 2% (w/v) agarose gel in 1x TAE buffer.

2.2.1.6 Microarrays

For microarrays analysis, total RNA was prepared from $5x10^6$ cells of PC4 wild-type (WT) and knockout (KO) ES cells using the Qiagen RNeasy Minikit (Qiagen) with the on column DNAase I (RNase-Free DNase Set, Qiagen, Cat. No. 79254) digestion according to the manufacturer's instructions. RNA samples (10 µg) were hybridized to GeneChip® mouse gene 1.0 ST arrays by the approved Affymetrix service provider KFB (Regensburg). Pre-processing of data, i.e. data acquisition and determination of up- and down-regulated genes, was also performed by KFB.

2.2.1.7 Bioinformatic analysis

Array data were analyzed further using Bibliosphere from Genomatix (www.genomatix.de) in order to create a hypothetical network amongst the target genes based on co–citation in literature databases (Scherf et al. 2005). Networks were generated using microarray target genes and transcription factors that were co–cited together with the corresponding gene at the “sentence level”, i.e. genes that were found cited in the same sentence in literature databases. Furthermore, gene ontology (GO) analysis was performed using MGI Gene Ontology Term Finder (http://proto.informatics.jax.org/prototypes/GOTools/web-docs/MGI_Term_Finder.html). In addition, a hierarchical clustering analysis was performed using MultiExperiment Viewer software (MeV) (http://www.tm4.org) (Eisen et al. 1998).

2.2.2 Cell Biology

2.2.2.1 Culture of human tumor cell lines and related methods

2.2.2.1.1 Cell lines

A549	Human lung adenocarcinoma epithelial cell line, adherent
HeLa	Human epithelial cell line, cervical carcinoma, adherent

HEK293T Human embryonic kidney cell line, adherent

2.2.2.1.2 Growth conditions

A549 and HeLa adherent cell lines were grown in Dulbecco's modified Eagle medium (DMEM plus 4500mg/ml glucose, L-Glutamine, without pyruvate; Invitrogen, Cat. No. 11971-025) supplemented with 10% (v/v) FBS (Invitrogen, Cat. No. 10270-106), L-Glutamine (Invitrogen, Cat. No. 25030024) and 1% (v/v) Penicillin-Streptomycin (Invitrogen, Cat. No.15140-122). Cells were grown in culture dishes ranging from 15 and 10 cm down to 6 and 12 well plates (Nunc, Cat. No. 157150, 150350, 140675, 150628) in a tissue culture incubator under 5% CO_2 and at 37°C. Confluent cells were detached from the plates by using 0.25% trypsin (Invitrogen, Cat. No. 25050-030) and seeded to a new plate in the ratio of 1:4.

2.2.2.1.3 Freezing and thawing conditions

Cells were grown to 90% confluence in 10 or 15-cm dishes, trypsinized and resuspended in 0.5-1ml of cold freezing medium containing 90% serum and 10% dimethyl-sulfoxide (DMSO) (Sigma, Cat. No. D2650). Subsequently, cells were transferred to cryovials (Nunc) and placed for 24 hours at -80°C by using Mr. Frosty freezing container (Nalgene Mr. Frosty, Cat. No. C1562) before stored in liquid nitrogen. For thawing, frozen aliquots were quickly hand warmed, resuspended in 10 ml of pre-warmed DMEM medium (10% FBS), pelleted to remove residual amount of DMSO and resuspended in fresh growth medium and seeded on an appropriately sized cell culture dish.

2.2.2.1.4 siRNA transfection in HeLa, A549 cells

The day before transfection 1.3-1.5x10^5 cells were seeded in a volume of 4 ml per 6-cm-plate. For siRNAs transfection, the following components in every plate were mixed as the following table.

	25 nM final siRNA concentration	50 nM final siRNA concentration	100 nM final siRNA concentration
DMEM plain medium (Invitrogen, Cat. No. 41965-039)	100 µl	100 µl	100 µl

20 µM siRNA	5 µl	10 µl	20 µl
HiPerFect (Qiagen, Cat. No. 301704)	20 µl	20 µl	20 µl

The siRNAs used in this work are: control siRNAs= non_si_AF488 (Qiagen, Cat. No. 1022563), non target siRNA (Dharmacon, Cat. No. D-001810-01-05), scrambled siPC4, mouse scrambled siPC4; Target siRNA= siRNA-PC4-NL, siRNA-PC4-WR and siRNA-PC4-TK (all the target sequences were listed in table 7). All the siRNAs used in HeLa and A549 cells could yield 70-80% knockdown in protein level at the 25 nM. The components were mixed by vortexing and incubated for 10 minutes at room temperature to allow the formation of transfection complexes. The complexes were drop-wise added onto the cells. Then the plate was gently swirled to ensure uniform distribution of the transfection complexes. Transfection efficiency was monitored by using the non-silencing control siRNA from Qiagen “non_si_AF488” (25 nM final concentration on the plate) at 12-20 hours after transfection. Two days after transfection the cells were expanded if necessary. The cells were harvested by adding 4 ml of 0.5 mM EDTA/PBS (500 µl 0.5 M EDTA was added into 500 ml PBS, pH 8.0) to the plate and incubation for 20-30 minutes at room temperature. Then the cell solution was centrifuged (Eppendorf 5415R, 13000 rpm 4°C, 5 minutes), the supernatant was removed and the pellet was stored at -80°C for further analysis.

2.2.2.2 Culture of mouse embryonic fibroblasts (MEFs) and related methods

2.2.2.2.1 Preparation of MEFs

Timed matings of CD1-M-TKNEO^R mice (Stewart et al. 1987) (From RCC) (for neo resistant MEFs preparation) and the C3H mice (for wild-type MEFs preparation)were set up. At E13.5, the pregnant female was sacrificed and the uterus was taken out. Then the uterus was washed with sterile PBS to remove blood. The embryos were isolated from the placenta and yolk sac. The head, heart and fetal liver were removed from the embryos. The left white tissues from 2 embryos were transferred into one sterile Erlenmeyer beaker (containing a magnetic stirring bar and glass pearls) (diameter 2.85-3.3 mm, Roth Art, Cat. No. A557.1) with 10 ml 0.25% trypsin (Invitrogen, Cat. No. 25050-030). The beaker was incubated at 37°C for 15 minutes on a stirrer to disaggregate the tissue. The trypsinization was stopped by adding 10 ml of fibroblast medium, then centrifuged (Multifuge 3SR+, Heraeus, 1000 rpm, 5 minutes, room temperature). The cell pellet was resuspended in 20 ml fibroblast medium and

10 ml cell suspension was transferred in a 10-cm culture plate. When the plate was confluent, cells were expanded on a 15-cm plate. The passage of these cells was annotated as passage one. When the plate reached confluent, the MEFs were frozen down with freezing medium.

Fibroblast medium (for 600 ml):

DMEM high glucose (Invitrogen, Cat. No. 41965-039)	500 ml
Pen/Str/Glu (Invitrogen, Cat. No. 10378-016)	6 ml
MEM None Essential Amino Acids (100x) (Invitrogen, Cat. No.11140-068)	6 ml
FBS (Invitrogen, Cat. No. 10270106)	90 ml
2-Mercaptoethanol (Invitrogen, Cat No. 31350-010)	1.2 ml

Freezing medium for MEFs (for 10 ml):

Fibroblast medium	8 ml
FBS (Invitrogen, Cat No.10270106)	1 ml
DMSO (Sigma, Cat. No. D2650)	1 ml

2.2.2.2.2 Knocking down PC4 in MEFs with retroviral transduction

To knock down PC4 in MEFs, MEFs were generated from $PC4^{flox/-}$ embryos obtained by intercrossing $PC4^{+/-}$ and $PC4^{flox/+}$ mice. Then they were infected initially with ecotropic retroviruses. The ecotropic retroviruses were freshly prepared from HEK293T cells by cotransfecting pNL-4 (mock plasmid) or pNL-5 (Cre expression plasmid) together with pNL-6 (packaging protein expression plasmid) with the calcium phosphate or FuGENE 6 (Roche, Cat. No. 11814443001) reagent. The HEK293T cells were seeded such that 60% confluence was reached at 24 hours before transfection. Following the handbook of FuGENE 6 transfection reagent, HEK293T cells were cotransfected with above plasmids for producing retrovirus. After 48 hours, the retrovirus packed with target gene was produced into the culture medium. A 45 µm sterile filter was used to isolate the retrovirus from the culture medium supernatant. The filtered culture medium together with 5 µg/ml polybrene (Sigma, Cat. No. H9268) was used to infect MEFs ($PC4^{flox/-}$). The MEFs were already seeded at 1×10^5 cells per well in a six-well plate. MEFs were grown for 48 hours and then selected for 7 days by adding 2 µg/ml puromycin. Then the cells were harvested and total RNA and/or whole extract was prepared for later analysis.

2.2.2.2.3 Preparation of feeder cells from MEFs

MEFs were inactivated by mitomycin C treatment and ϒ-irradiated to provide a matrix for ES cell growth.

Mitomycin C treatment:

Confluent MEFs were treated with 10 µg/ml mitomycin C (Sigma, Cat. No. M0503) in DMEM plus 15% FBS culture medium for 2-3 hours at 37°C in an incubator at 5% CO_2. After that, the dishes were washed extensively with several changes of PBS. The cells were harvested by trypsinization and centrifugation (Multifuge 3SR+, Heraeus, 1000 rpm, 5 minutes, room temperature) and diluted into appropriate density. One confluent 15-cm plate of MEFs cells generated approximately the following numbers of feeder plates:

5x 10-cm plates (10 ml each)
10x 6-cm plates (5 ml each)
40x 3.5-cm plates (2 ml each)
18x 4-well plates or 3x 24 well plates (0.5 ml/well)
3x 96-well plates (0.2 ml/well)

ϒ-Irradiation treatment:

The confluent cells were exposed to 3,000-10,000 rads of ϒ-irradiation and then harvested by trypsinization and expanded into culture plates as above.

2.2.2.3 Culture of mouse embryonic stem (ES) cells and related methods

2.2.2.3.1 Embryonic stem cell culture (TBV2)

The TBV2 ES cell line was derived from a 129/Ola strain, created in the Institute of Experimental Genetics (IEG) of Helmholtz-Zentrum München. It was grown on Mitomycin C inactivated MEFs feeder cells with ES growth medium. Routinely cells were splitted every 2-3 days at a ratio of 1:3 with daily replenishment of the culture medium. ES colonies were washed twice with PBS and then treated shortly with 0.25 % trypsin (Invitrogen, Cat. No. 25050-030) at 37°C, until the cells were detached from the dish. The dissociated clones were used for splitting, transfection and freezing. During freezing, the cell pellets were resuspended into ES growth medium, then slowly added 2x freezing medium. All the ES cell vials should be transferred in liquid N_2 as soon as frozen.

TBV2 ES cell growth medium (for 600 ml):

DMEM (Invitrogen, Cat. No. 41966-029)	500 ml
FBS (PAA, Cat. No. 2602-p242901 Lot.P242901ES)	90 ml
Pen/Str/Glu (Invitrogen, Cat. No. 10378-016)	6 ml

MEM None Essential Amino Acids (100x) (Invitrogen, Cat. No.11140-068)	6 ml
2-mercaptoethanol (Invitrogen, Cat. No. 31350-010)	1.2 ml
LIF (CHEMICON, Cat. No. ESG1107,10^7 units/ml)	90 µl

2x freezing medium for TBV2 ES cells (for 10 ml):

ES cell growth medium	3 ml
FBS (PAA, Cat. No. 2602-p242901 Lot.P242901ES)	5 ml
DMSO (Sigma, Cat. No. D2650)	2 ml

2.2.2.3.2 Generation of ES cell lines containing PC4 conditional knockout allele

For the transfection of the PC4 targeting construct (refer to figure 13), an aliquot of TBV2 ES cells at the 10^{th} passage was thawed and plated on a 6-cm plate. Cells were passaged in total 2 times before collecting enough cells for the electroporation. For electroporation, $0.9x10^7$ cells in 0.8 ml PBS were transferred into one 2 mm cuvette, and 30 µg linearized target DNA or mock DNA was added. The electroporation conditions were 500 µF, 0.23 kV with a Gene Pulser II (Bio-Rad) electroporator. Transfected cells were resuspended in 10 ml TBV2 ES cell growth medium, 9 ml of which were distributed equally onto 3x 10-cm feeder (prepared with M-TK NEO^R MEFs) plates. The remaining 1 ml was resuspended in 10 ml growth medium and divided into 2x 10-cm plates, which were used as control plates. The leftover in the cuvette (about 10 µl) was also transferred into another 6-cm plate as controls. The non-transfected cells were also kept as control. Three days after transfection, cells were placed under G418 selection (Geneticin G-418 sulphate, 200 µg/ml, Invitrogen, Cat. No. 11811-023). Selection against HSV-tk containing random integrants started at day 4 after transfection by supplementing the medium with 0.5 µg/ml gancyclovir (Sigma, Cat. No. G2536). One of the control plates containing transfected cells was also treated as just described, while the other two (one with tranfected cells and one with non transfected cells) were under G418 selection only. The comparison of these last two control plates allowed monitoring of selection specificity. The ratio of double selected colonies versus G418 selected colonies was defined as Ganciclovir enrichment, i.e. the theoretical enrichment of homologous recombinant versus random integrants while using ganciclovir. Ganciclovir killed 30% of the colonies that would have undergone G418 selection. At 14 days after transfection, 312 double resistant colonies were picked, trypsinized in round-bottom 96-well plates with 45 µl cold 0.05% trypsin-EDTA (Invitrogen, Cat. No. 25300-096). The U-bottom 96-well was incubated in 37°C for 5 minutes then 150 µl ES growth medium was added and transferred into

another 96-well feeder plate. About 4 days later, the clones were big enough to be frozen down. After washing with PBS, the cells were trypsinized in 35 µl 0.25% trypsin (Invitrogen, Cat. No. 25050-030), and then 65 µl of pre-warmed ES medium was added to stop the reaction. 65 µl of the cell mixture were transferred into a new 96 well plate (without MEFs), and an equal volume of 2x freezing medium was added. Plates were quickly closed and sealed with parafilm and embedded in several layers of cellulose paper sheets and stored at -80°C. The remaining 35 µl cells were added to 150 µl growth medium in the original 96-well plate for DNA extraction. Once the Southern blot analysis was finished, the candidate ES cell clones were thawed from the frozen 96-well plates. The candidate ES cell clones were frozen in early passage and also some DNA extraction of these cells were kept to confirm the genotype. For blastocysts injection, the earlier passage candidate ES cell clones were thawed and plated in a 6-cm dish containing feeders, and 2 days later splitted 1:3 in order to be injected the following day. The injection process was carried out in IEG of Helmholtz-Zentrum München. A schematic view (Figure 8) of the steps followed from the electroporation of PC4 targeting construct to the end of the selection process is given below.

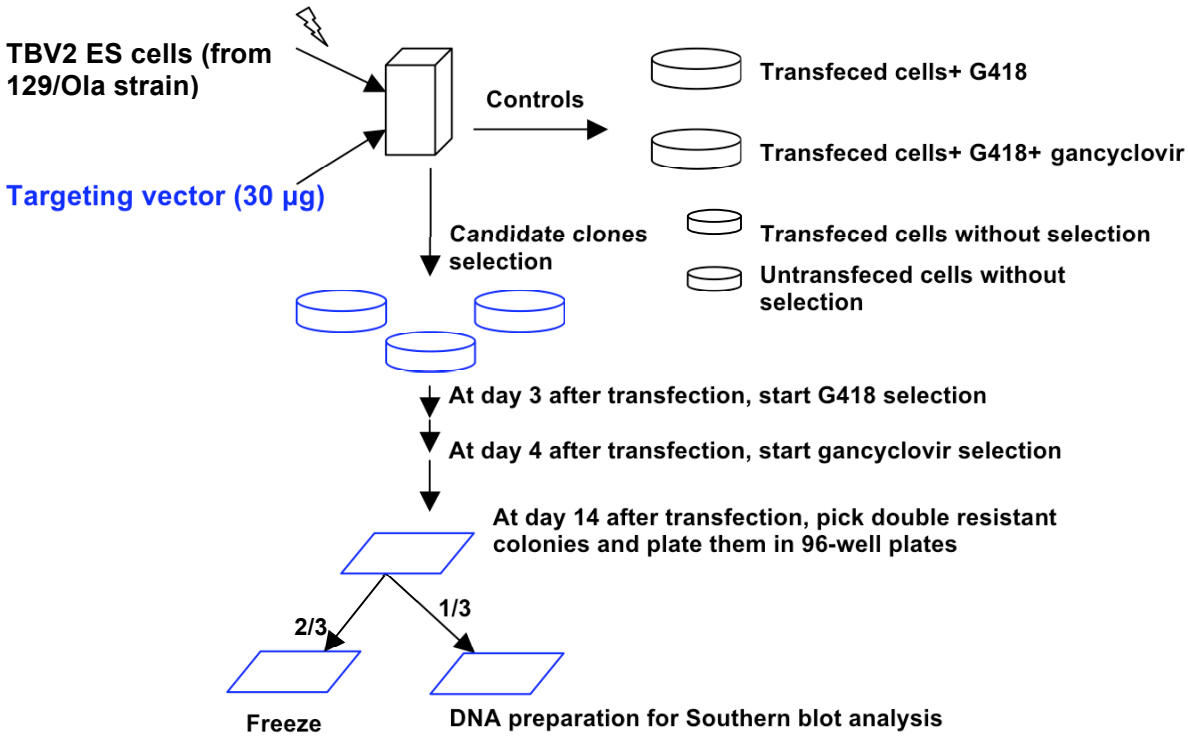

Figure 8: Scheme view of the generation of ES cell lines containing PC4 conditional alleles.

2.2.2.3.3 PC4 wild-type (WT) and knockout (KO) ES cells derivation from blastocysts

The E1.5 embryos from $PC4^{+/-}$ mice intercrosses were collected and cultured *in vitro* until E3.5. Zona pellucida was removed by pipetting up and down in Acid (Acid Tyrode's, Sigma, Cat. No. T1788), then the single blastocyst was transferred into a 48-well plate containing a monolayer of confluent mitomycin C-inactivated MEF feeder cells in ES growth medium. Blastocysts were allowed to attach to the MEF feeder layer, which usually takes 2 days. After attachment, medium was changed. About 6 days later, the inner cell mass was expanded to a ring-like morphology. The expanded blastocysts were washed with PBS, and 100 µl 0.25% trypsin (Invitrogen, Cat. No. 25050-030) were added to the well. After 15 seconds, the trypsin was aspirated. This procedure reduced stickiness of the cells and allowed easier detachment. To mechanically detach an expanded blastocyst and surrounding MEFs, a 20 µl pipette and 10 µl pipette tip were used. Under a microscope, 10 µl of 0.25% trypsin (Invitrogen, Cat. No. 25050-030) was added into the expanded clones and several circles with the pipette tip around the blastocyst were made to remove surrounding MEFs and separate the blastocyst (on the top of some MEFs) from the rest of the feeder layer. The clones were transferred into a drop of 10 µl 0.25% trypsin (Invitrogen, Cat. No. 25050-030). After 5 minutes trypsinization, the clones were dissociated into individual cells and small cell clumps by pipetting up and down approximately ten times with a 10 µl pipette tip. The cell suspension was transferred into a 48-well plate with feeders in ES cell medium. Several days after trypsinization, compact cell colonies with typical ES cell colony morphology were detected in some of the wells. The culture procedures of these ES cells were based on the standard method for TBV2 except the FBS was specific and MEFs were prepared from CH3 mice (none resistance for drug selection).

ES cell growth medium for PC4 WT and KO ES cells (for 600 ml):

DMEM low glucose (PAA, Cat. No. E15-005)	500 ml
FBS (Invitrogen, Cat. No.10270106, Lot 40G8251K)	90 ml
Pen/Str/Glu (Invitrogen, Cat. No.10378-016)	6 ml
MEM None Essential Amino Acids (100x) (Invitrogen, Cat. No. 11140-068)	6 ml
2-Mercaptoethanol (Invitrogen, Cat. No. 31350-010)	1.2 ml
LIF (bacterial recombination protein purified by ourselves) (added freshly)	600 µl

2x freezing medium for PC4 WT and KO ES cells (for 10 ml):

ES cell growth medium for PC4 WT and KO ES cells	6 ml
FBS (Invitrogen, Cat. No.10270106, Lot 40G8251K)	2 ml
DMSO (Sigma, Cat. No. D2650)	2 ml

2.2.2.3.4 Rescue of PC4 KO ES cells

In the rescue experiments, PC4 WT and KO ES cell lines were used, and *ApaI I* was used to linearize pWR12 and pWR23 for transfecting these cells. The electroporation conditions were 500 µF, 0.25 kV, in a 4 mm cuvette with gene Pulser II (Bio-Rad) electroporator. The cell number for one transfection was $4x10^6$, and the DNA amount for each transfection was about 20 µg. After electroporation, the transfected ES cells were transferred into a MEFs coated 10-cm plate for culturing. One day later, G418 was added to a final concentration of 300 µg/ml into the transfected and untransfected (control) ES cells for selecting resistant clones. After about 5 days selection, almost all untransfected cells were dead. Resistant ES cells were used for cell growth analysis. More specifically, the resistant ES cell colonies (green in fluorescent microscope) were picked with mouth glass pipette and transferred in a new culture dish. After trypsinization, the colonies were splitted into single cell suspension, and then equal number of cells were seeded in 6-well plates and counted every 24 hours till day 4.

2.2.2.3.5 Karyotyping of ES cells

Actively growing PC4 WT and KO ES cell lines (24 hours after 1:5 passage on feeder plates) were cultured in the presence of Nocodazol (3 µg/ml) for 4 hours, after removal of the MEFs by plating them on gelatin-coated (PBS/0.1% gelatin, Sigma, Cat. No. G1393) culture dish for a minimum of 5 minutes at 37°C. Then 50 ng/ml colcemid (Sigma, Cat. No. D7385) was added and cultured for another 2 hours. Chromosome spread of the cells for karyotyping analysis was obtained as follows. The cells were harvested by centrifugation (Multifuge 3SR+, Heraeus, 1000 rpm, 5 minutes, room temperature). The cell suspension was flicked by drop-wise adding 1 ml 0.56% (w/v) KCl. Another 3 ml 0.56% (w/v) KCl was slowly added to the cells. After 10 minutes incubation at 37°C in water bath, cells were pelleted by centrifugation (Multifuge 3SR+, Heraeus, 1000 rpm, 5 minutes, room temperature). The cells were fixed by adding FIX solution (3 volume methanol: 1 volume acetic acid) drop by drop while flicking the tubes. Then the cells were incubated at room temperature for 30 minutes, and pelleted by centrifugation (Multifuge 3SR+, Heraeus, 1000 rpm, 5 minutes, room temperature). The cells were resuspended in 4 ml FIX solution. This step was repeated before resuspending the cells in 200 µl FIX solution. The cell suspension was dropped onto a glass slide from a 10 cm distance. After the slides were air dried at room temperature, the slides were stained with DAPI solution and scanned with 40x objective for good

spreads. The chromosome spreads were analyzed on a microscope using 100x oil immersion objectives and 1000x magnification.

2.2.2.3.6 *In vitro* differentiation of embryonic stem cells

For *in vitro* differentiation, ES cells of PC4 WT and KO were feeder-depleted by being replated onto gelatin-coated dishes for 45 minutes. This step was repeated once more. Non-adherent cells were recovered and seeded onto bacterial grade (without adherence) dishes in ES cell growth medium in the absence of LIF for 4 days. After the formation of embryonic bodies (EBs), EBs were treated with 0.5 µM retinoic acid (RA) for 4 days in the bacterial grade dishes and reseeded onto new tissue culture dishes for 8-12 days. Differentiated ES cells were used for RNA isolation and RT-PCR (or qRT-PCR) analysis.

2.2.2.3.7 Cell cycle and apoptosis analysis with Flow Cytometer

Cell cycle analysis: PC4 WT and KO ES cells were resuspended in 1 ml PBS at a density of $3x10^6$/ml after feeder depletion. The single-cell suspensions were kept on ice until they were run on the flow cytometer. 900 µl DAPI (4,6-diamidino-2-phenylindole) solution (10 µg/ml DAPI and 0.1% Nonidet P-40 detergent in a Tris buffered saline) was added to 100 µl cell suspension for staining. The tube was mixed thoroughly for cell cycle analysis with Flow Cytometer (Partec Cyflow^R space).
Apoptosis analysis: ES cells were collected as above, and washed twice with PBS. $5x10^5$ cells were resuspended in 100 µl of 1x Annexin V Binding Buffer (BD Pharmingen™, Component No. 51-66121E) with 2 µl FITC Annexin V (BD Pharmingen™, Component No. 51-65874X) and 2 µl Propidium Iodide (PI) (BD Pharmingen™, Component No. 51-66211E). The cells were gently vortexed and incubated for 15 minutes at room temperature in the dark. 400 µl of 1x Annexin V Binding Buffer was added to each tube and analyzed by flow cytometry within 1 hour.

2.2.3 Mouse experiments

2.2.3.1 Mouse keeping

Mice were kept in the mouse facilities of Helmholtz-Zentrum München. Chimeras generated after blastocyst injection of PC4 homologous recombinant ES cells were mated with C57BL/6J wild-type mice in order to produce germ-line transmitted offspring. The F1 generation was mated with Cre deleter mice (C57BL/6J background)

for generating the PC4$^{+/-}$ mouse strain. The mouse strain PC4$^{+/-}$ was back-crossed to wild-type C57BL/6J mice for maintenance and further analysis.

2.2.3.2 Dissection of E7.5 to E9.5 mouse embryos

Timed matings between PC4$^{+/-}$ mice were set up. The day of the plug corresponds to day 0.5 of embryonic development. At the day of dissection, the female was sacrificed by cervical dislocation. The reproductive organs were dissected and the uterus containing the mouse embryos were removed and put in ice-cold PBS. The embryos including the placenta were released by rupture of the uterus muscle with two forceps. Between E6.5-9.5, the embryos are fully surrounded by the deciduas. At E7.5 the deciduas containing the embryos are pear-shaped. In order to reveal the small embryos, the deciduas were dissected by holding them at their broader end with a watchmaker #5 forceps using a dissection microscope. The embryos were shelled out by piercing the deciduas at the very tip of the “pear” and by pushing carefully to the direction of the holding forceps. After the embryos were released, the ectoplacental tissue and red blood cells was carefully removed with forceps and the embryos were transferred with a plastic Pasteur pipette. At E8.5 and E9.5, the deciduas are still fully surrounding the mouse embryo. After the decidua was carefully removed, the embryo was prepared by rupture and removal of the yolk sac membrane. The yolk sac was collected for genotyping.

2.2.3.3 Histological analysis of early embryos

Timed matings were conducted with interbreeding between PC4$^{+/-}$ mice. Females with copulation plugs were considered to be at embryonic development day 0.5 (E0.5) of gestation. Deciduas were isolated in ice-cold PBS at E5.5, E6.5, and E7.5, fixed overnight in 4% (w/v) paraformaldehyde (PFA) buffered with PBS overnight at 4°C. After rinsing three times with PBS, the fixed deciduas were incubated with 10% (w/v) sucrose buffered with PBS for 6 hours at 4°C, then with 25% (w/v) sucrose overnight at 4°C and washed with PBS. The deciduas were then dehydrated in an ethanol series (70%-95%-100% EtOH) and imbedded in paraffin for sagittal sections. Paraffin blocks were trimmed and serially sectioned at 5-7 µm. All the tissue sections were collected and fully extended on a SuperFrost/Plus slide (Fisher Scientific, Cat. No. 1255015). The slides were kept in an oven overnight at 40°C. At the following day, all the embryo sections were deparaffinized with Xylene (2 times 5 minutes each) and rehydrated in an ethanol series (100%-95%-80% EtOH). Then the sections were immerged in tap

water for 4 minutes, before they were stained with hematoxylin (Sigma, Cat. No. GHS216) for 3 minutes. After rinsing with tap water for 4 minutes, the slides were submerged into 70% EtOH (v/v) for 4 minutes and rinsed with water. After that, the slides were microscopically inspected. One slide for each embryo was kept for mechanically isolating embryonic tissues out of deciduas to achieve its genotype with PCR strategy. The remaining slides were stained with eosin solution (Sigma, Cat. No. HT110116) for 1 minute, and dehydrated from 95% (v/v) EtOH to 100% EtOH. Finally, the slides were immerged in Xylene for 15 minutes, then covered with coverslips using Permount mounting medium (Fisher Scientific, Cat. No. SP15-500) for microscopic evaluation.

2.2.3.4 Superovulation

Since large numbers of oocytes and preimplantation embryos are required for early phenotype analysis and ES cell derivation, gonadotropins were administered to females prior to mating for inducing superovulation. The efficient induction of superovulation in mice depends on age and weight of female mice, dose of gonadotropins, and time of administration. For C57BL/6J strain, it was empirically determined that 8 to 10-week-old females produced sufficient amounts of preimplantation embryos for subsequent analysis. Light cycle in mouse house of Muenster is 6 a.m. to 6 p.m., so 10 IU PMSG (pregnant mare serum gonadotropin, Calbiochem, Cat. No. 367222) was administered intraperitoneally between 4 to 5p.m. Then, 48 hours later, 10 IU hCG (human chorionic gonadotropin, Calbiochem, Cat. No. 230734) was administered intraperitoneally to the females, and then females were mated with males.

2.2.3.5 Collection of morulas and blastocysts

Morulas (E2.5) and blastocysts (E3.5) were located in the uterus of pregnant female mice. After superovulation, the pregnant mice were killed and the uterus was taken out for collecting embryos. All the isolated uteri were rinsed 2-3 times before flushed. Then the uterus was cut across the cervix, and ovary was removed. In a plastic tissue culture dish, a 30-guage needle was inserted into the base of each horn to flush with 0.5 ml M2 medium (Sigma, Cat. No. M7167) with 4 mg/ml BSA (Sigma, Cat. No. A3311). Because there may be some morulas left in oviduct, the oviduct was isolated and smashed to release all the embryos. The embryos were picked up and rinsed through several drops of fresh M2 medium containing 4 mg/ml BSA, then analyzed.

2.2.3.6 Immunofluorescence staining of morulas and blastocysts

Morulas (E2.5) and blastocysts (E3.5) were isolated from C56BL/6 female mice, which were mated with C56BL/6 male mice. The embryos were fixed in 1.3% PFA in 0.5x PBS (1:2 dilution of PBS with distilled water), incubated at room temperature for one hour, and transferred into a 4-well plate in PVP/PBS (1 mg/ml PVP40 in PBS) buffer at 4°C. After permeabilized with 0.5% Triton X-100 in PVP/PBS buffer for one hour at room temperature and washed two times with PVP/PBS, the embryos were ready for immunostaining. Incubation with the primary antibody (polyclonal rabbit-anti-PC4, 1:400 dilution was used for the immunostaining) was carried out in 100 µl PVP/PBS for one hour at 37°C in a humid dark chamber. To control the primary antibody specify, incubation with PBS (negative control) was included. After this, the embryos were washed with at least 3 times for 10 minutes each in PVP/PBS. Incubation with the secondary antibody (Goat-anti-Rabbit-Cy3 IgG) (Dianova, Jackson immnuoresearch Europe ltd, Cat. No. 111-165-144) conjugated to the fluorescent dye was performed as above except the incubation time was only 30 minutes. After washed with PVP/PBS for 3 times, the embryos were mounted with Vectashield mounting medium (Vector Laboratories, Cat. No. H1200) on 76x26 mm cover glass. The analysis of the embryos was carried out with a confocal microscope (Zeiss).

2.2.3.7 E1.5 embryos isolation from $PC4^{+/-}$ mice intercrosses for *in vitro* culture

Superovulated female $PC4^{+/-}$ mice were mated with male $PC4^{+/-}$ mice. At E1.5, the oviducts without ovary and fat were isolated from the female mice. Then all the oviducts were transferred into M2 medium (Sigma, Cat. No. M7167) in a 35-mm Petri dish covered with mineral oil (Sigma, Cat. No. M5310). The oviducts were flushed with M2 medium by thin glass pipettes. The embryos were collected and washed through several drops of fresh M2 medium to rinse off the debris. The embryos were transferred into a microdrop of KSOM medium in the culture dish, which was equilibrated for at least 2 hours in an incubator. The embryos were cultured *in vitro* until E2.5 for deriving ES cells.

KSOM medium:

EDTA (disodium salt)	0.01 mM
NaCl	95 mM
KCl	2.5 mM
$CaCl_2$	1.71 mM
KH_2PO_4	0.35 mM
MgSO4	0.2 mM

Na lactate (Sigma, Cat. No. L7900)	10 mM
Na pyruvate (Sigma, Cat. No. P4562)	0.2 mM
Glucose (MP Biomedicals, Cat. No. 194672)	0.2 mM
Phenol red (0.5%, Sigma, Cat. No.P0290)	100 µl/L
$NaHCO_3$ (MP Biomedicals, Cat. No.194553)	25 mM
MEM EAA (50x, Invitrogen, Cat. No.11130-077)	1x
MEM NEAA (100x, Invitrogen, Cat. No.11140-068)	1x
Pen/Strep/Glu (100x, Invitrogen, Cat. No.10378-016)	1x
BSA (sigma, Cat. No. A3311)	1 mg/ml

2.2.3.8 *In vitro* fertilization of mouse oocytes and immunofluorescence staining

To determine the localization of PC4 in zygote stage, *in vitro* fertilization was performed with wild-type mice. F1 generation mice (obtained from matings of C57BL/6J with CBA wild-type mice) were used as sperm and oocytes donors. Mature oocytes were collected 14 hours post human chorionic gonadotropin injection as outlined in 2.2.3.4. Sperm isolation and *in vitro* fertilization (IVF) procedures were performed as following. In briefly, the sperm was isolated from cauda epididimus of donor males and capacitated in pre-gassed HTF buffer for 1.5 hours. Isolated oocytes in cumulus cell mass were placed into 100 µl drop of HTF buffer with capacitated sperm and incubated in CO_2 incubator for 3, 5, or 8 hours. For longer incubation time the oocytes were incubated with sperm in HTF medium for 8 hours and then transferred into the drop of pre-gasses and pre-warmed M16 medium (Sigma, Cat. No. M7292) and incubated further for 2, 4 or 10 hours. After the removal of zona pellucida by treatment with Acidic Tyrode's solution, fertilized oocytes were fixed for 20 minutes in 3.7% (w/v) PFA in PBS, and permeabilized with 0.2% (v/v) Triton X-100 in PBS for 10 minutes at room temperature. The fixed zygotes were blocked overnight at 4°C in 1% (w/v) BSA (Equitech-Bio, Cat. No. BAC62-0050) and 0.1% (v/v) Triton X-100 in PBS. After blocking, the embryos were incubated in the same solution with anti-PC4 rabbit polyclonal antibody at room temperature for 1 hour, followed by several washes and incubation for 1 hour with anti-rabbit secondary antibodies coupled with Rhodamine Red-X (Jackson ImmunoResearch Laboratories Inc.). Then, after washing, the zygotes were placed on slides and mounted with a small drop of Vectashield mounting medium (Vector Laboratories, Cat. No. H1200). At least 20 zygotes were analyzed. The slides were analyzed on Zeiss Axiovert 200 M inverted microscope equipped with the fluorescence module and B/W digital camera for imaging. The images were captured, pseudocoloured and merged using AxioVision software (Zeiss).

HTF buffer:

NaCl (Sigma, Cat. No. S-5886)	101.6 mM
KCl (Sigma, Cat. No. P-5405)	4.69 mM
$MgSO4 \cdot 7H_2O$ (Sigma, Cat. No. M-1880)	0.2 mM
KH_2PO4 (Sigma, Cat. No. P5655)	0.37 mM
$CaCl_2$ (Sigma, Cat. No. C-7902)	2.04 mM
$NaHCO_3$ (Sigma, Cat. No. S-5761)	25 mM
Glucose (Sigma, Cat. No. G-6152)	2.78 mM
Na-pyruvate (Sigma, Cat. No. P-4562)	0.33 mM
Na-lactate (Sigma, Cat. No. L-1375)	21.4 mM
Penicillin (Sigma, Cat. No. P-7794)	0.075 g/L
Streptomycin (Sigma, Cat. No. S-9137)	0.05 g/L
Phenolred (1%) (Sigma, Cat. No. P-0290)	0.2 ml/L
BSA (Equitech-Bio, Cat. No. BAC62-0050)	4 mg/ml

The buffer was gassed for 5 minutes with 5% CO_2, 5% O_2 balanced with N_2 before supplementing it with BSA. Medium was stored at 4°C for no longer than 2 weeks, and regassed before used.

2.2.4 Biochemistry

2.2.4.1 Sodium dodecyl sulphate polyacrylamide gel electrophoresis (SDS-PAGE)

Proteins were separated on a SDS-PAGE gel using the mini-gel system from Bio-Rad. Depending of the size of the protein, 12-15% 170:1 acrylamide/bisacrylamide gels were used. For electrophoresis, proteins were mixed 1:6 with 6x loading buffer, heat denatured at 95°C and loaded onto the gel. Proteins were separated applying a current of 25 mA for the mini-gels and the running buffer was 1x TGS. For molecular weight determination, prestained marker (Bio-Rad, Cat. No. 161-0375) was run in parallel. Following electrophoresis, proteins were subjected to Western blotting.

Components for different percentages of SDS-PAGE:

	12%	15%	stacking gel
GelA (Roth, Cat. No. 3037.1)	4 ml	5 ml	1.7 ml
GelB (Roth, Cat. No. 3039.1)	0.35 ml	0.44 ml	0.7 ml
1.5 M Tris/HCl (pH 8.8)	2.5 ml	2.5 ml	
1 M Tris/HCl (pH 6.8)			1.25 ml
H_2O	3 ml	2 ml	6.2 ml
10% SDS	0.1 ml	0.1 ml	0.1 ml
30% APS	23 µl	23 µl	35 µl
TEMED	6 µl	6 µl	6 µl

2.2.4.2 Whole-cell extracts preparation

For cell pellets: Cell pellets were resuspended in 200-300 µl of 0.2% NP-40 lysis buffer, and incubated on ice for 5 minutes. Then, three to five freeze-thaw cycles were performed to complete lysis. Debris was removed by centrifugation (Eppendorf 5415R, 13000 rpm, 4°C, 10 minutes). The supernatant were stored at -80°C.

0.2% NP40 lysis buffer:
50 mM Tris/HCl, pH 8.0
150 mM NaCl
0.2% (v/v) NP40
1 mM EDTA, pH 8.0
Prior to use, add protease inhibitors to a final concentration of
2 µg/ml Leupeptin
2 µg/ml Aprotinin
2 µg/ml Pepstatin
1 mM PMSF

For organs: A piece of organ was homogenized in 0.1% (w/v) NP-40, 150 mM NaCl, 50 mM Tris (pH 7.5), 1mM EDTA, 1mM DTT with complete protease inhibitors (Roche, Cat. No. 1697498001) by electronic homogenizer. Then the tube was incubated on ice for 30 minutes. Insoluble material was removed by centrifugation (Eppendorf 5415R, 13000 rpm, 4°C, 10 minutes). Equal protein content was used for SDS-PAGE and Western blot analysis.

Measurement of protein concentration: Total protein concentration was determined using the Bradford assay (Bio-Rad protein assay) by detecting absorbance at 595 nm. A standard curve was made using serial dilution of BSA (100-250-500-750-1000 µg/ml) and protein concentration of the sample was calculated according to the standard curve.

2.2.4.3 Western blot

Proteins separated by SDS-PAGE were transferred to a PVDF membrane (Bio-Rad, Cat. No. 162-0177) using a Semi-Dry Transfer Cell (Bio-Rad, Trans-Blot^R SD), paper soaked in 1x transfer buffer and run for 50 minutes at 15 V (mini-gels). After transfer, the membrane was shortly stained with a Ponceau S solution to make the transferred marker visible. The membrane was then incubated for 1-12 hours in 1x TBS containing 5% (w/v) milk powder to reduce unspecific background binding. After blocking, the membrane was incubated for 1-12 hours with appropriate dilutions of the primary antibodies in 1x TBST containing 1% milk powder. To remove excess antibody, the membrane was washed 3 times for 15 minutes with TBST. Secondary antibodies (1:10,000 dilution) were applied for 1 hour in TBST containing 1% (w/v) milk powder and after 3 times washes in 1x TBST 15 minutes each and a final rinse in dH_2O, the antibodies were detected using the enhanced chemiluminescence detection system (Western Lightning, Perkin Elmer, Cat. No. NEL105) according to the manufacturer's instructions and exposed on BioMax MR Film (Kodak, Cat. No. 8736936).

3. RESULTS

3.1 PC4 knockdown in HeLa and A549 cells

In order to validate the physiological function of PC4, messenger RNA was knocked down by RNA interference in HeLa and A549 cells. We used several PC4-specific siRNAs, which are named as following: siRNA-PC4-NL (target sense in human PC4 cDNA is 177-197) (Figure 9), siRNA-PC4-TK [(target sense in human PC4 cDNA is 213-233, taken from (Das et al. 2006) (Figure 9)], siRNA-PC4-WR (target sense in human PC4 cDNA is 292-311) (Figure 9) and several non-sequence-specific control siRNAs which are named as following: non-targeting siRNA (from Dharmacon), scrambled siRNA (target sequence was listed in the table 7)and FITC-conjugated negative control siRNA AF488 (non_si_AF488, Qiagen). The efficiency of PC4 mRNA knockdown was usually 80% in A549 and HeLa cells. This is exemplified in Western blot analysis for siRNA-PC4-NL and siRNA-PC4-TK in A549 (Figure 10A left panel) and in HeLa cells (Figure 10B left panel) at day3 and day5 after transfection.

Cell proliferation rates were measured by counting viable cells at different time points after PC4 knockdown. As shown in Figure 10A (right panel), A549 cells proliferated normally upon application of non-targeting siRNA, scrambled siPC4. But sequence-specific siRNA-PC4-NL and siRNA-PC4-TK performed differently in these two cell lines. Only siRNA-PC4-TK reduced proliferation of A549 cells, whereas none of the siRNA had an effect on cell growth of HeLa cells. Lack of inhibition of proliferation was evident from further independent PC4-specific siRNA pool (Dharmacon). The siRNA pool knocked down PC4 significantly but did not interfere with cell proliferation (by Sanghamitra Singhal and Thomas Albert, unpublished data). Hence, reduced proliferation of A549 cells upon knocking down PC4 is most likely due to the off-target effects of the siRNA-PC4-TK, which contains repeated sequence (CAG) (Figure 9).

Another PC4-specific siRNA (siRNA-PC4-WR) (Figure 9) was tested in comparison with two other control siRNAs: non_si_AF488 and mouse scrambled siPC4 in HeLa cells. The knockdown efficiency of siRNA-PC4-WR and siRNA-PC4-NL were similar (Figure 10C, left panel) without effect on cell proliferation.

To investigate the effect of PC4 knockdown on global gene expression, we carried out gene profiling analysis with microarrays (Affymetrix GeneChip ‘Human Genome U133 Plus 2.0 Array’). A mixture PC4-specific siRNAs (siRNA-PC4-NL and WR) transfected cells was used and a mouse scrambled siPC4 served as control. The effects on

endogenous PC4 levels were tested in Western blots. As shown in Figure 10C, about 15% of PC4 was found after knockdown in HeLa cells. From four best-quality arrays, we identified 110 up-regulated genes and 12 down-regulated genes (more than 2 fold changes were considered and listed in table 9-10 in appendix) in response to the PC4 knockdown. Compared with previously published genes identified from microarrays in HeLa cells (Das et al. 2006), only two common genes were found: *RTRF* and *DSG2*. Taken together, all these results suggest that PC4 is not essential for human tumor cells or the residual levels of PC4 persisting after transient knockdown maintain the normal growth of tumor cells. To circumvent this difficulty, a knockout approach was proposed.

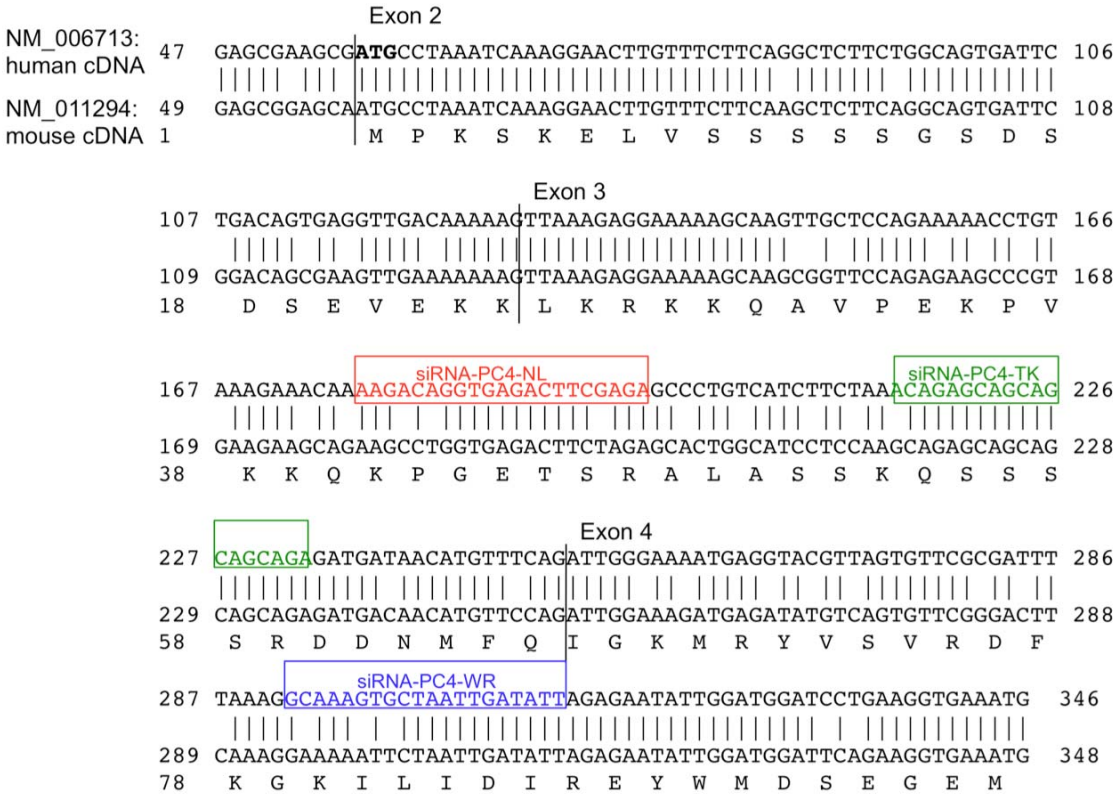

Figure 9: Target sequences of different siRNAs specific for PC4 mRNA in human cells.

Different target sequences of diverse siRNAs are indicated in different colored boxes in the alignment of human and mouse PC4 cDNA sequences.

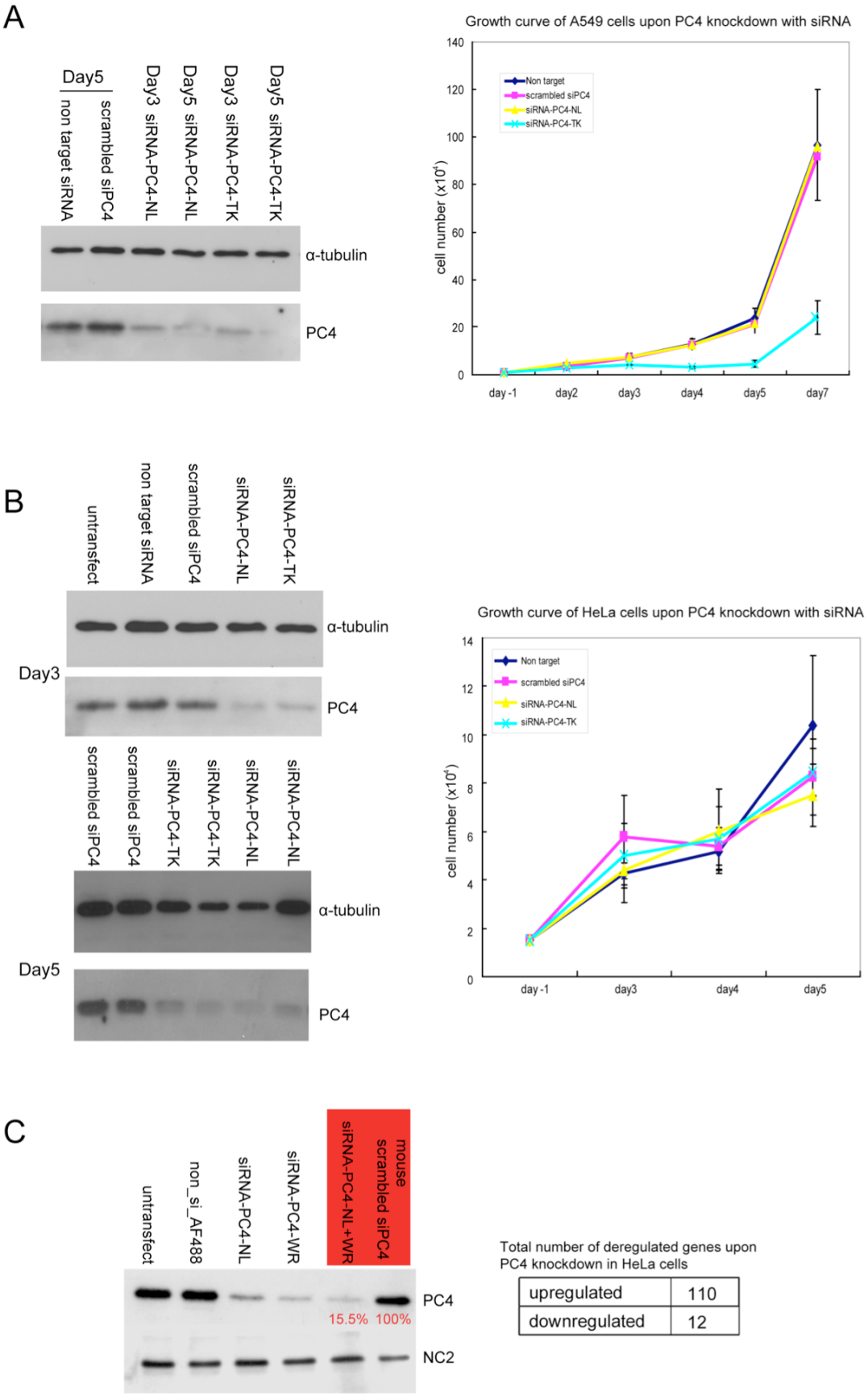

Figure 10: Effect of PC4 knockdown in A549 and HeLa cells.

(A) Western blot analysis of endogenous PC4 protein levels in A549 cells after siRNA transfection (left panel). Knocking down PC4 did not decrease A549 cell proliferation (right

panel). α-tubulin was used as a loading control. The numbers of cells were counted at different time points. Day1: cells were seeded, days 2, 3, 4, 5, and 7: days after transfection of siRNA. (B) Western blot analysis of endogenous PC4 protein levels in HeLa cells after siRNA transfection at different time points (left panel). Knocking down PC4 did not decrease HeLa cell proliferation (right panel). Cells were counted as shown in (A). (C) Microarray analysis of gene expression upon PC4 knockdown by siRNA. Western blot analysis of endogenous PC4 protein levels in siRNA-transfected HeLa cells used for microarray analysis (left panel). The samples shown in red were those analyzed by microarrays. NC2 was used as a loading control. The number of deregulated genes in response to PC4 knockdown is listed in a table (right panel). Only those genes whose expressions were more than double or less than half of control levels were considered.

3.2 Generation of PC4 conditional knockout mice

3.2.1 Organization of PC4 genomic locus

The murine PC4 gene consists of 5 exons on chromosome 15 encoding 127 amino acids (aa). The N-terminal part of PC4 contains a SEAC motif, which is encoded by exon 2 and exon 3. Exon 3 also encodes the lysine-rich motif (aa 23-41). The evolutionary conserved C-terminal domain (CTD) for ssDNA binding is encoded by exon 4 and exon 5 (aa 66-101). A schematic summary of the PC4 gene structure is shown in Figure 13A. PC4 is widely expressed in different tissues and cell lines in mouse and human as shown by northern blots (Figure 11, from Dr. Wera Roth).

3.2.2 Generation of constitutive knockout mice for PC4

To characterize the *in vivo* function of PC4, a loss-of-function study was carried out using a knockout mouse approach. Given that PC4 homolog (SUB1) in yeast was non-essential, we initially chose to eliminate gene in a non-conditional manner. A constitutive knockout mutant of PC4 was first generated by Gertraud Stelzer in our lab. A region comprising intron 3 to exon 5 was deleted which resulted in mice with a null allele (Figure 12A). After homologous recombination (Figure 12B), positive ES cells were injected into blastocysts to obtain chimeric mice. A single heterozygous mouse colony was established. These mice were viable and fertile. In contrast, live offspring lacking both PC4 alleles were never obtained (Figure 12C).

Examination of the embryos at different developmental stages suggested that homozygous embryos died at the preimplantation stage, as knockout blastocysts were obtained at a ratio far lower than that expected according to Mendelian inheritance (Figure 12C). Because the analysis of preimplantation stage embryos was difficult and without suitably established techniques at the time, further the analysis of this classical PC4 knockout was not pursued in the lab.

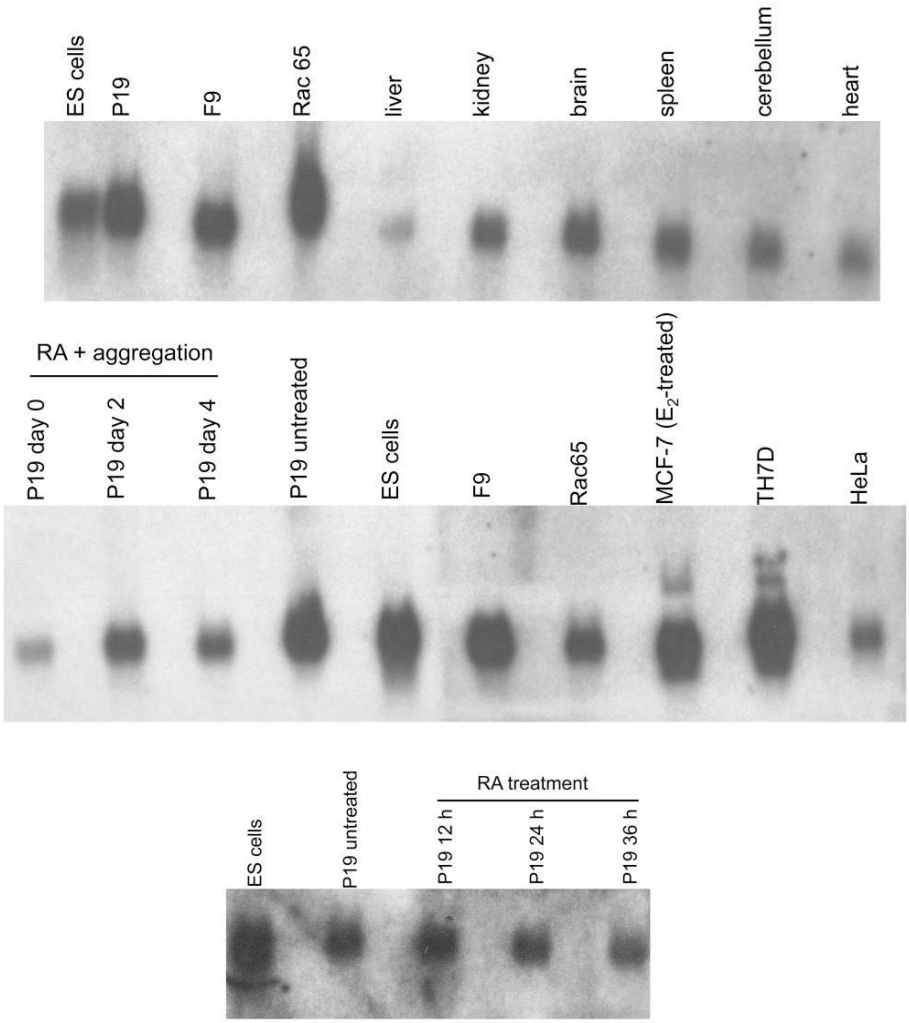

Figure 11: Northern blot analysis of PC4 in different mouse tissues and cell lines.
Total RNAs (30 µg) were isolated from mouse organs and different cell lines, and then analyzed by northern blotting using ^{32}P-labeled human PC4-cDNA. MCF-7 and TH7D: human breast adenocarcinoma cell line; P19: pluripotent murine embryonic carcinoma cell line; RA: retinoic acid, induces ES cell differentiation; Rac65: P19 EC-derived mutant cell line resistant to the differentiation-inducing activity of RA; F9: mouse embryonic carcinoma cell line; E_2: estradiol, induces MCF-7 proliferation.

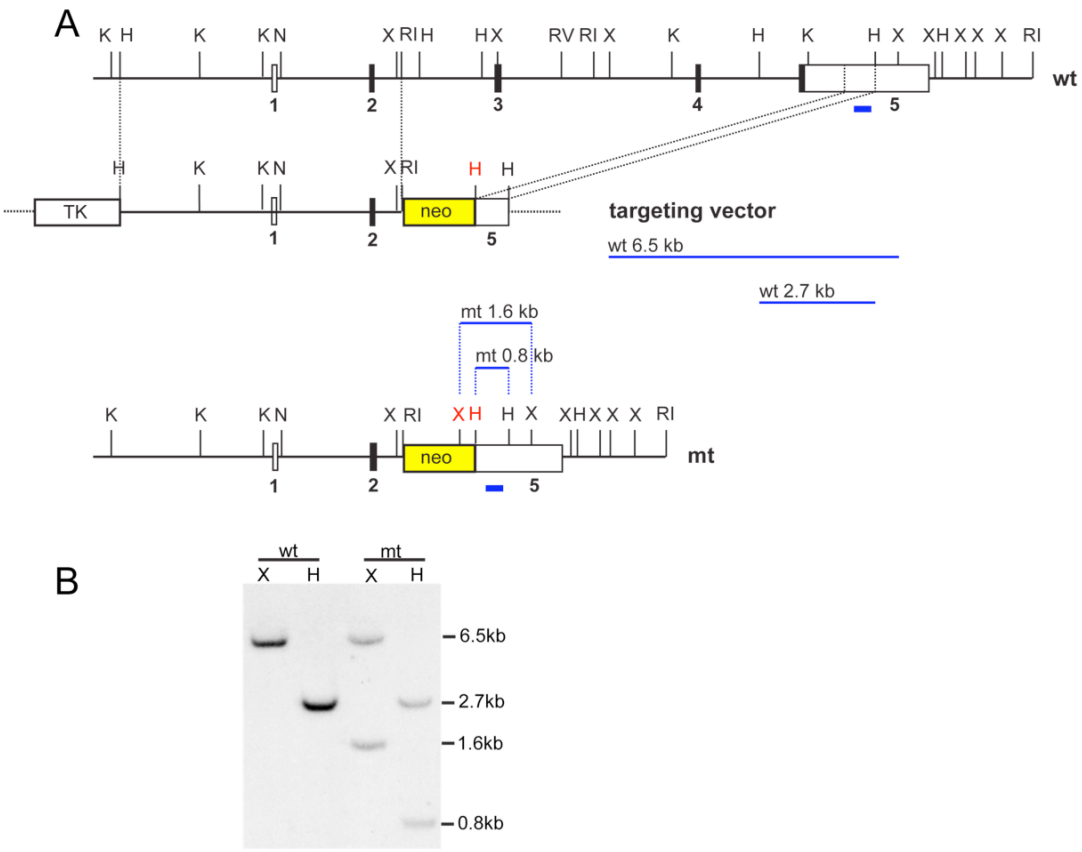

C

Genotype analysis of embryos derived from PC4 constitutive knockout mice crosses

No. with genotype		+/+	+ / -	- / -
weaning	71	19	52	0
E7.5	15	4	11	0
E8.5	14	4	10	0
E3.5	77	15	58	4

Figure 12: Constitutive gene knockout of PC4 (performed by Gertraud Stelzer).
(A) Genomic targeting of PC4 null allele. Exons 3 to 5 of PC4 were replaced by the neo-resistance cassette, which was flanked by two homologous arms for ES homologous recombination. (B) Southern blot analysis for identification of homologously recombined ES clones. (C) Summary of different embryonic stages for homologous null PC4 mice.

3.2.3 Conditional knockout of the PC4 gene

We used a conditional knockout approach to circumvent early embryonic lethality. In this approach, exon 4, which encodes the PC4-CTD, was flanked with two loxP sites. Deletion of exon4 eliminates all known functions of PC4 and abrogates binding to both dsDNA and ssDNA. Because the PC4-CTD is essential for ssDNA binding as well as

for the cofactor function of PC4, a loss-of-function allele was expected when Cre recombinase was present. A neo cassette flanked by two Flippase Recognition Target (FRT) sites was introduced into intron 4 (Figure 13A). As a consequence, the neo cassette can be removed from the mutant allele via recombination with FLP recombinase before conducting the Cre-mediated deletion of exon 4 in a tissue or cell lineage of interest.

3.2.4 Homologous recombination (HR) in ES cells

Double-selected TBV2 ES cell clones were analyzed in Southern blot to identify ES cell clones with that underwent distinct homologous recombination. To distinguish wild-type and mutant alleles 3 probes were used for the screening (Figure 13A). Probe A and probe B, which targeted upstream and downstream of the mutant allele, respectively, were used to distinguish homologous recombination from the random integration. Probe C was used to check the presence of the single loxP site so as to exclude cells with the mutation during recombination.

Restriction enzymes were selected in a manner that allowed to generate specific mutant and wild-type genomic patterns on Southern blots. For example, the digestion of the target vector with *Kpn*I and hybridization against probe A yielded a 7.8 kb fragment in the mutated allele versus a 9.2 kb fragment in the wild-type allele. The *Xba*l digestion yielded a 4.3 kb fragment using probe B in the mutant allele and a 6.5 kb fragment in the wild-type allele. An *Eco*RV digestion site was inserted between the loxP sites in the targeting allele. As a consequence, a 4.8 kb fragment in the mutant and a 10.5 kb fragment in the wild-type allele were detected with probe C.

Among 312 ES cell clones that survived antibiotics selection and were picked, 179 were successfully screened by Southern blot, and four clones were positive for homologous recombination on all events. These candidate clones were expanded and again confirmed by Southern blot. An example for screening of homologous recombination (HR) is shown in Figure 13B.

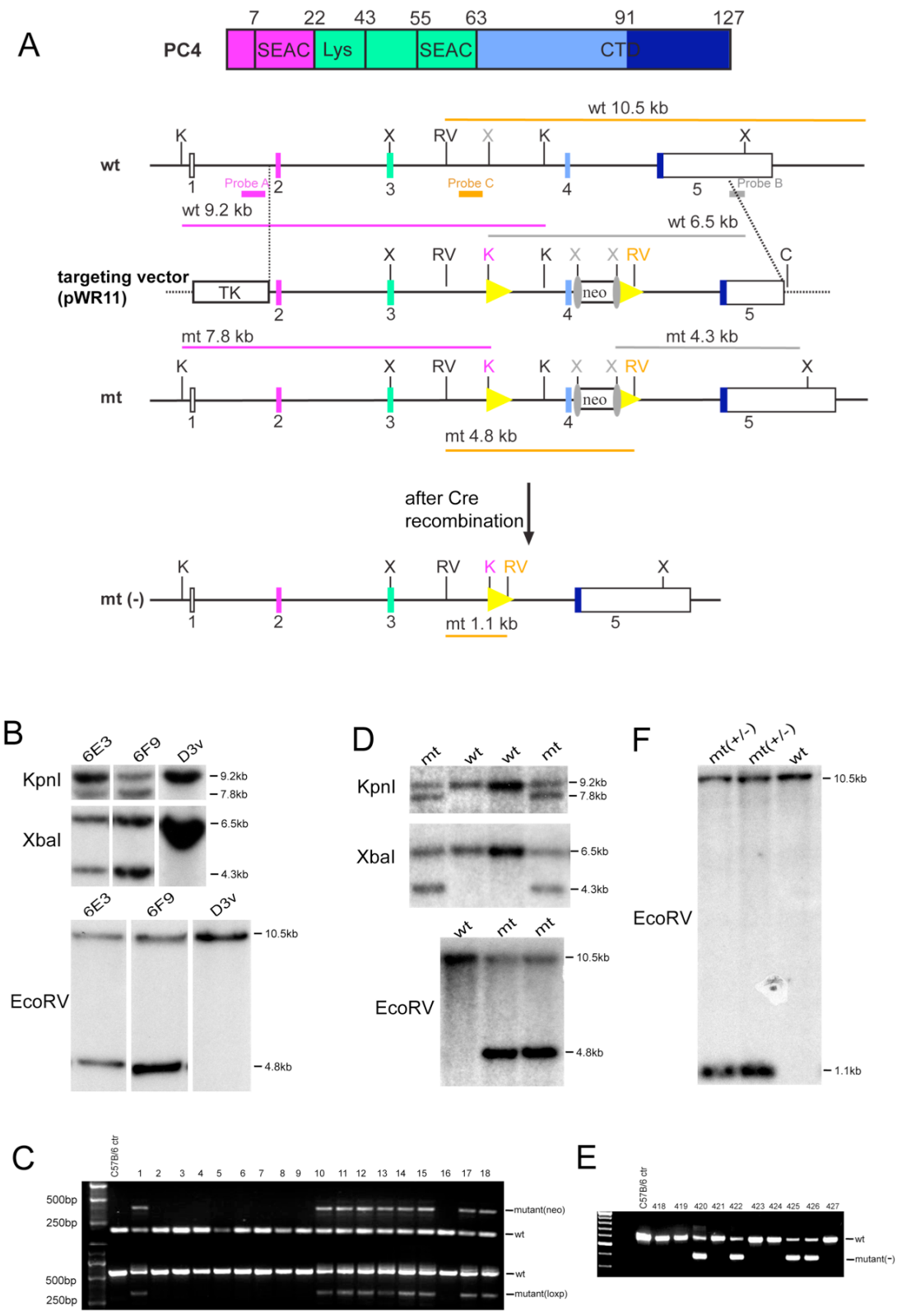

Figure 13: Construction of knockout mice and confirmation of targeting event.
(A) Organization of PC4 domains. Genomic regions encoding various domains of the protein are represented with different colors. Homologous recombination results in the insertion of the targeting vector, which included an FRT-flanked neomycin cassette (Neo) and exon 4 flanked by loxP sites. *Kpn*I, *Xba*I, and *Eco*RV: enzymes used for Southern blot analysis. *Cla*I was used

for linearization. The yellow arrows indicate the loxP sites. The mt (-) allele shows the genomic organization after exon 4 deletion by Cre-recombinase. The upstream (probe A) and downstream (probe B) probes used for Southern analysis are indicated in red and grey, respectively. The internal probe C, is indicated in orange. (B) Southern blot analysis of genomic DNA from double-selected clones (6E3, 6F9) after digestion with *Kpn*I, *Xba*I, *Eco*RV and hybridization with the probe A, probe B, and probe C, respectively. These fragments distinguish between the targeted event and the wild-type allele. (C) PCR genotyping of F1 generation. Upper panel checks the existence of the neo cassette (primer used: oWR77, oWR78, oWR79, see method section 2.2.1.3), and lower panel checks whether the single loxP side is inserted upstream of exon 4 (primer used: oWR80, oWR81, oWR83, see methods section 2.2.1.3). Both methods yielded the same results. Numbers from 1-18 in the figure indicate the mouse identification number. (D) Southern blot analysis of tail genomic DNA from the F1 generation to confirm the genotype. (E) PCR genotyping for heterozygous mice (+/-) (primers used: oWR79, oWR83, oWR81, see methods section 2.2.1.3). Numbers from 418-427 indicate the mouse identification number. (F) Southern blot analysis of heterozygous mouse (+/-).

Figure 14: Chimerism percentage for PC4 conditional knockout chimeras.
The three photos on the left show three male chimeras and the three photos on the right show the pairs of corresponding chimera and C57BL/6J female mice. Mouse ET42_6E3 exhibited germ line transmission. Mouse ET44_6F9 and ET49_6F9 were sterile. ET42, ET44, ET49 in indicate the chimeras' identification numbers. 6F3 and 6F9 indicate the homologous recombination ES cell clones used for microinjection. The percentage in each picture represents the estimated chimerism judged by fur color.

3.2.5 Heterozygous PC4 knockout mice

Three out of four positive ES HR clones carrying the mutated allele were injected into mouse blastocysts to generate chimeric mice by the staff at the Institute for

Developmental Genetics, Helmholtz-Zentrum München. After microinjection blastocysts were transferred into the uterus of pseudopregnant foster mice. Of the 14 pups born from two ES lines, three male chimeric mice were identified that showed chimerism of estimated 80%-95% as judged by coat colors (Figure 14). Chimeric mice were mated with wild-type C57BL/6J mice for germ line transmission. The ES cell line TBV2 stems from 129/Ola mice that have chinchilla-colored fur, while the C57BL/6J are black. Hence, the offspring derived from the ES cell clones have brown coat color, if the recombinant ES cells went into the germ line in the previous generation. From these crossings, one of the chimeras (ET42_6E3), showed 100% germ line transmission because all of its pups (F1) were brown, and the other two chimeric mice are sterile.

Eighteen of the F1 offspring were genotyped using PCR and Southern blotting on DNA extracted from their tails (see methods section 2.2.1-3). The PCRs were run with 3 primers targeting the neo cassette and the single loxP site of the mutant allele, as shown in Figure 13C and confirmed that all F1 mice carried the mutant allele. As the PCR strategy we used did not reveal homologous recombination, Southern blot was used to confirm the mouse genotypes. As shown in Figure 13D, it is clear that the F1 mice ($PC4^{Neo\ flox/+}$) contained one mutant allele at the target locus. PC4 is expressed in many if not all tissues tested (Figure 11). Since the constitutive knockout mouse strain was lost because of unsuccessful recovery from frozen embryos, a heterozygous mouse line (termed $PC4^{+/-}$), which contained one wild-type PC4 allele ('+') and one mutated PC4 allele lacking both exon4 and the neo cassette ('-'), was generated via ubiquitous Cre recombinase-mediated excision [F1 mice were mated with Cre-deleter mice (CMV-Cre) (Schwenk et al. 1995; Rodriguez et al. 2000)] in order to investigate its general physiological function. The heterozygote state was confirmed by PCR and Southern blot analyses (Figure 13E-F). Since the first generation of $PC4^{+/-}$ mice contains the Cre transgene initially, the heterozygous mice were back-crossed with C57BL/6J mice to exclude this gene. After the $PC4^{+/-}$ mouse strain (without Cre transgene) was established, it was maintained by crossing with wild-type C57BL/6J mice. All mice used for further phenotypic analyses used in this work are on a C57BL/6J background (at least 5 generation crossed back with C57BL/6J mice).

The conditional knockout mice can be used to investigate tissue-specific roles of PC4. This requires mouse strains that express Cre recombinase from a tissue-specific promoter. Initially, the neo cassette had to be removed via mating with mice that express FLP recombinase in all tissues (Rodriguez et al. 2000). Figure 15A shows the

genomic organization of the PC4$^{+/flox}$ strain. The genotype was confirmed by Southern blot analysis with *Eco*RV digestion and PCR analysis (Figure 15B-C).

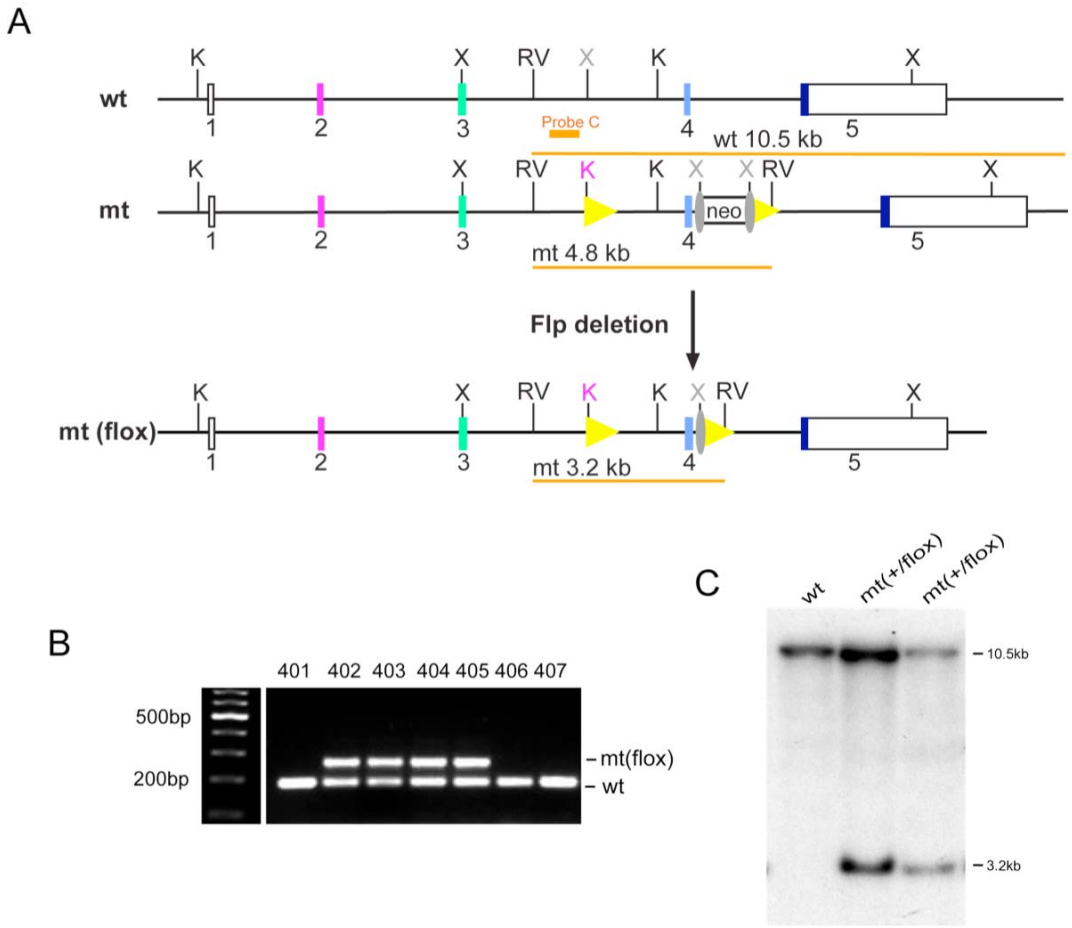

Figure 15: Construction of PC4$^{+/flox}$ mouse strain and confirmation of genotype.
(A) Genome organization of the mt (flox) allele. The F1 generation was mated with FLP recombinase transgenic mice, and the neo resistant cassette was removed. (B) PCR genotyping for PC4$^{+/flox}$ mouse strain (primers used: oWR77, oWR78, oWR79, see methods section 2.2.1.3). 401-407 indicates the mouse identification number. (C) Southern blot confirmation of PC4$^{+/flox}$ mouse strain. Genomic DNA was digested by *Eco*RV and analyzed with the probe C.

3.3 Phenotypic analysis of heterozygous and homozygous PC4 knockout mice

Although these heterozygous mice were viable, fertile, and indistinguishable from their wild-type siblings in growth rates and litter sizes, no homozygous PC4 (PC4$^{-/-}$) offspring resulted from crossing PC4$^{+/-}$ mice with one another.

3.3.1 Heterozygous ($PC4^{+/-}$) and hypomorphic PC4 ($PC4^{Neo\ flox/-}$) mice contain reduced protein

To study protein levels in $PC4^{+/+}$ and $PC4^{+/-}$ mice, spleen extracts (see methods section 2.2.4.2) taken from heterozygous and wild-type mice were analyzed by Western blot analysis. Extracts from $PC4^{+/+}$ spleens had higher PC4 protein levels than $PC4^{+/-}$ (Figure 16). Furthermore, there are reports (Frank et al. 2002; Hu et al. 2004) indicating that hypomorphic alleles (containing the neo allele) can decrease the mRNA levels of target genes. So we tested whether tissues from the PC4 hypomorphic ($PC4^{Neo\ flox/-}$) mutant mice (obtained by cross $PC4^{Neo\ flox/+}$ with $PC4^{+/-}$) contain less protein. As demonstrated in the western blot shown in Figure 16, the amount of PC4 in the hypomorphic ($PC4^{Neo\ flox/-}$) mice was markedly less than that in either the $PC4^{+/-}$ or $PC4^{+/+}$ mice. Although the $PC4^{+/-}$ and $PC4^{Neo\ flox/-}$ mice had less PC4 protein, they were viable and showed no obvious abnormalities.

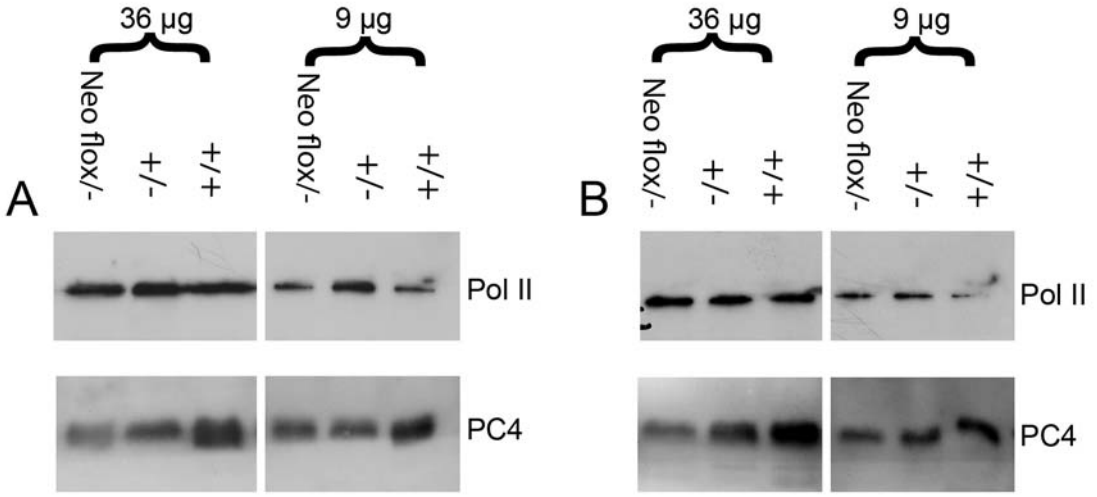

Figure 16: Analysis of PC4 protein levels in spleen of $PC4^{+/-}$, $PC4^{Neo\ flox/-}$ and $PC4^{+/+}$ mice.
(A) Western analysis of whole spleen lysates of heterozygous ($PC4^{+/-}$), hypomorphic ($PC4^{Neo\ flox/-}$) and wild-type ($PC4^{+/+}$) mice. Lysates (9 µg, 36 µg) were analyzed with polyclonal antibodies directed against PC4 and RNA Polymerase II. (B) Western blot analysis of spleen lysates from other three different genotype mice versus A.

3.3.2 Loss of PC4 causes embryonic lethality in postimplantation stage

Intercrosses of $PC4^{+/-}$ mice (Figure 17A) never resulted in viable $PC4^{-/-}$ mice. To determine the precise time point of embryonic death, embryos from different stages of development were collected for PCR genotyping and phenotype analysis. At E9.0, only embryonic debris genotyped to be homozygous for the knockout allele could be

A

Stage	Genotype (number of embryos and weanings)			
	WT	PC4$^{+/-}$	PC4$^{-/-}$	Total
weaning	11	31	0	42
E9.0	5	8	2[a]	15
E8.5	4	19	5[b]	28
E7.5	5	11	6[b]	22
E3.5	9	30	11	50

a. Only embryo debris were left.
b. Abnormal morphology and small size.

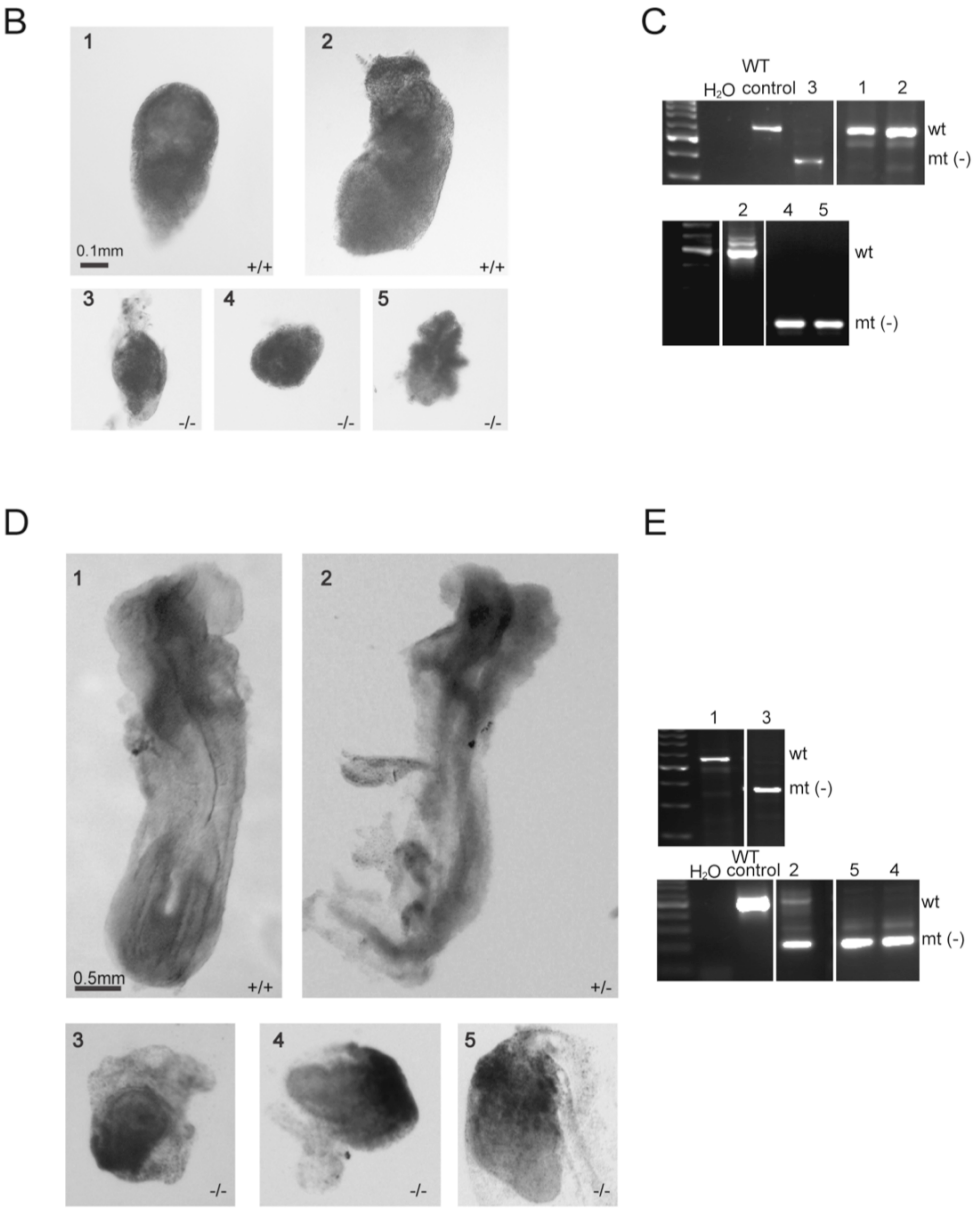

Figure 17: Analysis of PC4-deficient embryos.
(A) Genotype analysis of PC4$^{-/-}$ newborns and embryos in different development stages (B)

Morphology of $PC4^{+/+}$ versus $PC4^{-/-}$ embryos at E7.5. (C) PCR genotyping of E7.5 embryos shown in panel B (upper panel: PCR genotyping with primers oWR83, oWR79, oWR81, see methods section 2.2.1.3; lower panel: nested PCR genotyping with primers oNL1, oNL36, oNL37, oNL38, oWR80, oWR83, see methods section 2.2.1.4) (D) Morphology of $PC4^{+/+}$ versus $PC4^{-/-}$ embryos at E8.5. The PC4 deficient embryo is much smaller and disorganized than its wild-type littermate. (E) PCR genotyping of E7.5 embryos shown in panel D (upper panel: PCR genotyping with primers oWR83, oWR79, oWR81, see methods section 2.2.1.3; lower panel: nested PCR genotyping with primers oNL1, oNL36, oNL37, oNL38, oWR80, oWR83, see methods section 2.2.1.4).

collected from small deciduas, while wild-type and heterozygous embryos were isolated from normal-sized deciduas. This suggests that $PC4^{-/-}$ embryos died before E9.0. At E7.5, the $PC4^{-/-}$ embryos reached normal Mendelian frequencies, but were dramatically smaller than wild-type embryos and did not contain normal structures (Figure 17B). At E8.5, the $PC4^{-/-}$ embryos were collected that were developmentally retarded, having a smaller size and abnormal morphology (Figure 17D), whereas the wild-type and $PC4^{+/-}$ embryos formed a visible embryonic axis, a defined head, somites, and other embryonic structures. Although the E8.5 mutant embryos exhibited some variation in size, even the largest mutant embryo was much smaller than its littermate control. All of the disorganized embryos seemed to be in the process of resorption.

Intact deciduas of E5.5-E7.5 embryos were subjected to histological sectioning to better understand the defects present in the $PC4^{-/-}$ embryos. At E5.5, wild-type, heterozygous, and $PC4^{-/-}$ embryos showed similarities in size and structures (Figure 18A). At E6.5, normal embryos underwent a process of rapid cell division and elongation to form the egg cylinder (Figure 18B, left). A clear boundary was seen between embryonic and extraembryonic portions and wild-type embryos exhibited a well-organized ectoderm, endoderm, and primitive streak region. In contrast, the mutant embryos showed various defects. The less severe mutant (Figure 18B middle) had no detectable primitive streak and thin embryonic endoderm and ectoderm. However, the more severe mutant $PC4^{-/-}$ embryo (Figure 18B right) was much smaller and underdeveloped, and no defined structures could be identified. At E7.5, wild-type embryos had a well defined mesodermal layer between the endoderm and ectoderm, and the amnion was clearly visible (Figure 18C left), the $PC4^{-/-}$ embryos morphologically lacked a distinguishable extraembryonic portion and an ectoplacental cone. There was two-layered, round egg cylinder embryonic tissue, which was about half the size of the wild-type embryo (Figure 18C right). Embryonic endoderm and ectoderm were visible, but the mesoderm cell layer seems to be absent in these mutants. From these results, we conclude that $PC4^{-/-}$ embryos survived through the blastula stages and exhibited normal implantation, but arrested at around E7.5. Thus, PC4 appears to be essential for embryonic development beyond E7.5 in mouse.

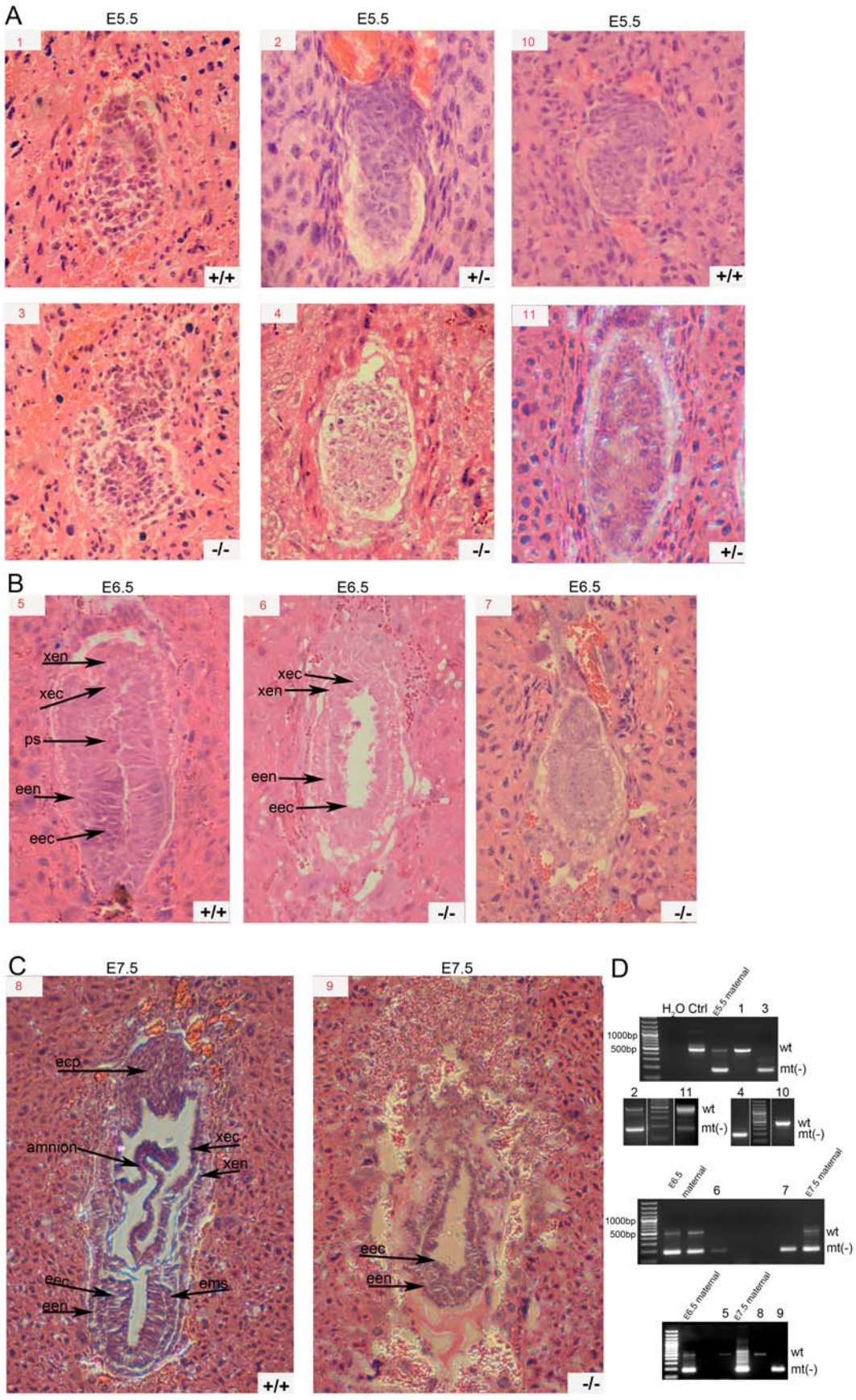

Figure 18: Histological sections of embryos between E5.5 to E7.5.

(A) Hematoxylin and eosin staining of sagittal sections of E5.5 $PC4^{+/+}$, $PC4^{+/-}$, and $PC4^{-/-}$ embryos. (B) Hematoxylin and eosin staining of sagittal sections of E6.5 $PC4^{+/+}$ and $PC4^{-/-}$ embryos. Wild-type embryos have initiated the formation of a primitive streak and show an elongated egg cylinder, however, the knockout embryos (middle) show underdeveloped embryonic endoderm and ectoderm or are smaller. (C) Hematoxylin and eosin staining of sagittal sections of E7.5 $PC4^{+/+}$ and $PC4^{-/-}$ embryos. The wild-type embryo has well-defined embryonic and extra-embryonic structures. A layer of mesodermal cells is visible between the ectoderm and endoderm. The $PC4^{-/-}$ embryo has only a two-layered, rounded egg cylinder and no extra-embryonic ectoderm, endoderm, or mesoderm. (D) Genotype analyses (primers used: oNL1, oNL36, oNL37, oNL38, oWR80, oWR83, nested PCR, see methods section 2.2.1.4) of all embryos shown in A, B, C. Arrows indicate the corresponding structures of the embryo. Numbers are the embryo identification numbers used for genotyping analyses. ecp, ectoplacental cone; eec, embryonic ectoderm; een, embryonic endoderm; ems, embryonic mesoderm; ps, primitive streak; xec, extra-embryonic ectoderm; xen, extra-embryonic endoderm; xms, extra-embryonic mesoderm.

3.3.3 $PC4^{-/-}$ embryos exhibited normal preimplantation development

To evaluate the effects of PC4 knockout on preimplantation development, embryos at the blastocyst stages were derived from $PC4^{+/-}$ mice crosses and genotyped. In this stage, homozygous blastocysts achieved normal Mendelian frequencies (Figure 17A). Furthermore, a time-lapse experiment was performed on preimplantation embryos for morphological analysis. Embryos at the two-cell stage were flushed from oviducts at E1.5 and cultured on a microscope stage with time-lapse image recording. After finishing the observation, each embryo was genotyped by nested PCR (Figure 19D). It was found that $PC4^{-/-}$ embryos cleaved normally from the two-cell to the eight-cell stage (Figure 19A-B), then compacted quickly and cavitated normally to form regular blastocysts at E3.5 (Figure 19C). Compared with wild-type preimplantation embryos, $PC4^{-/-}$ embryos did not differ in morphology, size, or total cell numbers during development. Hence, these observations clearly indicated that the knockout of PC4 did not compromise embryo development at the preimplantation stage.

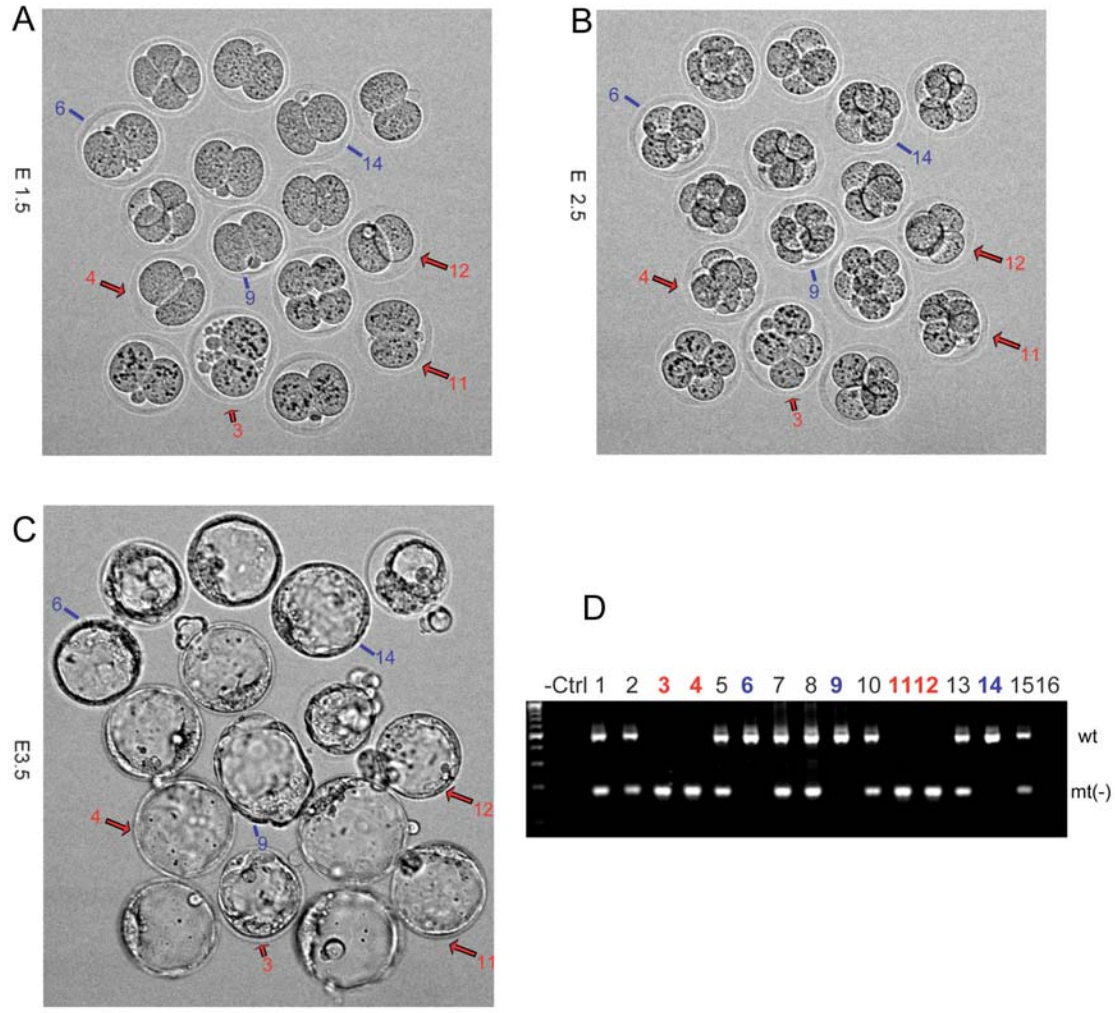

Figure 19: Preimplantation development of PC4-deficient embryos.
(A) Morphology of two- to four-cell stage embryos isolated from oviducts. (B) Morphology of eight-cell stage embryos after one day culture *in vitro*. (C) Blastocyst-stage embryos at E3.5. (D) Nested PCR genotyping analysis of preimplantation embryos shown in A-C (primers used: oNL1, oNL36, oNL37, oNL38, oWR80, oWR83, nested PCR, see methods section 2.2.1.4). Red arrows and numbers indicate homozygous embryos; blue lines and numbers indicate wild-type embryos.

3.4 PC4 expression in mouse preimplantation embryos

PC4, as a general positive transcription cofactor, is very active during preimplantation development, when the expression of a vast number of genes is initiated during activation of the zygotic genome around the two-cell stage. Eventually, differential gene expression results in differentiation of cell lineages for the three germ layers (trophoblast, hypoblast, and epiblast). Due to the lack of data concerning the pattern of PC4 expression at early embryonic stages, *in vitro* fertilization oocytes were studied for the presence of PC4 using immunostainning with a specific PC4 polyclone antibody (Figure 20). In unfertilized eggs, PC4 is diffusely localized in the cytoplasm and is excluded from

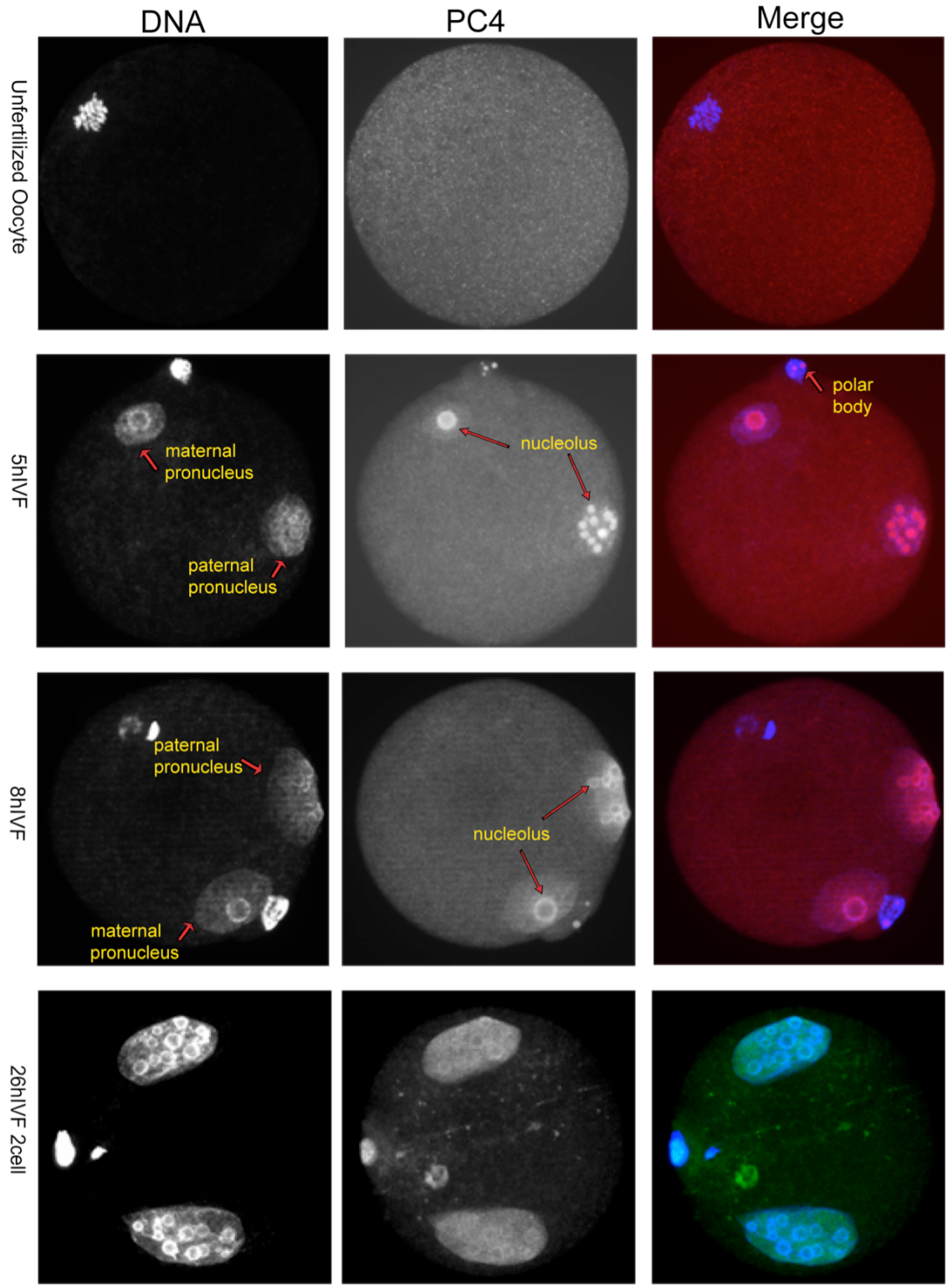

Figure 20: Immunodetection of PC4 in fertilized oocyte.
Unfertilized oocytes and *in vitro* fertilized zygotes as well as two-cell stage embryos were histochemically stained to detect nuclear localization of PC4 during preimplantation development. Heterochromatic DNA was visualized by DAPI *(blue*) staining. PC4 was detected by primary polyclonal antibody from rabbit with Rhodamine Red-X-conjugated anti-rabbit secondary antibodies (*red or green*). Red arrows indicate the structures of zygotes.

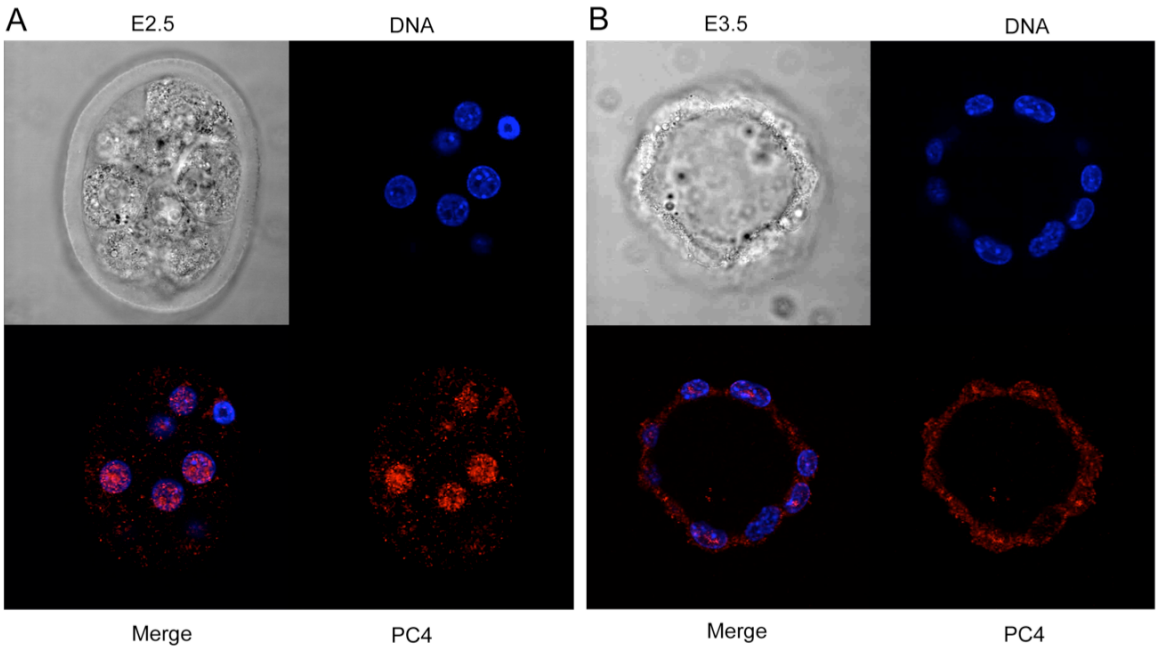

Figure 21: Distribution of PC4 in mouse morula and blastocyst.
(A) Localization of PC4 at the 8-cell, morula stage. (B) Localization of PC4 at the blastocyst stage. PC4 was detected by primary polyclonal antibody and Cy3-conjugated secondary antibody (*red*)

the condensed metaphase chromosomes. After fertilization, in addition to its cytoplasmic localization, PC4 enters into the two maternal and paternal pronuclei. Interestingly, the factor accumulates at the nucleoli few hours after fertilization [till 5 hours after *in vitro* fertilization (5h IVF)]. At 8hIVF, PC4 is then localized in the nucleus and highly overlapped with DAPI staining (heterochromatin). At the two cell stage, PC4 signals become more pronounced. At the morula (Figure 21A) and blastocyst (Figure 21B) stages, PC4 is concentrated in nucleus versus the cytoplasm. The nuclear localization is unrelated to DAPI staining, indicating that PC4 was localized with euchromatin instead of heterochromatin at the morula and blastocyst stages. The dynamic localization of PC4 might indicate a role in early embryo development.

3.5 Generation and phenotypic analysis of PC4 knockout (KO) ES cells

3.5.1 Reduced proliferation rates of PC4 KO ES cells

Based on the observation that PC4 knockout blastocysts are viable and morphologically normal, we hypothesized that ES cells could be generated from them. PC4 KO ES cells could serve as a model to dissect the molecular functions of PC4. Beyond it, ES cells have the inherent capacity to develop into different cell types *in vitro*. Hence, they could be used as a differentiation model to study the role of PC4 in it.

Cell proliferation and differentiation events are closely involved in the processes of early embryogenesis. *In vivo,* the cell population initially doubles every 24 hours, and doubling time decreases to 12 hours close to the onset of gastrulation. ES cell lines were established following the procedure described below. After plating the blastocysts on inactivated mouse embryonic fibroblasts (MEFs) with ES cell culture medium, the outgrowth of ICM of the embryos were formed around 7 days later. The ES cell like colonies that were derived from the outgrowth were detected after several weeks (see methods section 2.2.2.3.3). Since the PC4 knockout embryos grew so slowly and were very sensitive to the environment, it took around one year to establish the two homozygous PC4 null ES cell lines. When compared at high magnification (200x), both WT and KO cell lines showed the same typical morphology of ES cell colonies (Figure 22A). However, at lower magnification (40x), colony densities of PC4 KO ES cells were reduced compared to wild-type ES cells. As expected, PC4 KO ES cells did not contain detectable levels of PC4 as determined by Western blotting (Figure 22B). Deletion of the wild-type allele was also confirmed in PC4 KO ES cells by using PCR analysis (Figure 22B). Growth rates of KO cell lines were significantly below the one of the wild-type cell lines (Figure 22C). The doubling time of PC4 null ES cells was 34 hours, while wide-type ES cells had a doubling time of approximately 15 hours. These observations suggest that PC4 is necessary for normal cell proliferation rates.

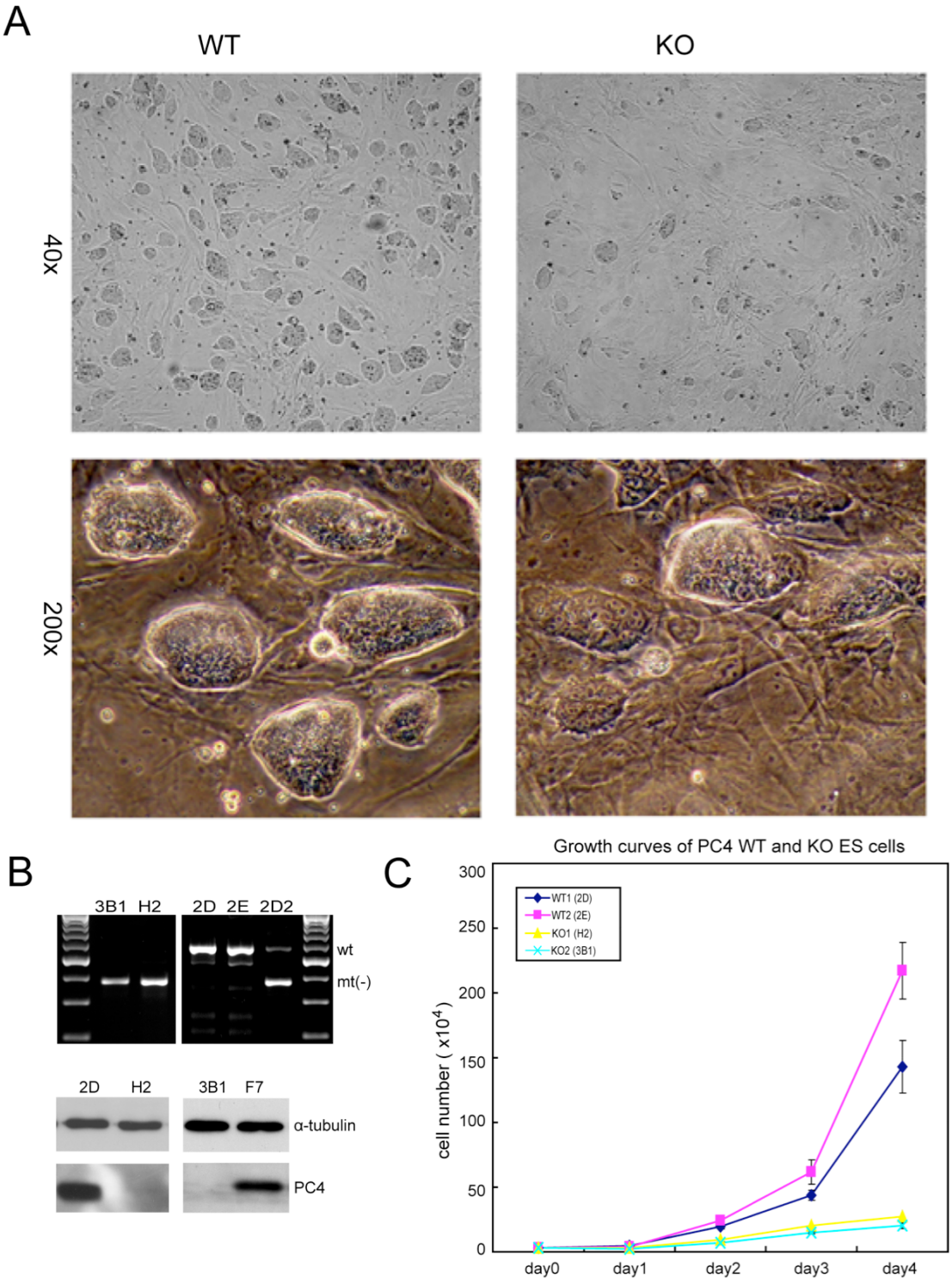

Figure 22: Morphology and growth curves of PC4 wild-type (WT) and knockout (KO) ES cells.

(A) Morphology of wild-type (WT) and knockout (KO) ES cells at 40x and 200x magnification. (B) PCR genotyping and western blot analysis of different WT versus KO ES cell lines. ES cell lysates were analyzed with polyclonal antibodies against PC4 and a mouse monoclonal antibody against α-tubulin (as a loading control). (C) Cell growth curves. WT and KO ES cells were seeded in culture dishes, and the cell numbers were determined at the indicated times thereafter. Data are means ± SD from three independent experiments. 3B1, H2, 2D, 2E and F7 in this figure indicate clone numbers of the ES cell lines. These clone numbers are used thereafter.

3.5.2 The reduced proliferation in PC4 KO ES cells is not due to an increase in apoptosis

Because the depletion of PC4 in ES cells resulted in a significantly lower growth rate, the question arose whether this might have been due to cell loss via apoptosis. To investigate this possibility, we performed an apoptosis assay. The apoptotic program is characterized by certain morphological changes, including one of the earliest features, loss of plasma membrane integrity. In apoptotic cells, the membrane phospholipid phosphatidylserine (PS) is translocated from the inner to the outer leaflet of the plasma membrane, thereby exposing PS to the external cellular environment. Annexin V is a 35-36 kDa Ca^{2+}-dependent phospholipid-binding protein that has a high affinity for PS, and can bind to cells with exposed PS. Conjugated to FITC, Annexin V serves as a sensitive probe for flow cytometry analysis of cells that are undergoing apoptosis at the early stage. Another fluorescent agent, propidium iodide (PI), is excluded by viable cells with intact membranes, whereas the membranes of dead and damaged cells are permeable to PI. Therefore, using flow cytometry analysis, FITC Annexin V- and PI-negative cells represent viable, non-apoptotic cells, FITC Annexin V-positive and PI-negative cells represent early apoptotic cells, FITC Annexin V- and PI-positive cells represent end stage apoptotic cells or early necrotic cells, and PI-positive cells represent the late necrotic or dead cells. We analyzed two WT and two KO ES cell populations for apoptosis. As shown in Figures 23, the percentages of viable cells, pre-apoptotic cells, late apoptotic or early necrotic cells, and late necrotic or dead cells, did not differ significantly between the WT and KO ES cell lines. Thus, the loss of PC4 did not induce apoptosis, and apoptosis cannot be considered an explanation for the proliferation defective phenotype observed in PC4 KO ES cells.

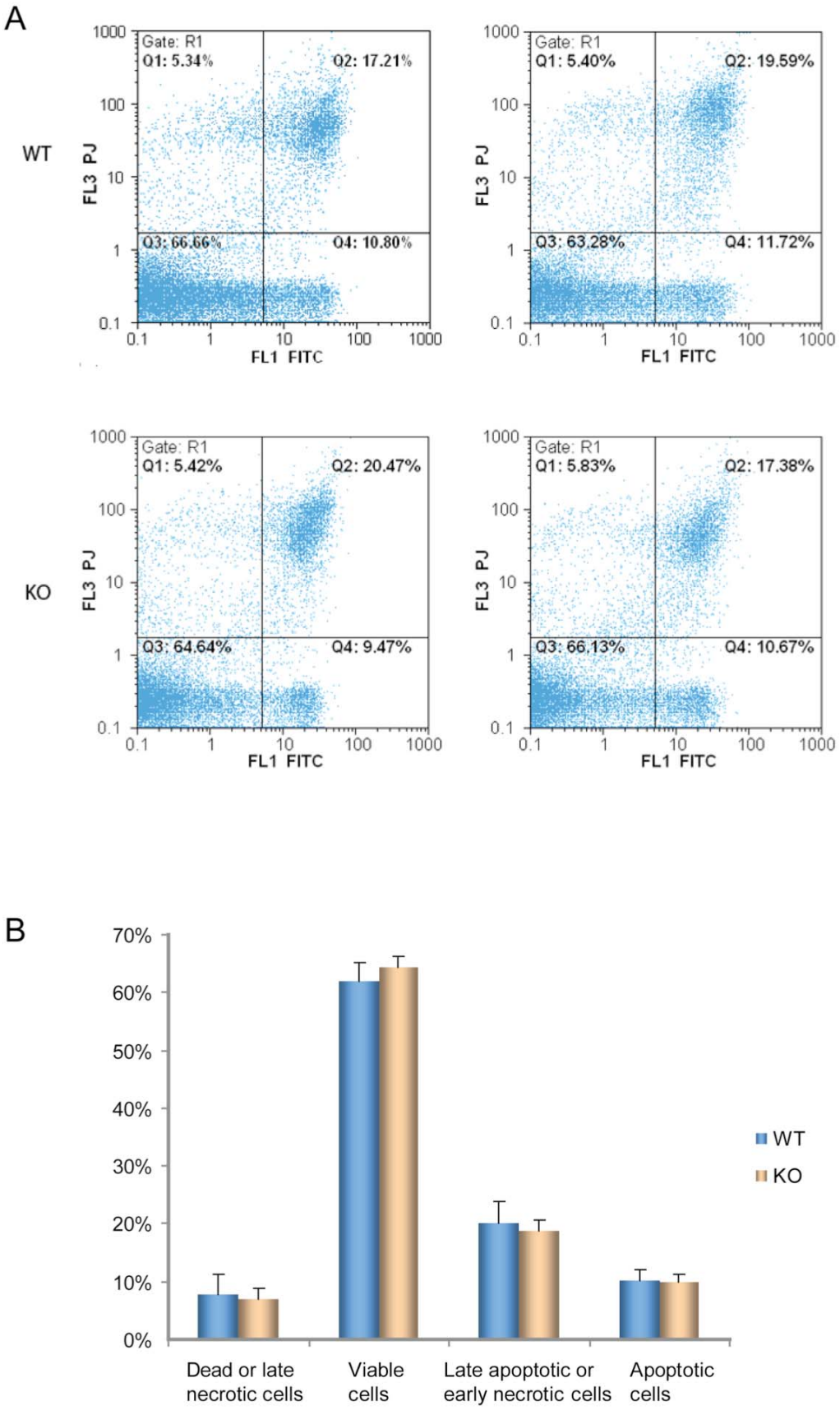

Figure 23: Flow cytometry analysis to determine the number of apoptotic cells induced by PC4 deletion

(A) Representative dot plots from flow cytometry. The WT and KO ES cells were stained with FITC Annexin V in conjunction with propidium iodide (PI) ('FL3 PJ' channel) for Fluorescence-activated cell sorting (FACS) analysis. (B) Percentages of apoptotic cells (as assayed by Annexin V expression), dead or late necrotic cells (as assayed by PI-positive cells), late apoptotic or early necrotic cells (as assayed by both Annexin V- and PI-positive cells), viable cells (as assayed by both Annexin V- and PI-negative cells). Error bars represent SD and means are of three independent experiments with two biological samples. WT and KO ES cell lines used here were F7, 2D, H2, 3B1.

3.5.3 Human PC4 partially rescues the slow growth phenotype seen in PC4 KO ES cells

To ascertain whether the low growth rate of PC4 KO ES cells could be rescued by ectopic expression of PC4, a plasmid vector with human PC4 cDNA was transiently transfected back into the KO ES cells. The human PC4 full length DNA, which is highly conserved in mouse, was fused with an EGFP-coding sequence at its N-terminal end to visualize the transfection efficiency (Figure 24A). The resulting fusion protein was assumed to be functional as it replaced endogenous PC4 in both human and mouse cell lines in DNA damage recognition (Mortusewicz et al. 2008). After electroporation of the linearized EGFP-mock and EGFP-PC4 vectors, approximately 30% of the ES cells were transfected, based on EGFP expression. We also confirmed the fusion protein expression in KO ES cells by Western blot (Figure 24B). After neomycin selection for five days, the growth rates of the transfected WT and KO ES cells were evaluated. The growth rate of KO cells transfected with EGFP-PC4 was higher than that of the mock-transfected KO cells; however, it was still lower than that of the mock-transfected WT ES cells (Figure 24C). The doubling time changed from 35 hours in KO to 28 hours in the rescue situation. These results demonstrated that PC4 did play a role in cell proliferation regulation. Further proof for the crucial role of PC4 in cell proliferation came from conditional knockdown experiments (Xiaoli Li, Jianming Xu, Sanghamitta Singhal, Thomas Albert unpublished observation). Together data suggested that the KO ES cell lines contained no artificial genetic mutation that caused the observed proliferation defect, and re-expression of human PC4 in mouse cells partially rescued the reduced proliferation phenotype observed following PC4 depletion.

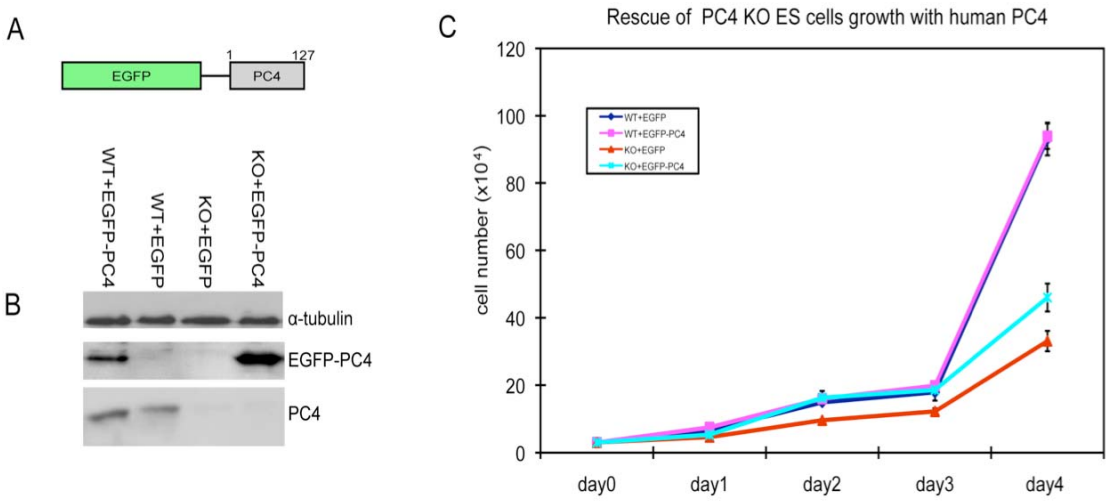

Figure 24: Human PC4 partially rescues the slow growth of KO ES cells
(A) Arrangement of EGFP-PC4 fusion expression vector. PC4 is from human cDNA that encodes 127 amino acids. (B) Western blot analysis of transfected WT (F7) and KO (3B1) ES cell whole lysates prepared after 10 days following transfection and selection. ES cell lysates were analyzed with polyclonal antibodies against PC4 and a mouse monoclonal antibody against α-tubulin. (C) Viable cells were counted at various time points (0-4 days) after transfection with mock and EGFP-PC4 vectors.

3.5.4 Tetraploidy was occasionally observed in ES cells lacking PC4

Cell cycle arrest might be another explanation for the reduced cell proliferation seen in PC4 KO ES cells. To examine this possibility, we analyzed the cell cycle progression in three WT and two KO ES cell lines by flow cytometry. All the WT ES cells showed the expected, normal cycle progression (Figure 25A): about 28% of the cells were in G1 phase, 60% in S phase, and 12% in G2/M phase. One of the KO ES cell lines also exhibited a normal cell cycle, whereas the other proceeded through S-phase without an intervening mitosis, and became tetraploidy (Figure 25A). The tetraploid cell population in G1 is difficult to distinguish from the G2 phase of the normal cell population. Furthermore, the observed tetraploidy in PC4 KO ES cells was documented by karyotype analysis. As shown in Figure 25B, many metaphase plates of the KO ES cells contained nearly double the number of chromosomes. However, it was reported that hypoeuploid and hypereuploid metaphases could be found throughout the period of ES cell culture (Rebuzzini et al. 2008). From passage 6 to 34, the frequency of tetraploid cells in metaphase ES cells is about 1-2.2% (Rebuzzini et al. 2008). To exclude that the tetraploidy observed was due to high passage culturing, we used early passages of ES cells (less than 20 passages) with the same conditions for both WT and KO ES cells. Our data reveal that the WT and PC4 KO ES cells have a similar frequency of hypoeuploid chromosomes, about 7% and 10%, respectively. On the other hand, the proportions of cells with 40 chromosomes in the WT and PC4

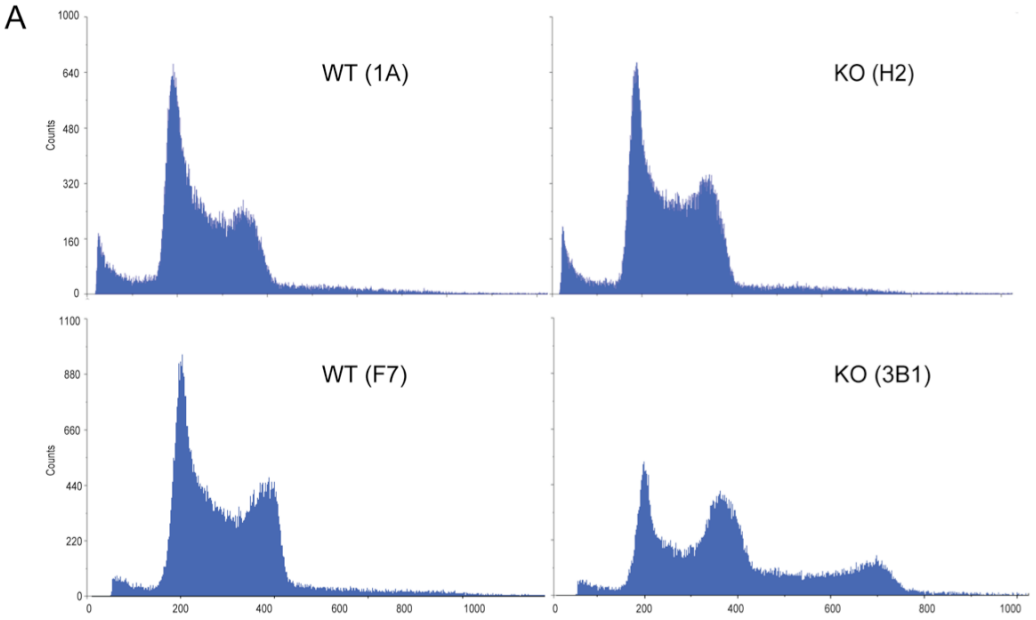
A
WT (1A)
KO (H2)
WT (F7)
KO (3B1)
Counts
1000
640
480
320
160
0
1100
880
660
440
220
0
200
400
600
800
1000

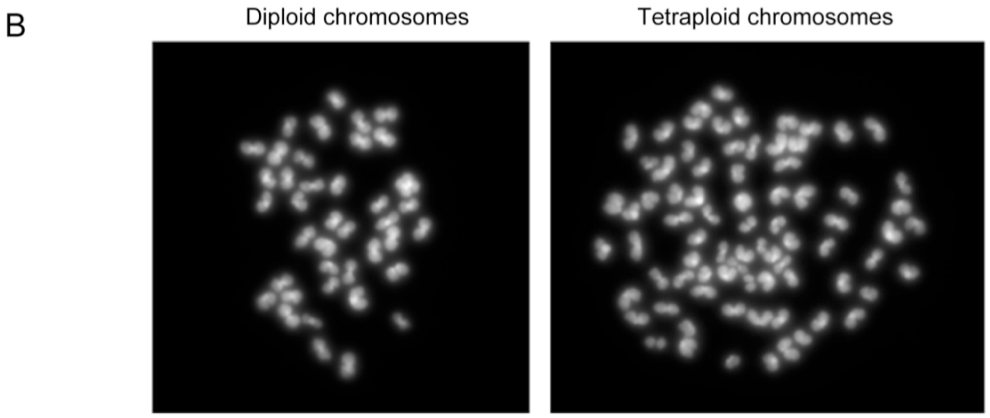
B
Diploid chromosomes
Tetraploid chromosomes

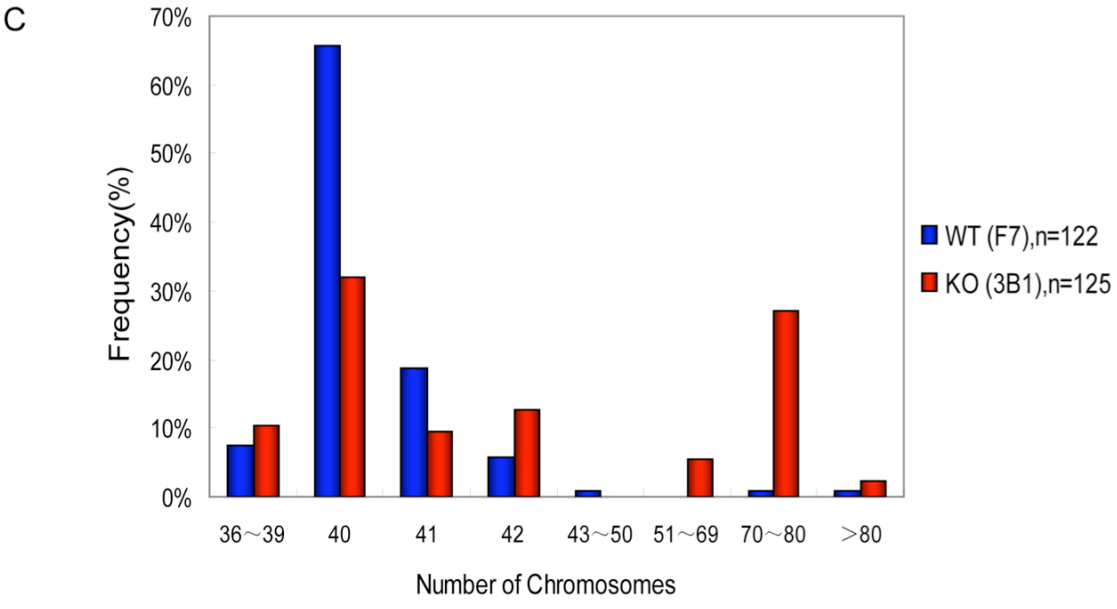
C
Frequency(%)
70%
60%
50%
40%
30%
20%
10%
0%
36～39
40
41
42
43～50
51～69
70～80
>80
Number of Chromosomes
WT (F7),n=122
KO (3B1),n=125

Figure 25: Lack of PC4 could induce tetraploidy in ES cells.
(A) Cell cycle analysis of WT and KO ES cell lines. F7 and 1A are WT ES cell lines. H2 and 3B1 are KO ES cell lines. (B) Metaphase chromosomes of diploid and tetraploid cells. (C) The frequency of chromosome number distribution in WT (F7) and KO (3B1) ES cells.

KO ES cells were notably different (66% versus. 32%, respectively). The percentage of KO ES cells with 70-80 chromosomes was 27%, which was remarkably higher than the 1% in the WT ES cells (Figure 25C). Furthermore, the tetraploid frequency was also much higher than that found in high passage ES cells, which suggested that the tetraploidy was a consequence of the loss of PC4. But the tetraploidy was not seen in short term knockdown experiments (Xiaoli Li, Jianming Xu, Sanghamitra Singhal, Thomas Albert unpublished observation). From these results, we conclude that loss of PC4 in ES cells may promote tetraploidy in the cells as a survival mechanism.

3.5.5 PC4 is important for embryonic stem cell differentiation

To explore the potential role of PC4 in differentiation we used embryoid body (EB) *in vitro* differentiation assay and *in vivo* teratoma formation assays**.** Two WT and two PC4 KO ES cell lines were used for EB differentiation. We observed that PC4 KO ES cells formed EBs, but they were slightly smaller than those differentiated from the WT ES cells (Figure 26A), which is due to their slower growth rate. After 16 days differentiation, we observed many beating cardiomyocytes (around 10%) in the culture dishes of WT cells *in vitro*. In contrast, the KO ES cells generated only few cardiomyocytes (about 1%).

To investigate the genetic defects in PC4 KO ES cells, we monitored transcripts of well-documented markers of the three embryonic germ layers. Initially, we utilized end-point RT-PCR analysis to monitor gene expression (Figure 26B). Undifferentiated ES cells highly expressed the *Oct4* pluripotency marker, whereas differentiated WT and KO ES cells also expressed *Oct4*, but at lower levels, possibly due to contamination from remaining undifferentiated ES cells. While undifferentiated WT and KO ES cells did not express the three layer-specific markers: *GluR6*, hepatocyte nuclear factor 3β (*HNF3β*), α-fetoprotein, *βH1*, and α-cardiac myosin, all except the mesoderm marker *βH1*, were expressed in differentiated WT and KO ES cells; *βH1* was not detected in differentiated KO ES cells. We used *βH*1 (hematopoietic lineage marker) and α-cardiac myosin (cardiomyocyte lineage markers) as markers because mesoderm cells can develop into cardiomyocytic and hematopoietic cell lineages incipiently. Consistent with our observation of beating cardiomyocytes in the differentiated PC4 KO ES cells, α-cardiac myosin, which functions to control cardiac contractility, was detected in these cells. Because the differentiated PC4 KO ES cells did not express *βH1*, we

hypothesize that PC4 might play a role in the differentiation of hematopoietic cells during embryogenesis.

Because the traditional RT-PCR did not detect quantitative differences between KO and WT EBs, we analyzed further samples with more differentiation markers [(taken from (Landry et al. 2008)] using quantitative real-time PCR. During the differentiation time course (8 days and 16 days), *Nestin*, a marker of neural stem cell progenitors derived from the primitive ectoderm, was elvated in KO compared with WT EBs at day 8, whereas it dropped to wild-type level at day 16. This indicated that loss of PC4 induced the ES cells to differentiate into neural cells early on. However, we did find significantly lower expression of the primitive ectoderm markers *Fgf5* and *Otx2* in the KO compared with the WT differentiated ES cells during the entire differentiation time course (Figure 27), indicating connections between PC4 and the differentiation of primitive ectoderm. As markers of endoderm differentiation, we observed overexpression of *Sox17*, *Gata4*, and *Hnf4*α in KO differentiated ES cells compared to WT during the entire period, implying that depletion of PC4 may moderately favor endoderm differentiation. In other words, PC4 might normally play a role in repressing endoderm differentiation. Although the mesoderm markers *T* and *Fgf8* were significantly underexpressed in PC4 KO EBs compared to WT (Figure 27), especially at day 8, two other mesoderm markers, *Evx1* and *Wnt3*, were highly expressed in the early PC4 KO EBs. At a later stage, when both genes were upregulated in WT differentiated cells, their levels in KO were still lower than in WT. In summary, the qPCR results clearly indicated that PC4 was involved in certain processes related to the differentiation of all three germ layers, although some differentiation markers were not affected by its loss.

To evaluate the effects of PC4 KO on the differentiation of ES cells *in vivo*, we carried out a teratoma formation assay by transplanting PC4 KO ES cells into 'severe combined immunodeficient' (SCID) mice. Four weeks after subcutaneous injection, PC4 KO ES cells formed teratomas in 5/5 injected mice. In hematoxylin and eosin stained teratoma sections (Figure 28) we found tissues from all three germ layers, such as neural cells and keratinized epithelium (ectoderm), muscle and osteroid island cells (mesoderm), and columnar epithelium and pancreatic follicles (endoderm). We did not yet detect any cell types missing from the teratoma sections due to the PC4 depletion. This may be due to the fact that there are more than 200 different cell types in mouse, and the number of tissues that can be morphologically identified in teratomas is very limited. Nevertheless, the gene expression studies on differentiated cells strongly suggest that PC4 was closely involved in cellular differentiation

processes.

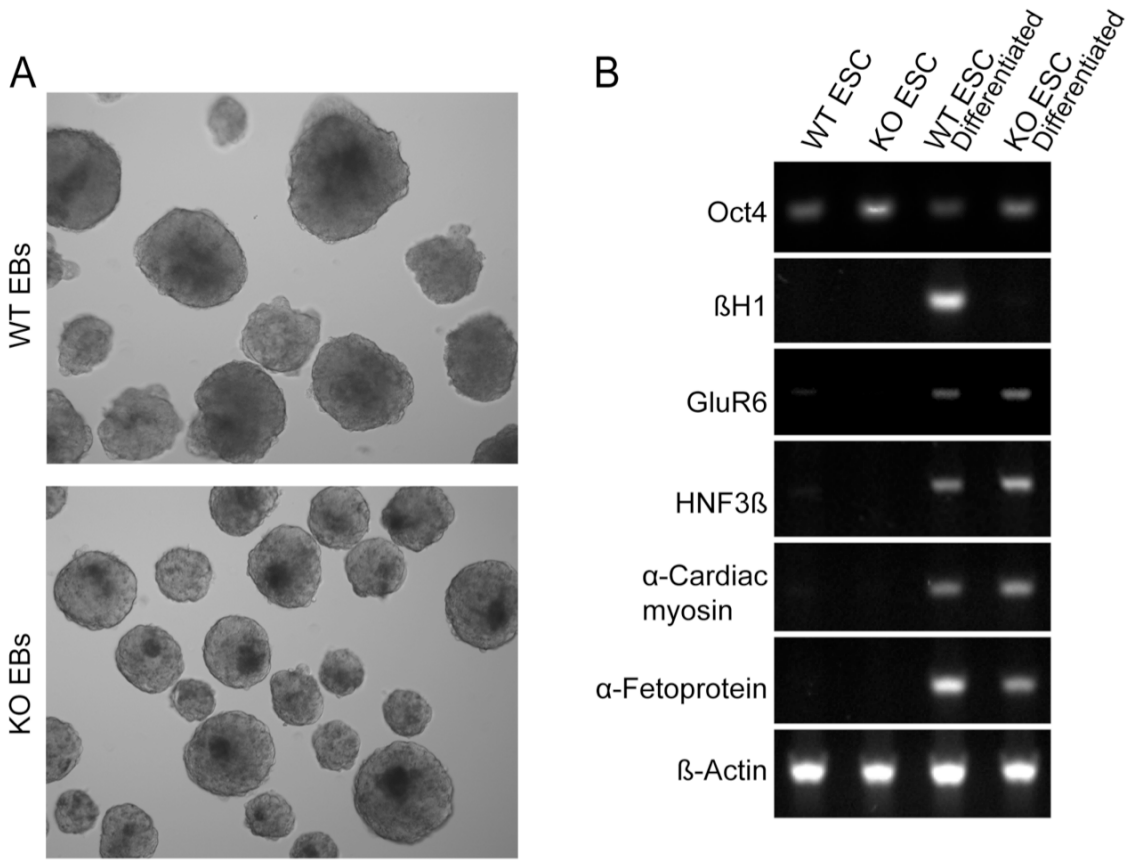

Figure 26: Differentiation of WT and KO ES cells *in vitro*.
(A) Morphology of WT embryoid bodies (EBs) (upper left) and PC4 KO EBs (lower left) (Both KO ES cell lines showed the same results, and the representative photos are from F7 and 3B1 cell lines). (B) RT-PCR analysis showing expression of layer-specific markers in differentiated WT and KO ES cells (Both KO ES cell lines showed the same results and the representative gels are from F7 and 3B1). β-Actin was used as a loading control.

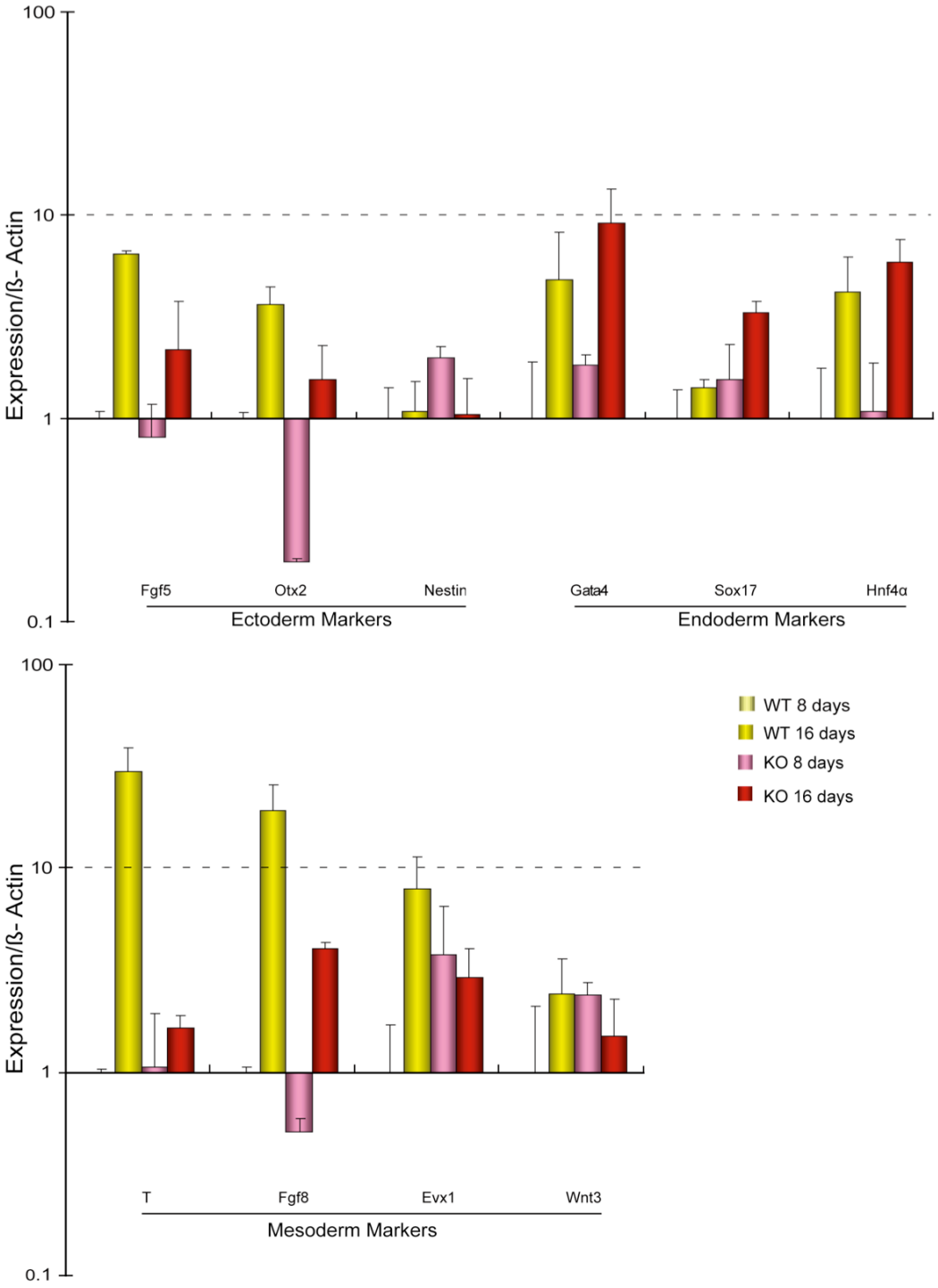

Figure 27: Quantitative PCR analysis of gene expression in PC4 WT and KO differentiated ES cells.

Relative expression of developmental markers during the time course of embryoid body differentiation (all the sequences of primers used here are listed in table 7). The expression of many markers of ectoderm, mesoderm, and endoderm tissue lineages were decreased or increased during differentiation. The mRNA levels of the various markers in 8 days differentiated WT ES cells were set to one, and ß-Actin expression was used as an internal control. Error bars represented ±SD. WT and KO ES cell lines used here were F7, 2D, H2, 3B1.

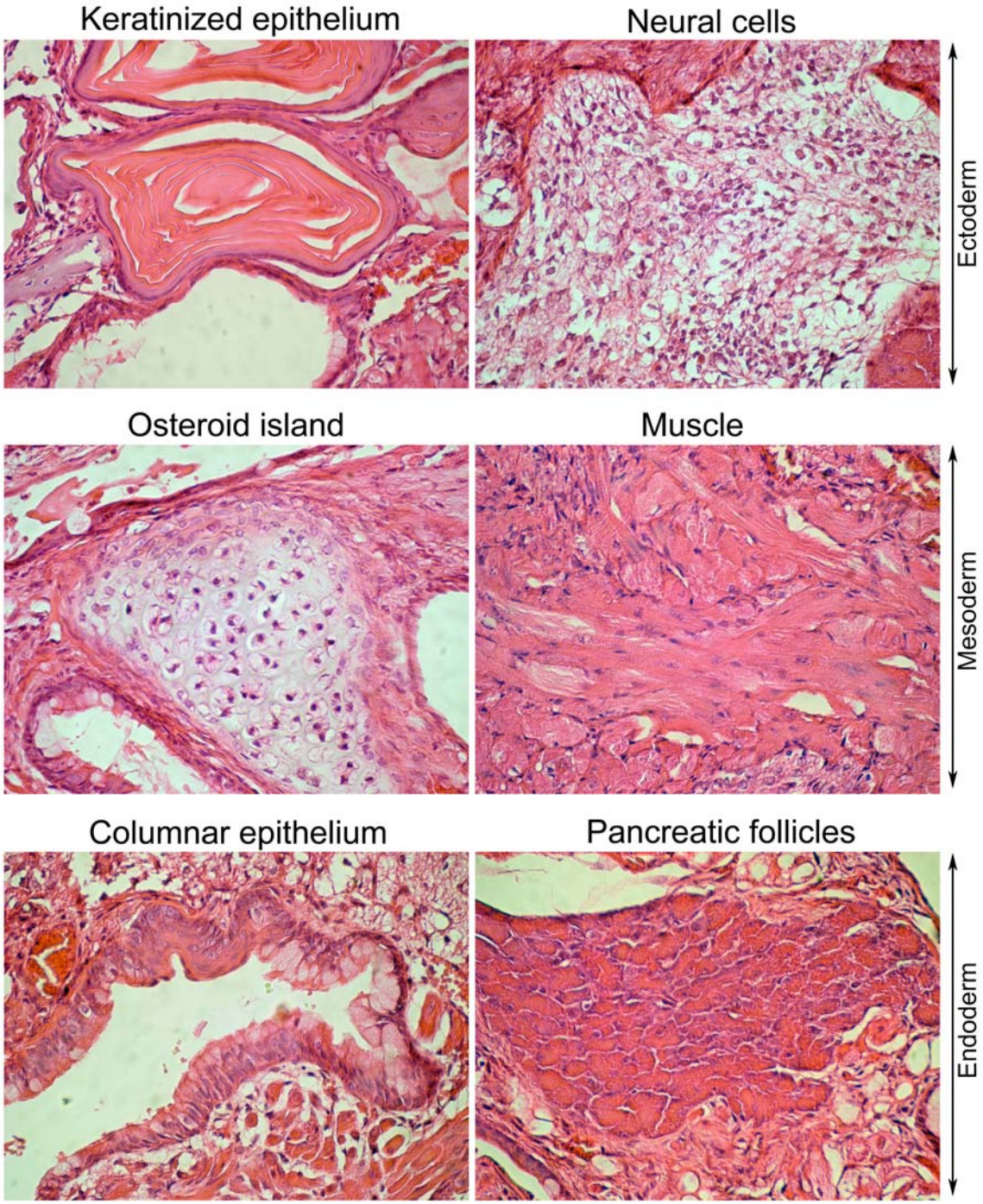

Figure 28: *In vivo*, teratoma formation assay following injections of PC4 KO ES cells into SCID mice.

Four weeks after the injections, teratomas were sectioned and stained with hematoxylin and eosin. The micrograph shows a teratoma containing ectoderm: neural cells and keratinized epithelium; mesoderm: muscle and osteroid islands; and endoderm: columnar epithelium and pancreatic follicles.

3.5.6 Gene expression profiling analysis in ES cells upon loss of PC4

3.5.6.1 Microarray data analysis

Currently, there is very limited data available regarding the target genes of PC4. The number and identity is expected to provide insight into the mechanism of gene control by PC4. It may further explain the mechanism underlying the proliferation defect in PC4 KO cells. Gene expression profiling was conducted with a mouse gene 1.0ST array (Affymetrix) representing 28853 genes (offering whole-transcript coverage). Total RNA was isolated from 2 independent WT and 2 independent KO ES cell lines and equal amount of total RNA was analyzed by KFB (Center of Excellence for Fluorescent Bioanalytics, Regensburg, Germany). Eight independent arrays were used for the WT ES and KO ES cells. Only those genes whose expressions in all KO ES cells were significantly ($p < 0.05$) more than double or less than half of that in the WT ES cells, were considered to be 'differentially expressed' between WT and KO cells. We found 80 genes that fulfilled these criteria. Among them, 54 genes were upregulated and 26 were down regulated. The latter include 4 microRNAs genes. Unsupervised cluster analyses of the expression patterns of the differentially expressed genes are shown in Figure 29A. The candidate PC4-regulated genes were also classified based on the biological process annotations according to the Gene Ontology (GO) terms (Figure 29B). Although many genes were associated with more than one biological process, the GO analysis gave us some clues about the PC4-regulated networks. The biological processes that were deregulated include proliferation, cell death, development (differentiation), cell communication, cell metabolism, cell cycle, and transcription. As the *p* values (observed frequency vs. genome frequency) for these processes were less than 0.05, the differences observed are significant at the whole genome level. Hence, PC4 may directly or indirectly modulate these physiological processes.

We further analyzed the differentially expressed genes using Bibliosphere (www.genomatix.de), a bioinformatics tool developed recently to facilitate literature-based array data analysis. This software sorts the genes according to their co-citation in the NCBI database to identify gene-gene relationships. Of the 80 differentially expressed genes we had identified, 68 of them were annotated in the Bibliosphere database. For example, transcription factors were listed with their co-cited candidate target genes. As shown in table 8, it is intriguing that out of the 37 genes co-cited with one of the transcription factors, Nfkb1, Stat3, Trp53, Jun, or Fos, 21 of them were co-cited with Nfkb1, and all had binding sites for it in their promoter regions. Seventeen of

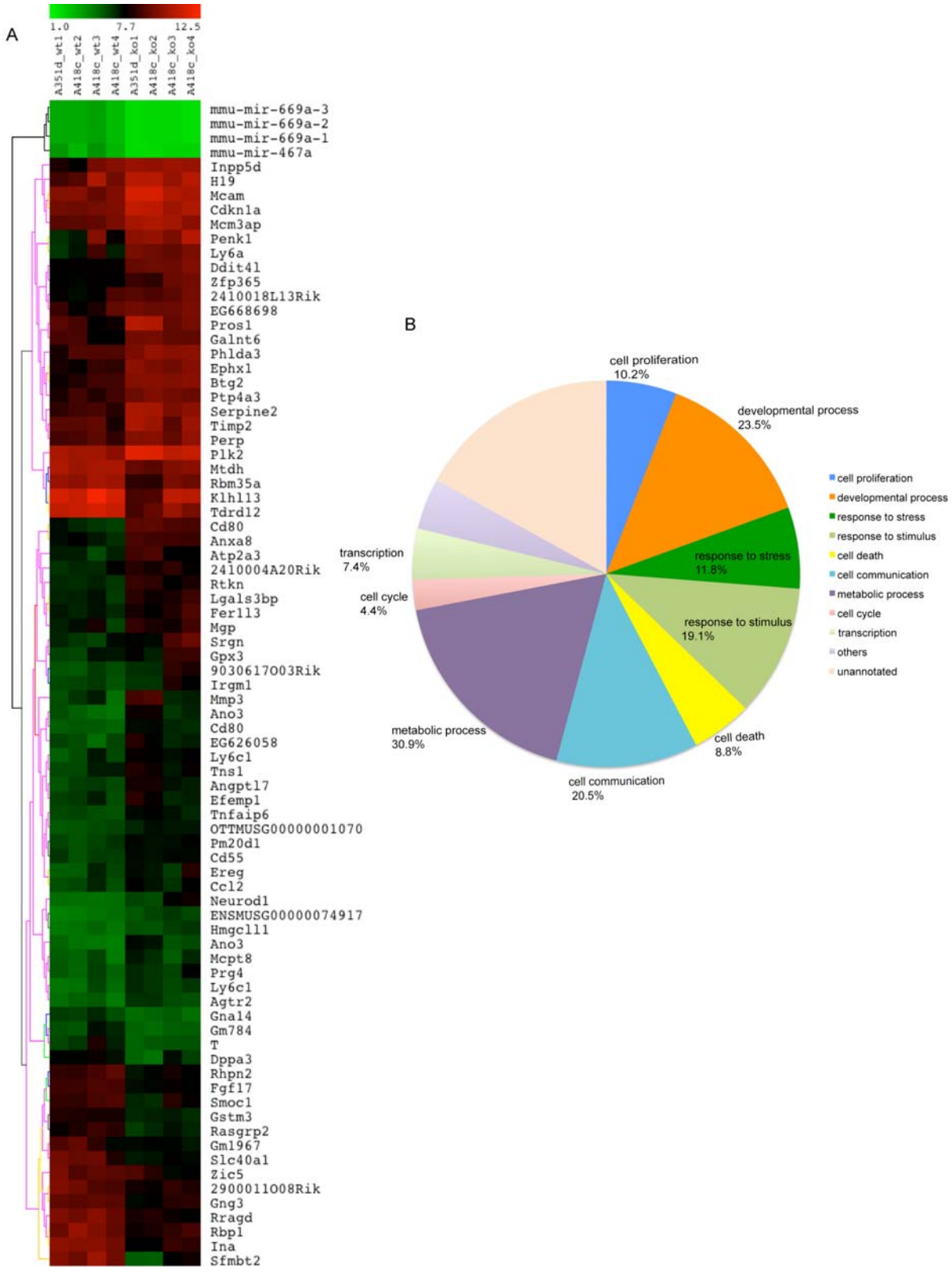

Figure 29: Biological features of above two fold regulated genes in microarrays.
(A) Hierarchical clustering of the gene expression profiling data obtained by microarray analysis

of PC4 KO ES cells versus WT ES cells. Hybridizing samples are listed to on the top and the target genes are listed to the right. wt1 and wt3 are from two independent WT cell lines: F7 and 2D. wt2 and wt4 is the duplicate of wt1 and wt3, respectively. Likewise, ko1 and ko3 are from two independent KO cell lines: 3B1 and H2. Ko2 and ko4 is the duplicate of ko1 and ko3, respectively. (B) GO (Gene Ontology) analysis of the differentially expressed genes using the filter of biological processes.

Gene/TF	Nfkb1 (V$NFKB)	Stat3 (V$STAT)	Trp53 (V$P53F)	Jun (V$AP1F)	Fos (V$AP1F)
Mmp3	+	+	+	+	+
Cdkn1a	+	+	+	+	+
Timp2	+	+	+	-	-
Cd80	+	+	+	+	+
Btg2	+	+	+	+	+
Ccl2	+	+	+	+	+
Penk1	+	+		+	+
Rbp1	+	+		-	
Ereg	+	+		-	-
Ly6a	+	+		-	-
Inpp5d	+	+		+	
Mcam	+	+		-	
Serpine2	+	-		-	-
Cd55	+		+		
Ptp4a3	+		+		
Mcm3ap	+			+	
Gpx3	+			+	
Ina	+				
Srgn	+				
Rtkn	+				+
Mtdh	+				
T	-	+	+		-
Agtr2	-	-		-	-
Perp	-		+		
Lgals3bp	-		-		
Irgm1	-				
Pros1		+			
Ly6c1		+			+
Neurod1		+		-	
Dppa3		+			
Plk2			+	-	-
Ephx1			+		
Phlda3			+		
Rbm35a					+
Tnfaip6				+	+
Rasgrp2				+	
Fgf17					+

+ TF cocited and bing sites found in the promoter

- Cocited but no binding sites

Not cocited

Table 8: Microarray target genes that were co-cited together with transcription factors.

Differentially expressed genes and presence of transcription factors binding sites were shown here.

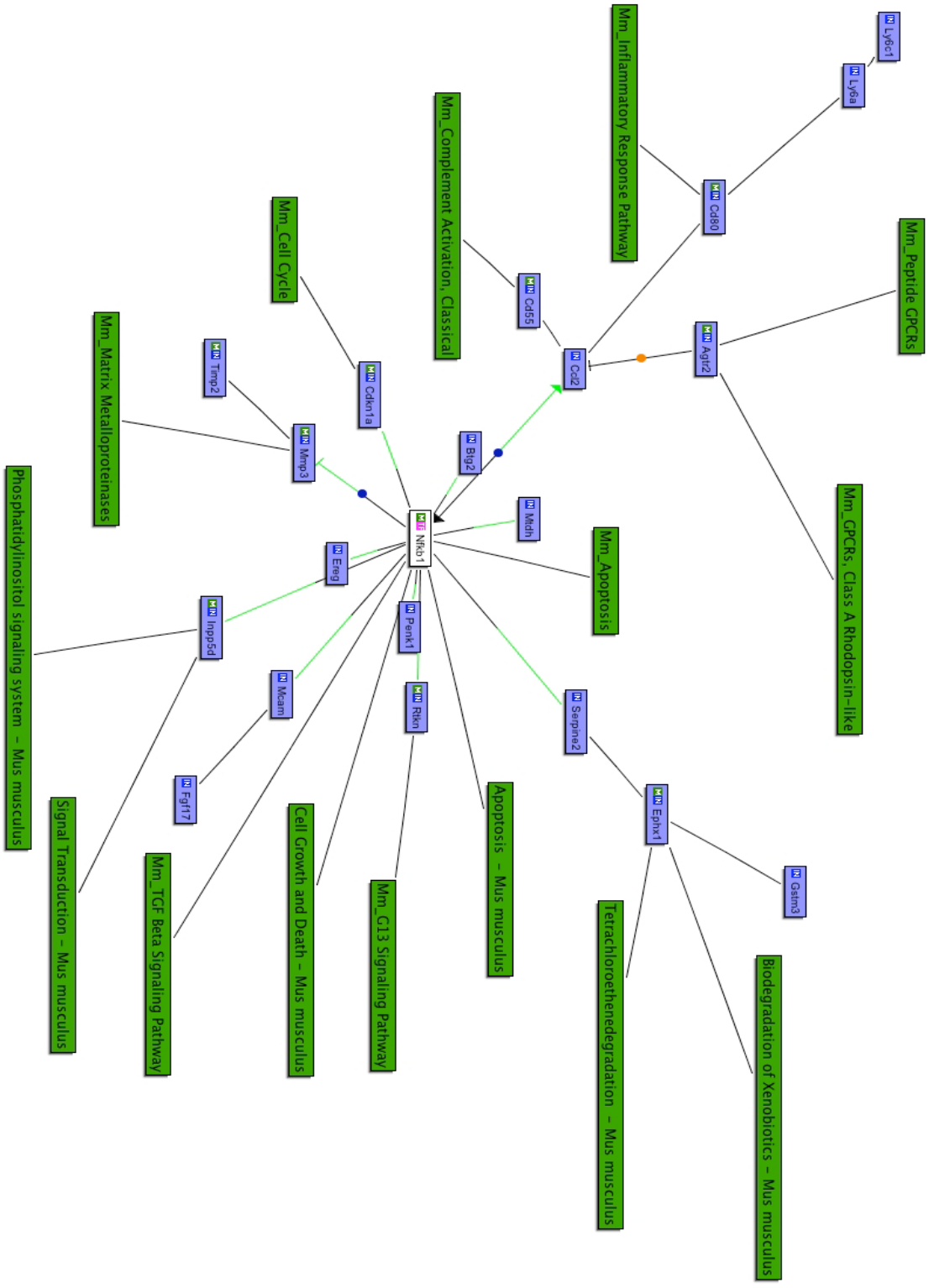

Figure 30: Bibliosphere-predicted regulatory network based on differentially expressed genes revealed by microarray.

Blue box: differentially expressed genes identified from microarray; white box: transcription factors; green line: transcription factor binging site match in target promoter; filled arrowhead: activation; blocked arrowhead: inhibition; red connection ball: connection annotated by molecular connection experts; blue connection ball: connection annotated by Genomatix experts; green box: BioCyc pathways. Co-citation filter used: GFG level B3, meaning that two

genes were co-cited in the same sentence as ‘gene...function word . . . gene’.

the 37 genes were co-cited with and bind to STAT3, and 13 genes were similarly related to Trp53, and 11 of them to Fos and Jun. These data suggest that PC4 might regulate its target genes by forming complexes with certain transcription factors, such as Nfkb1. An Nfkb1-regulated network (Figure 30) was generated by the Bibliosphere pathway software, demonstrating its central role in these biological processes, and which might be connected to the phenotype we observed in the PC4 KO ES cells.

3.5.6.2 Validation of PC4-dependent genes

It is well known that PC4 functions as a co-activator for Pol II transcription. It was further reported that human PC4 (Wang and Roeder 1998) and SUB1 (the yeast homolog of PC4) (Rosonina et al. 2009; Tavenet et al. 2009) binds to Pol III genes. Moreover, SUB1 activates Pol III genes. So far, SUB1 was not found at the Pol I-transcribed ribosomal DNA promoter. Therefore, we anticipated that the loss of PC4 might also have an impact on the expression of Pol III-transcribed genes. Because a role in Pol III is not disclosed by gene expression profiling on microarrays, we analyzed endogenous expression of Pol III- and Pol I-transcripts using quantitative PCR (qRT-PCR) on total RNA from PC4 KO ES and WT cells (Figure 31). ß-Actin was used as an internal control. Pol I transcripts, included 5.8S, 18S, and 28S rRNAs, together with the Pol III-dependent transcripts, 5S rRNA, 7SKRNA and U6snRNA were examined. The results show that PC4 does not affect Pol I-transcribed ribosomal rRNAs. In contrast, expression of Pol III-dependent genes is upregulated about 1.5 fold. Hence, loss of PC4 does not alter Pol I transcription. The increase of Pol III transcription level, however, could be indirect, i. e. a consequence of an altered number of grams in the cell.

In addition, it was reported that p53 was a potential target gene of PC4 (Banerjee et al. 2004; Batta and Kundu 2007). Therefore, we analyzed the expression of *p53*, and *p*53 target genes with qRT-PCR upon loss of PC4. It is shown that the expression of *p*53 and its target gene *Bax* is unaffected by the PC4 knockout. However, *p21* expression in KO ES cells is 2.27 times that in WT cells. All these results suggest that loss of PC4 may consequently upregulate *p21* expression, but can not regulate the expression of *p53* or its target gene *Bax*.

Considering the low growth rate phenotype of PC4 KO cells, at the beginning, we hypothesized that cell cycle-related genes might also be influenced in these cells. The cell cycle, G1, S, G2, and M phases, is crucial for cell proliferation and growth, as well

as for cell division after DNA damage. Progression of a cell through the cell cycle is promoted by a number of cyclin-dependent kinase (CDK) complexes with specific regulatory proteins called cyclins (Schwartz and Shah 2005). Cyclin D isoforms (D1-D3) (Pontano et al. 2008) interacting with CDK2,-4, and -6 drive a cell to progress through the G1 phase. Cyclin E/CDK2 directs the G1/S phase transition and the cyclin A (ccna2)/CDK2 complex controls S phase progression. In addition, cyclin A (ccna2) complexed with CDK1 (cdc2) is important in the G2/M phase transition. Compared with WT ES cells, depletion of PC4 in KO ES cells led to slightly reduced expressions of cyclin E1 (ccne1), cyclin D1 (ccnd1), and CDK2, but not of cyclin A (ccna2). This was confirmed on microarrays.

To validate the microarray results, we listed differentially expressed genes as potential target genes. Seven of the genes that were upregulated and seven of those that were downregulated in the KO ES cells, all reported to be involved in regulation of cell proliferation and differentiation, were verified by qRT-PCR from two independent WT and two KO ES cell lines. Results showed that the corresponding transcripts were markedly increased by at least 100% or decreased by at least 50% in the KO ES cells compared to the WT, thus confirming the accuracy of our microarray data. Of the upregulated genes, *Ddit4l* was upregulated more than 4-fold in the knockout ES cells. *Ddit4l* was reported to negatively regulate the mTOR (mammalian target of rapamycin) pathway, which plays an essential role in cell growth control (Corradetti et al. 2005). Likewise, other up-regulated genes, *Perp*, *p21*, *Rb1*, *Plk2* and *Phlda1* function in cell proliferation, cell apoptosis and cell death processes (Burns et al. 2003; Hossain et al. 2003; Young and Longmore 2004; Singaravelu et al. 2009). Furthermore, over-expressing of *Neurod1,* which is reported to facilitate the differentiation of ES cells towards endocrine and insulin-producing cells (Marchand et al. 2009), could also slow down the proliferation of pluripotent ES cells. Among the downregulated genes, *Sfmbt2* was dramatically repressed in PC4 KO ES cells to only 10% of the expression level in WT ES cells. *Tdrd12* was decreased by 80%, and *Gng3, Rbp1, Rragd, Fgf17,* and *Dppa3* were each reduced by around 60% in PC4 KO ES cells. *Dppa3* null embryos were shown to rarely reach the blastocyst stage (Payer et al. 2003), so downregulation of *Dppa3 in vivo* may result in the early embryo lethality of PC4 knockout mice. Two other pluripotent genes, *Nanog* and *Oct4*, shown to be unchanged in microarray analyses, were shown by qPCR to be slightly upregulated (increased about 50% and 40%, respectively) in KO ES cells. These data suggest that PC4 regulates proliferation by altering the expression of other genes involved in proliferation.

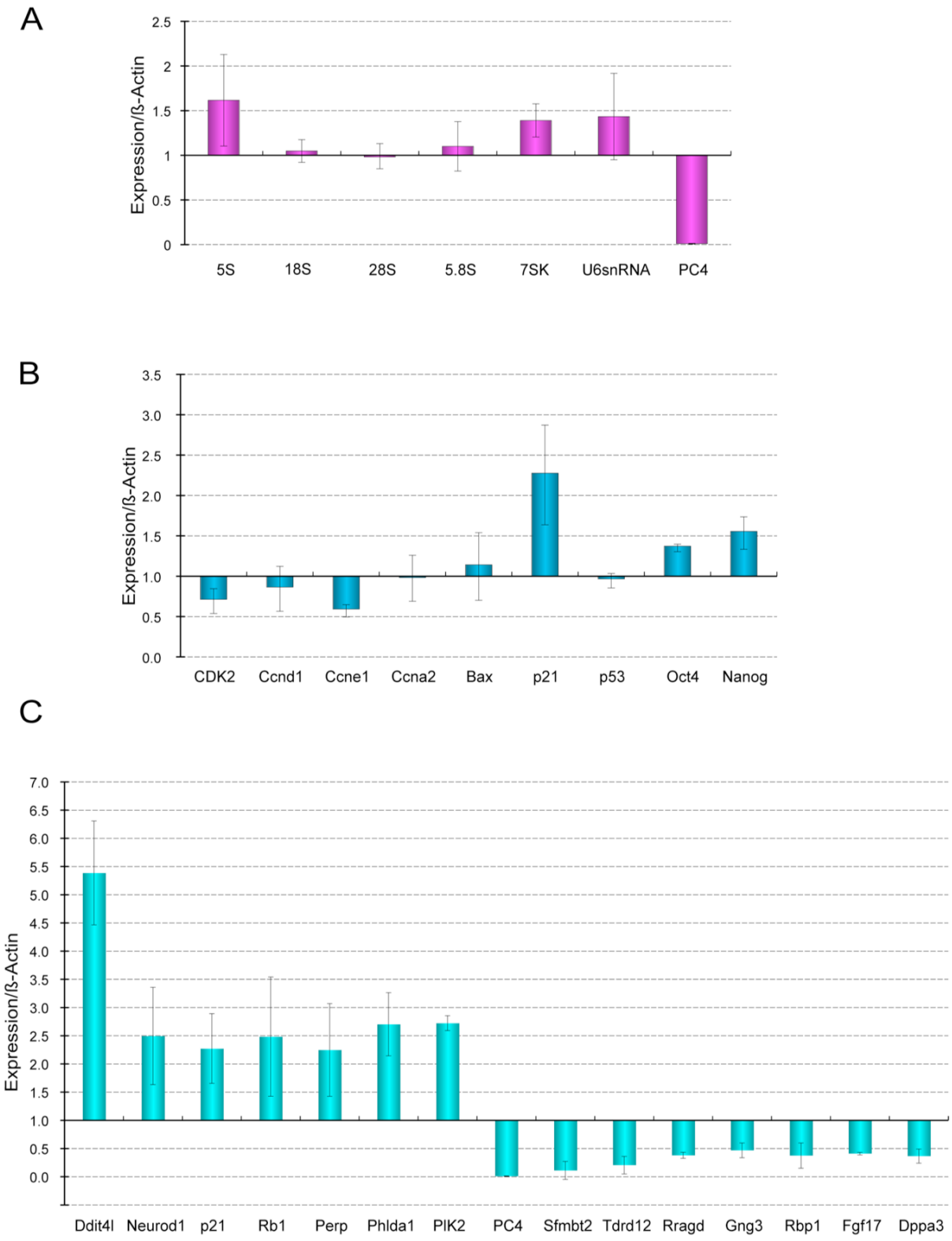

Figure 31: Quantitative PCR analysis of candidate genes in WT and KO ES cells validates the microarray data.

(A) Relative Pol I- and Pol III-transcribed gene expression in KO ES cells. (B) Relative expression of cell cycle-related genes, *p53* and its target genes, and pluripotent genes in KO ES cells. (C) Validation of the expression of PC4 potential target genes by qRT-PCR analysis.

For the qRT-PCR analyses (all the sequences of primers used here are listed in table 7), gene expression in KO ES cells was normalized to that in WT ES cells, which was arbitrarily set to one. WT cell lines used in this experiment were 2D, F7 and KO cell lines used here were H2 and 3B1. β-Actin was used as an internal control gene. Error bars indicated ±SD.

3.5.7 Loss of PC4 does not affect p53 activation

It has been reported that PC4 mediate gene activation by the tumor suppressor p53. Furthermore, the PC4 gene is p53 target gene and p53 itself drives PC4 expression (Banerjee et al. 2004; Batta and Kundu 2007; Kishore et al. 2007). Mechanistically PC4 triggers p53 recruitment to its target genes by inducing a bent. (Batta and Kundu 2007). Here we asked whether PC4 is critical for p53 expression and activation of the factor by genotoxic signals and subsequent activation of target genes. We analyzed protein levels and mRNA in PC4 KO and WT ES cells following their treatment with the p53-inducing agent doxorubicin. Four hours after the treatment, we found that the levels of p53 protein were highly increased in both WT and KO ES cells (Figure 32A). In KO ES cells, p53 was induced in a dose-dependent manner, while in WT ES cells p53 was induced independently of doxorubicin concentration. In the presence of doxorubicin, p53 was phosphorylated at Ser15 in both WT and KO ES cells, which is crucial for arresting the cell cycle and a sensor for DNA damage (Siliciano et al. 1997). The phosphorylation impairs the ability of Mdm2 to bind p53, promoting both the accumulation and functional activation of p53 in response to DNA damage. We also analyzed the mRNA levels of p53 target genes. *Bax*, *p21*, and *Mdm2* were all induced in the PC4 KO ES cells. This was also true for *p21* that was already upregulated in non-treated PC4 KO ES cells, and that was still markedly upregulated by doxorubicin treatment. In addition, doxorubicin led to a slightly higher expression of *p21* in PC4 KO cells than in WT cells (Figure 32B). Bax, a pro-apoptotic member of the Bcl-2 family, has p53 binding sites in its promoter; thus, direct activation by p53 could provide a link with the apoptotic machinery (Miyashita and Reed 1995). However, the p53 target gene *Bax* was upregulated to a slightly lesser extent in KO ES cells than in WT cells following such treatment, suggesting that PC4 might play a role of in of *Bax* activation in ES cells. Another p53 target gene *Mdm2* was similarly overexpressed in both KO ES cells and WT ES cells upon doxorubicin treatment, indicating that PC4 deletion did not affect *Mdm2* activation.

It was reported that p53 activation induces ES cell differentiation by suppressing *Nanog* expression (Lin et al. 2005). Nanog, a homeodomain protein expressed, as is Oct4, exclusively in ES cells, is required to maintain renewal and the undifferentiated state of ES cells. As expected, we found that *Nanog* mRNA was massively

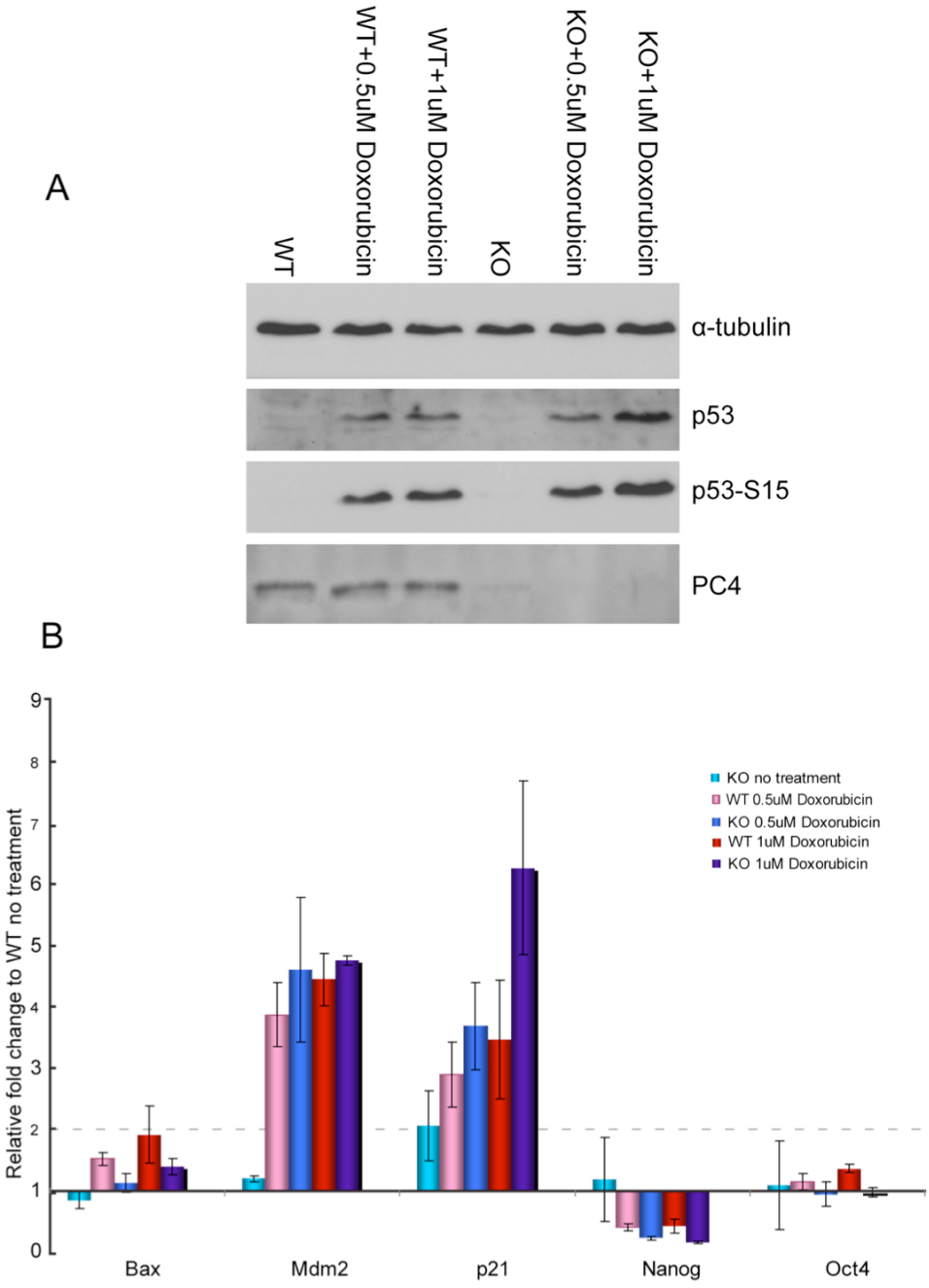

Figure 32: p53-dependent gene expression can be activated in absence of PC4.
(A) Upregulation of p53 protein levels at different concentrations of doxorubicin. p53 and α-tubulin expression are shown following 0.5 μM and 1 μM doxorubicin treatment for 4 hours (Whole cell lysates were prepared as methods section 2.2.4.2 and the representative Western blots from F7 and 3B1 cell lines are shown.). (B) mRNA levels of p53 target genes under different treatments in WT (F7) and PC4 KO (3B1) ES cells. The quantitative PCR (all the sequences of primers used here are listed in table 7) was normalized with ß-Actin, and the mRNA levels in untreated WT ES cells were set to one.

downregulated in both WT and KO ES cells after p53 activation, without any effect on *Oct4* mRNA. However, the downregulation of *Nanog* was more severe in PC4 KO ES cells than in WT cells in response to doxorubicin (Figure 32B). In conclusion, these results indicate that, although PC4 is not required for p53 activation, PC4 is important for maintaining embryonic stem cell homeostasis and it might be involved in the DNA damage response.

3.6 Down-regulation of PC4 in MEFs induced a similar proliferation phenotype as PC4 KO ES cells

To extend our findings of PC4 in differentiation cells, we further investigated PC4 function in mouse embryonic fibroblasts (MEFs). PC4 protein is present in MEFs, but only at a level of about 10-20% of that detected in ES cells (Figure 33A). To explore the function of PC4 in MEFs, we preformed knockdown experiments by transient Cre expression in $PC4^{flox/-}$ MEFs. We used Cre recombinase plasmids to transfect the MEFs and to induce genome deletion, and one week of drug selection to concentrate the transfected cells. Then we evaluated the numbers of surviving cells from the mock and Cre transfection. As shown in Figure 33B, we seeded the same number of cells for transfection at Day -1, then transfected (Day 1) and selected until Day 9. The number of surviving cells was much lower in the Cre-transfected MEFs than in the mock-transfected cells (Figure 33B), indicating reduced proliferation of the PC4-depleted MEFs, as we observed for the PC4 KO ES cells. Therefore, we assume that PC4 is important for cell growth in general in different types of cells.

At the molecular level, we tried to elucidate whether the PC4 target genes affected by the loss of PC4 in ES cells were also targets in other cell types, or whether they were targets only in ES cells. When PC4 was downregulated to about 5% of that in WT MEFs, 5S rRNA, 7SK, and U6 snRNA transcriptions were reduced about 50-60% (Figure 33C), contrary to the results found in ES cells. However, 5.8S rRNA, 28S rRNA, and 18S rRNA transcriptions were not significantly affected (increased or decreased about 10-20%) by the depletion, which is in agreement with the results from ES cells. Therefore, PC4 seems to regulate Pol III- rather than Pol I-dependent gene expression *in vivo*. Hence, in various cell types, PC4 is involved in regulation of Pol III transcription.

Because of the low transfection efficiency and reduced proliferation of PC4 knockdown MEFs, it was impossible to get enough material to repeat all experiments performed in the ES cells, but we did test a few potential target genes in PC4 knockdown MEFs. We found that *p21* and *Ddit4l* were consistently upregulated and *Sfmbt2* was

downregulated in MEFs and ES cells upon PC4 depletion, but the changes were less in MEFs than is ES cells. However, *Rragd*, which was reduced in PC4 KO ES cells, was increased about 50% upon PC4 knockdown in MEFs. Furthermore, *Rb1* was decreased by only about 20% in knockdown MEFs, whereas it was increased by 130% upon PC4 knockout in ES cells. These data indicate that PC4 regulates its potential target genes in different ways during cell differentiation *in vivo.*

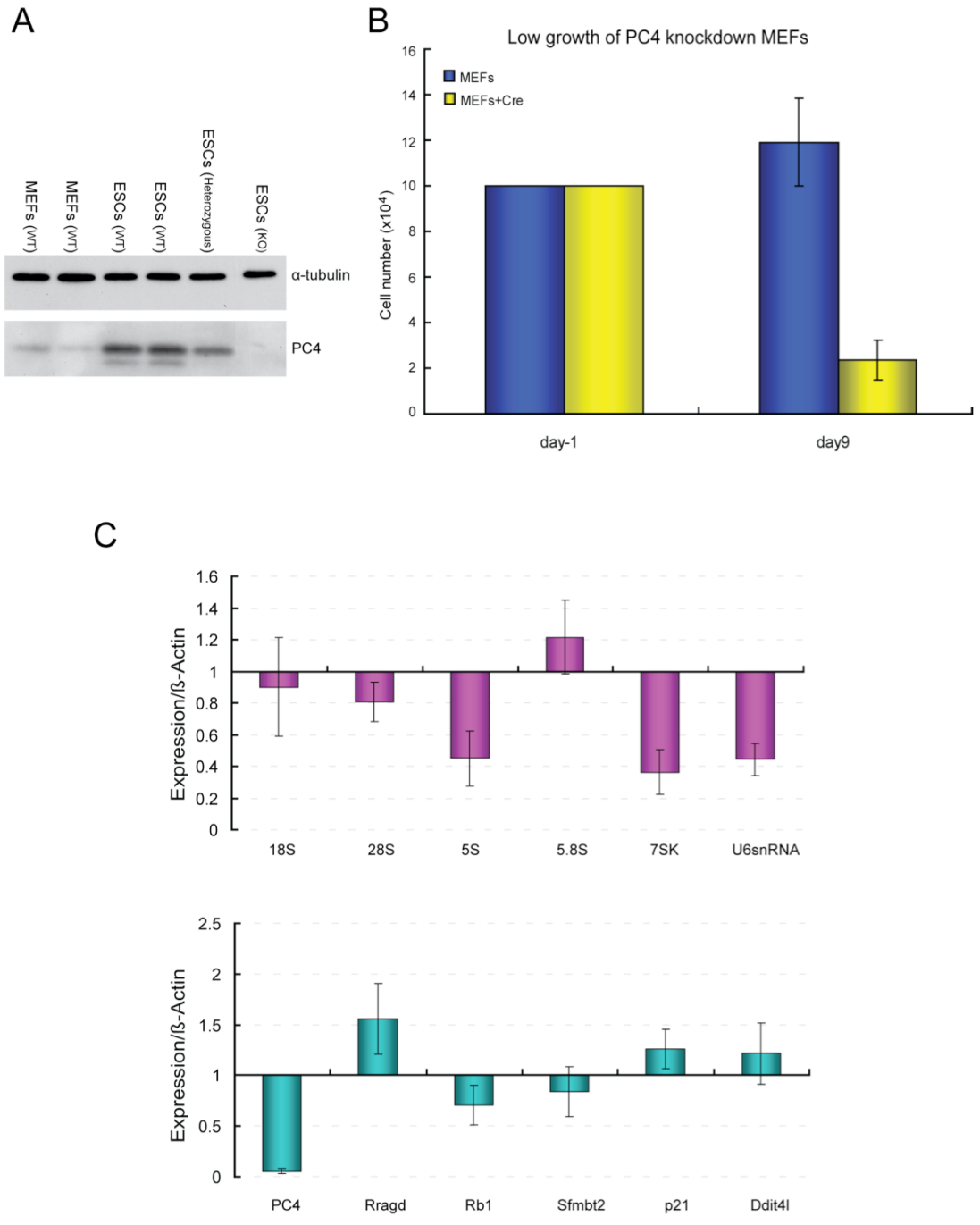

Figure 33: Phenotype analysis of MEFs upon PC4 knockdown.
(A) Western blot analysis of endogenous PC4 protein levels in WT MEFs compared with those in WT (F7), heterozygous (clone number of this cell line is 2D2), and PC4 KO (3B1) ES cells.

(B) Lower growth of MEFs when PC4 was downregulated. Day -1: flox/- MEFs seeded for transfection; Day 9: MEFs cultured after drug selection. (C) Analysis of the mRNA levels of each gene in mock and Cre-induced MEFs. The quantitative PCRs were normalized with ß-Actin and relative gene expression was normalized to mock transfected WT MEFs (set to one)

4. DISCUSSION

4.1 PC4 is required for embryogenesis

The classical *PC4* knockout mouse generated by Gertraud Stelzer in our lab showed embryonic lethality as early as the preimplantation stage, indicating that PC4 is essential for mouse embryonic development. However, not all physiological processes could be assessed by this constitutive gene inactivation strategy, and this mouse strain could not be recovered from frozen embryos. Therefore, the new conditional knockout model provided a powerful tool to gain insights into the biological roles of PC4. Although the constitutive knockout mouse already showed lethality in preimplantation embryos, it was still of great significance to identify whether PC4 null embryos could survive in the new PC4 knockout mouse strain. The fact that homozygous $PC4^{-/-}$ mutants died *in utero* around E7.0, confirmed that PC4 is essential for early stage embryogenesis. Compared with constitutive knockout mice, in which both exons 3 and 4 were deleted, the new "constitutive" exon 4 knockout mice exhibited a less severe embryonic lethality phenotype. This might possibly have been explained by the different targeting strategies; however, the early embryo lethality phenotype was present using both targeting strategies. As $PC4^{-/-}$ embryos were smaller and disorganized at E6.5 when gastrulation (characterized by massive cell proliferation) starts, the major cause of embryonic lethality was possibly due to impaired proliferation. This brings up the question of whether the preimplantation mutant embryos could have developed normally. After viewing cultured two-cell stage embryos *in vitro* via time-lapse microscopy, we concluded that preimplantation embryos did not appear to suffer from the loss of PC4. The survival of embryos to the blastocyst stage was likely due to maternal PC4. However, as the embryos developed, cell proliferation and differentiation become more important, and the lack of PC4 did not support life. Surprisingly, $PC4^{+/-}$ mutant mice did not exhibit developmental problems. Even though there was much less PC4 protein in hypomorphic mice, there were no differences in the viabilities of homozygous, heterozygous, and hypomorphic mice. This suggests that PC4 functions in a dose-independent way, and that small amounts of PC4 are sufficient.

This study is the first to characterize the physiological roles of PC4 in a knockout model and there are, as yet, few knockout studies of other positive transcription cofactors. PC1 (PARP) and other transcription cofactors show little sequence

homology, which proved to be nonessential *in vivo* for most of the functions suggested by the *in vitro* studies, with knockout mice showing few defects in nucleotide excision and base excision-repair (Wang et al. 1995). Four genetic studies of the murine TRAP/Mediator (PC2) have shown that TRAP220, SRB7, Trap100, and Med23 subunits are essential for embryogenesis but with quite different degrees of phenotypic severity. Trap220$^{-/-}$ embryos are viable up to E11.0, and the differentiation of primitive organs expected at this stage is apparent but incomplete (Ito et al. 2000; Zhu et al. 2000). It also showed that TRAP220$^{-/-}$ primary embryonic fibroblasts impaired cell cycle regulation (Ito et al. 2000). In contrast, Srb7$^{-/-}$ embryos are viable only up to the blastocyst stage, through which maternal SRB7 remains (Tudor et al. 1999). Culturing of homozygous knockout blastocysts yielded no outgrowth, indicating that Srb7 was essential for ES cell viability. The phenotypic severity of the Trap100$^{-/-}$ embryos is intermediate between that of the Trap220 and Srb7 mutations, and the Trap100 and Trap220 double mutations augment the phenotypic severity (Ito et al. 2002). The present studies showed that Med23$^{-/-}$ mice were embryonic lethal around 10.5 days of gestation (Wang et al. 2009). These indicate that TRAP/Mediator is essential for cell viability, but that a given mutant phenotype is variable and dependent upon the subunit composition of the residual TRAP/Mediator. Taken with our results, these data suggest PC4 is as important as other cofactors in mammals, although SUB1 is nonessential for the yeast growth in standard growth conditions.

4.2 Distinct localization of PC4 during fertilization implies a role in maintenance of genome methylation

In unfertilized eggs, PC4 was localized in the cytoplasm and excluded from condensed metaphase chromosomes. After fertilization, PC4 was mainly located in the two pronuclei, while cytoplasmic localization increased initially and then decreased significantly in late stage zygotes. From the 2-cell to the blastocyst stage, PC4 was mainly restricted to the nucleus. The dramatic change in the localization of PC4 indicated that it must play a crucial role after fertilization and before the 2-cell stage. During this developmental phase, many molecular events occur, including zygotic genome activation (Hamatani et al. 2006) and drastic alterations in genome methylation status (Mayer et al. 2000b; Mayer et al. 2000a; Santos et al. 2002). The increased PC4 in pronuclei after fertilization was attributed to either the translation of maternal stored mRNA or translocation of cytoplasmic protein. As a transcription cofactor, PC4 is very active and involved in genome activation, which was borne out

by the large amounts of PC4 concentrated for rRNA preparation in nucleoli after fertilization. Although the intensity of PC4 expression was less in the 2-cell to blastocyst stages compared with that found in zygotes, it was preferentially localized to euchromatin rather than heterochromatin to activate transcription. Similar to the PC4 localization pattern we observed during fertilization, PGC7/Stella/Dppa3, a maternal factor essential for early development, translocates from the cytoplasm to pronuclei to protect the maternal genome from demethylation (Nakamura et al. 2007). Does PC4 play a similar role or co-function in genome demethylation in early embryogenesis? If PC4 were involved in maintenance of methylation after fertilization, it would be interesting to determine whether it is associated with epigenetic regulation. To address this issue it might be useful to explore the methylation status of histone H3K9 (H3K9) (Santos et al. 2005), or to compare the sequences of maternally imprinted, paternally imprinted, and non-imprinted genes in PC4 null zygotes with those in wide-type zygotes. From our microarray data on PC4 knockout ES cells showing that Dppa3 was decreased, we expect that demethylation was increased in many target genes.

4.3 PC4 is important for the embryonic stem cell growth

To improve our understanding of the functions of PC4 in early embryonic development and ES cell differentiation, we tried to generate knockout ES cells. Because the heterozygous knockout mice was viable and no obvious phenotype was observed, we established PC4 KO ES cells from blastocysts obtained from $PC4^{+/-}$ mice intercrosses. Blastocysts from different genotypes were cultured on feeder layers of MEFs, and outgrowths were observed after 5 days *in vitro* culture. The morphologies of outgrowths from knockout and wild-type blastocysts were similar, and inner cell masses (ICM) developed in both genotypes. Although the ES cell-like colonies in the outgrowths grew and proliferated much more slowly from knockout blastocysts than from wild-types, the PC4 KO ES cells still survived and were suitable for *in vitro* culture. Taken together, these observations provided strong evidence that PC4 was important for ES cell proliferation. Together with the observed formation of morphologically normal blastocysts, this experiment suggests that the differentiation of ES cell equivalents *in vivo* was not initially disturbed, but the amplification of this population was partially compromised, thereby resulting in inhibition of *in vitro* proliferation of ICM-derived ES cells. Because the ES cells were similar to epiblasts at the blastocyst stage, we suggest that the PC4 null embryos died around gastrulation *in vivo* due to a repressed proliferation of PC4 knockout ES cells in the ICM, which could decrease

expansion in preimplantation embryos. Once the embryos are implanted, gastrulation becomes stronger and faster proliferation is required. The slow proliferation speed of epiblasts cannot provide enough cells for differentiation and organogenesis, which leads directly to embryonic death. Furthermore, the constant presence of maternal PC4 protein and other possible factors provided by the developing trophectoderm and/or maternal tissues in the *in vivo* situation might have temporarily compensated for the loss of PC4 until gastrulation.

4.4 Does PC4 have similar proliferation phenotypes in primary cells as in somatic cells?

Because ES cell lines are a unique system and are pluripotent compared with other somatic cell lines, it is meaningful to examine whether PC4 functions similarly in other cell types. The first candidate was mouse embryonic fibroblasts (MEFs), a primary mouse cell line. Although MEFs have lower PC4 protein levels than ES cells do, it seems this protein is very important for cell growth, because dramatically slower proliferation occurred after PC4 was knocked down. These data suggest that the effect of PC4 in proliferation is same. As MEFs are derived from late stage embryos (E13.5) and ES cells are from preimplantation embryos, one might suspect that PC4 functions differently in distinct developmental stages, especially because proliferation is so important in early embryonic stages. Moreover, the large amounts of PC4 exist in early developmental stages may suggest that it is more important for embryogenesis than for organogenesis.

Do carcinoma cell lines show similar phenotypes when PC4 is knocked down? We used a siRNA strategy for knocking down PC4 *in vivo*, and found that HeLa cells did not show any inhibition of proliferation with two different siRNAs targeting endogenous PC4. In contrast, A549 cells exhibited opposite effects following two different siRNA: one had no effect and the other reduced proliferation. HeLa cells contain no detectable p53 protein due to the degradation of endogenous E6 protein, whereas A549 cells express p53. Could it be that p53 was influenced to affect cell growth when PC4 was knocked down? This is one possibility, and another might be off-target effects of the siRNA-PC4-TK, recently reported by Das et al (Das et al. 2006). To clarify this issue, we have already tried a new siRNA pool targeting human PC4 consisting of a mixture of four siRNAs. The results showed that A549 cells did not proliferate slowly when PC4 was downregulated by this pool of siRNAs. Current ongoing research clearly answered the question of whether siRNA-PC4-TK has side effects. Taken together,

our results in carcinoma cell lines demonstrate that PC4 knock down did not alter proliferation, contrary to what happened in ES cells and MEFs. The reason for this difference appears to be incomplete deletion of PC4 carried out with siRNA in these cells. This abundant protein can apparently function very well even though only small amounts are left, which bodes well for the viability of hypomorphic PC4 knockout mice. Furthermore, PC4 might be substituted by other factors in somatic cell lines to rescue the deficiencies induced by PC4 knockdown.

4.5 Mechanisms underlying reduced proliferation upon loss of PC4

4.5.1 Loss of PC4 induced abnormal cell cycle, which inhibited cell proliferation.

All of the PC4 knockout ES cells derived from blastocysts showed similar morphologies and were slower to proliferate than wild-type ES cells. To understand how this phenotype arose, we performed cell cycle analyses. Surprisingly, one of the two PC4 knockout ES cell lines exhibited tetraploidy in about 30% of the cells, which is quite high compared with that found in wild-type ES cells. Polyploidy (e.g., tetraploidy, octaploidy) is observed in a large variety of both plant and animal cells during normal development or under stress, while aneuploidy is never detected in normal cells. Tetraploidy or aneuploidy can be induced by several signals and is prevalent in different forms of cancer cell lines. Because the PC4 KO ES cells proliferated with tetraploidy, we wondered whether the tetraploidy was a protective mechanism against stress, or rather a maladaptive response. Numerous studies have shown that normal diploid cells can be induced to undergo polyploidization via endomitosis. For example, hypertension can induce vascular smooth muscle cells and cardiac myocytes to become polyploid (Chobanian et al. 1984; Hixon et al. 2000). In these cases, polyploidy is believed to be a protective mechanism to prevent cellular proliferation. Similarly, based on the phenotype of PC4-depleted ES cells, we hypothesized that tetraploidy inhibits proliferation to compensate for mutations introduced by the knockout of PC4. In addition to tetraploidy, there might be other unknown pathways to coordinate this abnormal cell status.

Does PC4 regulate cyclin complexes to influence the cell cycle? It is reported that tetraploidy can be induced by the aberrant expression of proteins regulating the G2/M transition (Cyclin-B1, Aurora-A, Forkhead transcription factor, M3) (Hauf et al. 2003; Shin et al. 2003), or by mitotic spindle checkpoint proteins (BUBR1, Mad2, Aurora-B,

Survivin) (Barr et al. 2004; Meraldi et al. 2004), leading to abortive cytokinesis. Our qRT-PCR study showed that *CyclinE1* and C*dk2* were slightly downregulated upon PC4 depletion, *Ccna2* and *ccnd1* were unaffected, and *p21* was highly upregulated. It is reported that p21 plays an important role in regulating mitotic cell cycles and induces polyploidy together with p27 (Ullah et al. 2009). p27 is primarily responsible for preventing the cell from premature entrance into S-phase, a role that is common to mitotic cells and endocycles. p21 can facilitate this role and helps to prevent premature entrance into M-phase. The upregulation of p21 is responsible for DNA damage and maintenance of polyploidy cells, and is also involved in preventing polyploid cells from undergoing apoptosis through suppression of the checkpoint pathway. p21 is identified as a Cdk2 inhibitor, so the over-expression of p21 may also inhibit the activity of the Cdk2-CyclinE complex. As the Cdk2-CyclinE complex is constitutively active throughout the cell cycle in mouse ES cells, the diminished Cdk activity resulting from p21 inhibition may delay progression from G1 to S phase, thus lengthening overall generation times. Taken together, our experiments and those of others suggest that when PC4 is knocked out, cell cycle regulators are positively or negatively affected. PC4 takes part in many regulatory steps to maintain an orderly cell cycle. Once this balance is upset by the depletion of PC4, cells are under stress and try to adapt to their environment by adjusting the cell cycles.

4.5.2 Deletion of PC4 did not affect the expression of GTFs, but affected the transcription of cell growth- and death-related genes.

Based on the microarray data, deletion of PC4, a positive transcription cofactor, did not change the expressions of general transcription factors. The expressions of transcription factors that interact with PC4 in the basal transcription machinery, such as TFIIH and TFIIA, were not changed in PC4 knockout ES cells. These results indicate that the physiological deficit in PC4 did not correlate with those of other transcription factors, perhaps because the cofactor activities of PC4 may be substituted by other similar factors.

At the molecular level, many negatively regulated genes (e.g., *Rb1*) were expressed at higher levels upon PC4 deletion. Many genes related to cell death were also deregulated. Although the level of apoptosis in knockout ES cells was not different than that in wild-type cells, cell proliferation was inhibited upon deregulation of many genes involved in cellular growth processes, such as cell communication and metabolism. Many target gene promoters contain similar transcription factors: NFKB1,

STAT3, p53, Jun, and Fos, which are involved in the mitogen-activated protein kinase (MAPK) signaling pathway. The MAPKs are a group of serine/threonine protein kinases that are activated in response to a variety of extracellular stimuli and mediate signal transduction from the cell surface to the nucleus. In combination with several other signaling pathways, they can differentially alter the phosphorylation status of numerous proteins, including transcription factors, cytoskeletal proteins, kinases, and other enzymes, and greatly influence gene expression, metabolism, cell division, cell morphology, and cell survival. Therefore, we hypothesize that the mechanism underlying reduced proliferation following the loss of PC4, is that a large number of genes involved in the MAPK pathway were deregulated in their ability to modulate cell proliferation and metabolism.

4.5.3 P21 might be the key factor regulated by PC4 in the control of cell proliferation

Gene expression profiling showed that some miRNAs were downregulated when PC4 was depleted in ES cells. Could be these miRNAs involved in cell proliferation? Recent work from Robert Blelloch's laboratory described a role for mouse ES cell-specific miRNAs in establishing rapid cell cycles (Wang et al. 2008). The miRNAs they screened suppressed many key regulators of the G1/S transition to enable rapid proliferation in mouse ES cells. One miRNA, miR-20a, rescued the proliferation defects of *Dgcr8*$^{-/-}$ ES cells. Similarly, miR-20a was remarkably downregulated (1.63 fold downregulation) in our PC4 KO ES cells. Likewise, two other miRNAs, miR-17 and miR-467a, were also downregulated (1.75 and 2.87 fold decrease individually). Furthermore, *p21* was identified as a potential target of all three miRNAs by the computational program, Targetscan. In addition, qRT-PCR confirmed that *p21* transcription was enhanced in knockout cells (2.3 fold upregulation). Therefore, we hypothesized that PC4 might suppress p21 protein expression by enhancing the expression of miRNAs. Alternatively, PC4 may also directly regulate *p21* transcription by binding its promoter, a claim that is confirmed by a chromatin immunoprecipitation (ChIP) assay (performed by Jianming Xu, unpublished data). Furthermore, deletion of PC4 reduces the occupancy of Pol II and TBP in *p21* promoter, which implies PC4 is involved in regulation of p21 activation. Other inhibitors that play roles in the Cdk2/Cyclin E regulatory pathway, such as *Rb1* and *Lats2*, were also upregulated (2.5 and 1.4 fold upregulation individually) in PC4 knockout ES cells. Therefore, when PC4 was depleted, an increase in p21 together with other cell cycle inhibitors may delay

progression from G1 into S phase by restraining Cdk2/Cyclin E activity, thus lengthening overall generation times (Figure 34). Therefore, the rapid cell cycle in ES cells has been finally impaired and proliferation is reduced *in vivo*. One approach to confirm the key role of p21 in the PC4 regulation network is to knock down p21 in PC4 knockout ES cells. If the deletion of p21 rescues the reduced proliferation, the mechanism underlying the PC4 physiology function could be elucidated.

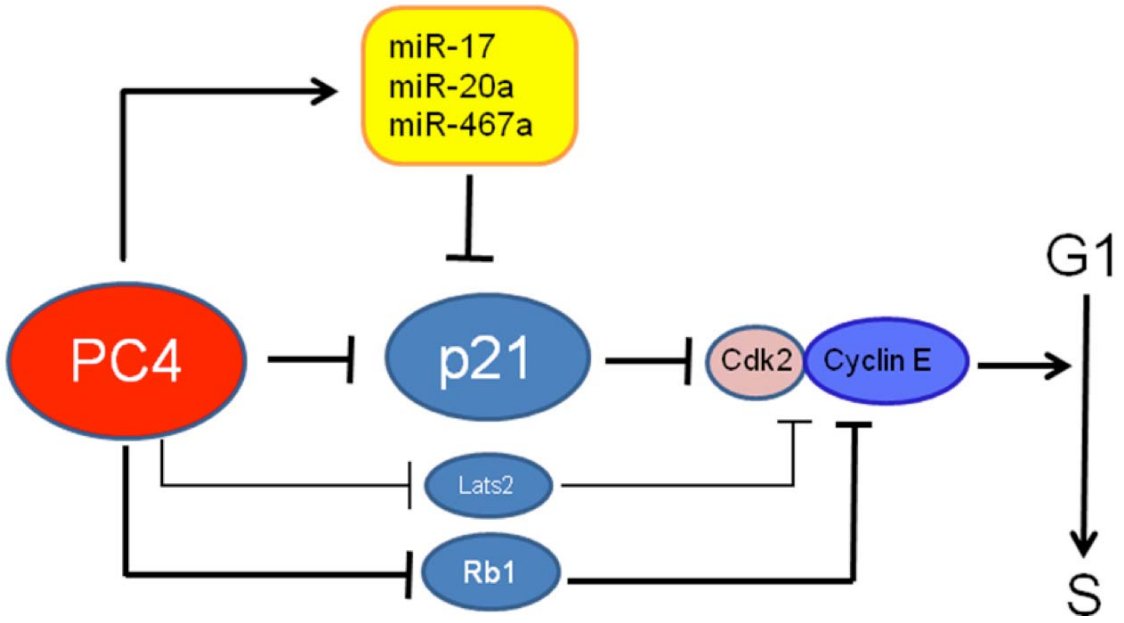

Figure 34: Proposed mechanism for PC4 regulation of G1 progression in mouse ES cells.
Mouse PC4 knockout ES cells exhibit high miRNA levels including miR-17, miR-20a and miR-467a, leading to elevated p21 protein level. Together with other upregulated Cdk2/Cyclin E pathway inhibitors (Lats2 and Rb1), the activity of Cdk2/Cyclin E is inhibited and progression from G1 to S phase is delayed, thus lengthening overall cell cycle time.

4.6 PC4 is required for differentiation

Because the differentiation of ES cells has been known to recapitulate changes in embryonic development, factors that have essential functions during early embryogenesis are also expected to be involved in the formation of embryoid bodies. Therefore, to characterize the role of PC4 in differentiation, we examined the potential of PC4 mutant cells to form embryoid bodies *in vitro*. Based on similar expressions of germ layer markers detected by RT-PCR, we concluded that the loss of PC4 did not influence the differentiation of ectoderm and endoderm tissues, but did affect mesoderm formation. In addition, pluripotency markers were still expressed in differentiated ES cells, probably due to incomplete differentiation *in vitro*. However, to

our surprise, qRT-PCR analysis in PC4 KO ES cells identified many ectoderm and mesoderm markers that were poorly expressed and some endoderm markers that were relatively overexpressed during embryoid body formation. Although RT-PCR and teratoma assays showed no effects of the knockout on differentiation, these results were probably due to the use of improper methodologies. The relatively low expression of ectoderm and mesoderm markers during knockout embryoid body formation *in vitro* and proper teratoma generation *in vivo*, indicate that PC4 plays a role in regulating differentiation and that the process was delayed somehow when PC4 was depleted. Therefore, we conclude that the delayed differentiation and reduced proliferation in the inner cell mass might result in the early embryo lethality observed in the PC4 knockout mice. To further explore differentiation defects in PC4 knockout ES cells, a microarray analysis should be performed on embryoid bodies. In addition, the histological analysis of PC4 mutant embryos at E5.5, E6.5, and E7.5 provide enough evidence to confirm that the early embryonic lethality is partially due to germ layer defects. In agreement with *in vitro* differentiation data, at E6.5 the embryonic ectoderm layer was thinner or unformed and the embryonic endoderm was not affected. At E7.5, no mesoderm layer was formed in PC4 knockout embryos, confirming observations made in the embryoid body differentiation assays. Taken together, these data suggest that PC4 is required for embryonic ectoderm, mesoderm, and endoderm formation in early embryonic developmental stages.

The gene profiling analysis also gave some clues to predict the function of PC4 in differentiation. From the microarray data, it is possible to conclude that the deletion of PC4 in ES cells may contribute to self-renewal and prevent the differentiation of specific cell lineages. This idea is supported by the upregulation of *STAT3* (1.26 fold) and *ID1* (1.53 fold) upon loss of PC4 in ES cells. Furthermore, *STAT3* is the target gene of the miR-17 family of miRNAs, which are differentially expressed during early mouse embryo development and is involved in stem cell differentiation. Thus, the downregulation of the miR-17 family of miRNAs including miR-17 (1.75 fold), and miR-20a (1.63 fold) triggered the possible self-renewal of their target genes, which are linked with STAT3 and bone morphogenetic protein (BMP) self-renewal pathways. The consequence of this is that the ES cells don't differentiate well. However, the upregulation of *Smad7* (1.56 fold), another target of the miR-17 family, antagonizes BMP signaling and induces differentiation. By contrast, downregulation of *T* (2.3 fold) limits mesoderm specification, which was confirmed by our embryoid body differentiation assays. Surprisingly, the gene *Neurod1* is highly expressed in PC4 null ES cells, which indicates these cells can differentiate towards endocrine lineages

(Marchand et al. 2009) and neurons**.** This is also supported by our embryoid body differentiation assays, which showed that *Nestin* expression was fast and high in PC4 knockout embryoid bodies. Taken together, our data and that of others suggest that the STAT3 and BMP signaling pathways were deregulated by PC4 in KO cells, which finally altered their fates.

4.7 Human PC4 can functionally replace its mouse counterpart

To rule out the possibility that the low growth phenotype of PC4 KO ES cells was attributed to the carry over of automatic genetic mutations during *in vitro* derivation, we rescued PC4 null ES cells by transfecting them with human EGFP-PC4 fusion protein. $PC4^{-/-}$ ES cells expressing the hPC4-EGFP fusion protein proliferated faster than vector-transfected PC4 null cells, showing that human PC4 (hPC4) can functionally replace mouse PC4 in mouse ES cell lines and suggesting that hPC4 can enter into the various murine PC4-containing complexes. This is in good agreement with the high homology between the mouse and human proteins. However, the proliferation of rescued PC4 KO ES cells was still slightly slower than that of the wild-type cells. This partial rescue might reflect the functional difference between the human fusion protein and the mouse protein. In addition, low transfection efficiency might be another reason for the partial rescue. The PC4 null ES cells also exhibited inhibited proliferation, which might have been due to deregulation of the network of growth signals. Even though a functional PC4 protein was reintroduced into the null ES cells, the low growth of the cells could not be completely reversed, possibly due to pre-established damage, such as epigenetic changes. In other words, PC4 is important for maintaining the homeostasis of the cells. Once this homeostasis is broken down, the cells are under stress and some permanent damages might occur to compensate for the abnormal status.

4.8 PC4 and DNA damage

4.8.1 Loss of PC4 doesn’t inhibit p53 activation in ES cells

The tumor repressor p53 can be activated in response to stress, for example DNA damage, and cause cell cycle arrest, DNA repair, and apoptosis. It was reported that PC4 could activate p53 and facilitate its DNA binding ability. In addition, the activation of p53 by PC4 is dependent on their physical interaction, DNA binding, and posttranslational modifications. Furthermore, the expression of PC4 is also regulated

by p53, which means PC4 is a p53-responsive gene. As all the above results were gathered from somatic cell lines (e.g., A549, H1299), and there was previously no evidence to show whether p53 was activated while PC4 was downregulated, we addressed this issue with our PC4 null ES cells. Surprisingly, depletion of PC4 did not influence either the expression or the phosphorylation of p53. Additionally, transcription of the p53 target genes *p21* and *MDM2* were enhanced following p53 induction due to genotoxic insult in PC4 KO ES cells. These results clearly indicated that PC4 was not functionally associated with p53, at least not in ES cells. This might be because pluripotent ES cells have their own specific players in p53 activation that are far different from those in somatic cells. Even though PC4 did not affect p53 activation, PC4 appeared to weaken the expression of p53 and its target genes. In contrast to wild-type ES cells, the expressions of *p53*, *p21*, and *Mdm2*, but not *Bax*, were slightly increased in PC4 null ES cells. Actually, *p21* was already upregulated in PC4 KO ES cells even before doxorubicin treatment. Therefore, it is possible that when PC4 is deleted, ES cells become more sensitive to stress signals, and to some degree, PC4 could be thought of as safeguarding the stable physiological situation of the cell for normal growth.

For ES cells, maintaining self-renewal is very important, and is controlled by Oct4, Nanog, and other transcription factors. During embryonic stem cell differentiation, Oct4 and Nanog expressions are downregulated; however, if cells constitutively express Nanog, differentiation is inhibited. If, for example, ES cells are exposed to a DNA damage-inducing drug, p53 binds to Nanog to suppress its expression, which induces differentiation. In our PC4-depleted ES cells, Nanog was largely downregulated upon doxorubicin treatment, similar to what happened in wild-type ES cells. But the level of Oct4 did not change so much in response to the DNA damage. Therefore, we predict that PC4 null ES cells are prone to differentiate upon p53 activation induced by DNA damage.

4.8.2 PC4 is involved in DNA damage response from yeast to mammals

Absence of the PC4 yeast homologue SUB1 renders the cells to undergo spontaneous and peroxide-induced hypermutability, suggesting the importance of PC4 expression under DNA-damaging conditions (Wang et al. 2004). If the HOG pathway fails, SUB1 becomes important to ensure survivals under osmotic stress. This is because the cell turns to an alternative pathway that makes use of SUB1 to target Pol II to enhance the expression of the necessary osmoresponse genes (Rosonina et al. 2009). All these imply PC4 may play a role in response to stress signals probably due to its DNA repair

activity. In our study, we proved that PC4 can be recruitment to the DNA damage site independent of poly (ADP-ribosyl)ation and phosphorylation of H2AX, but it functions in the very early steps of the DNA damage response. Although knockdown of PC4 in HeLa cells didn't show elevated DNA damage because of the low efficiency and short term of the knockdown treatment (data unpublished), it is expected that the repair function of PC4 is important for DNA damage response because it was observed to be recruited to the DNA damage sites. In our PC4 knockout ES cell model, we found slight enhancement of p53 dependent gene activation and increase of membrane damage (based on the observation), which implies PC4 might be important for sensing and signaling DNA damage. Probably the early embryo lethality of PC4 knockout embryos is due to the increasing of the DNA damage upon loss of PC4. Taken together, the DNA repair activity from yeast to mammals is consistent and important for normal cell growth and development of the mammals.

4.9 PC4 regulates **Pol III-dependent transcription *in vivo***

Pol I and III are specialized for transcribing only non-coding RNAs, which contribute up to 80% of all nuclear transcription in rapidly growing cells. Moreover, tRNA, 18S, 5.8S, 28S, and 5S rRNAs transcribed by Pol I and Pol III can comprise as much as 95% of the RNA content of a cell. Pol III regulates Pol II transcription by synthesizing *7SK*, *Alu*, and *B2* RNAs. In our PC4-deficient ES cells, Pol I-dependent transcription of rRNAs was not affected, whereas Pol III-dependent 5S rRNA, 7SK and U6snRNA transcriptions were enhanced, the latter indicating that PC4 might repress Pol III-dependent transcription. Tumor suppressors are able to inhibit transcription by Pol I and Pol III. For example, while p53 represses Pol III transcription, the p53 substitution mutation R175H (the most common p53 mutation in tumors) converts p53 from a repressor to an activator of Pol III transcription (Chesnokov et al. 1996; Cairns and White 1998; Stein et al. 2002; Crighton et al. 2003; Gridasova and Henry 2005; Morton et al. 2007). As PC4 is a potential tumor repressor, Pol III transcription should be increased when PC4 is reduced, but this issue needs to be carefully tested again by checking the transcription levels of other non-coding RNAs in PC4 KO cells. In contrast to PC4 KO ES cells, PC4 knockdown MEFs exhibited downregulation of Pol III transcription and almost no change in Pol I transcription. One explanation for the different Pol III responses in ES cells and MEFs is that PC4 depletion directly inhibits Pol III-dependent transcription as does SUB1 in yeast, but the ES cells try to circumvent this defect, leading to the overregulation of Pol III-dependent transcription.

Can the inappropriate expressions of the products of Pol III transcription in PC4 KO ES cells and knockdown MEFs have detrimental consequences, such as the abnormal proliferation we observed? Maf1, an essential mediator of Pol III repression in response to starvation in *Saccharomyces cerevisiae*, can repress Pol I- and Pol III-dependent tRNA and rRNA gene activity (Johnson et al. 2007), which causes anchorage-independent growth inhibition and cell morphology alternation. In view of this, one can hypothesize that the strikingly slower growth of PC4 KO ES cells and knockdown MEFs is due, in part, to the deregulation of Pol III. Although Manley's group claimed that SUB1, the yeast homolog of PC4, positively regulates Pol III recruitment to its target genes, which is contradictory to the PC4 repression effects seen in our mouse ES cells but in agree with the effect in MEFs, the role of PC4 in transcription other than that of only Pol II was confirmed by our studies (Rosonina et al. 2009).

4.10 Conclusions

To summarize the possible mechanisms underlying the phenotype upon loss of *in vivo*, the following diagram can be drawn (Figure 35). *In vivo*, PC4 is critical for mouse early embryo development. Loss of PC4 results in early embryo lethality via decreasing cell proliferation and impairing differentiation. Based on the gene expression analysis, many mechanisms underlying reduced proliferation were proposed, including abnormal cell cycle, deregulation of MAPK pathway and Pol III transcription. Furthermore, increase of DNA damage upon PC4 depletion may also lead to failure in early development of PC4 knockout embryos.

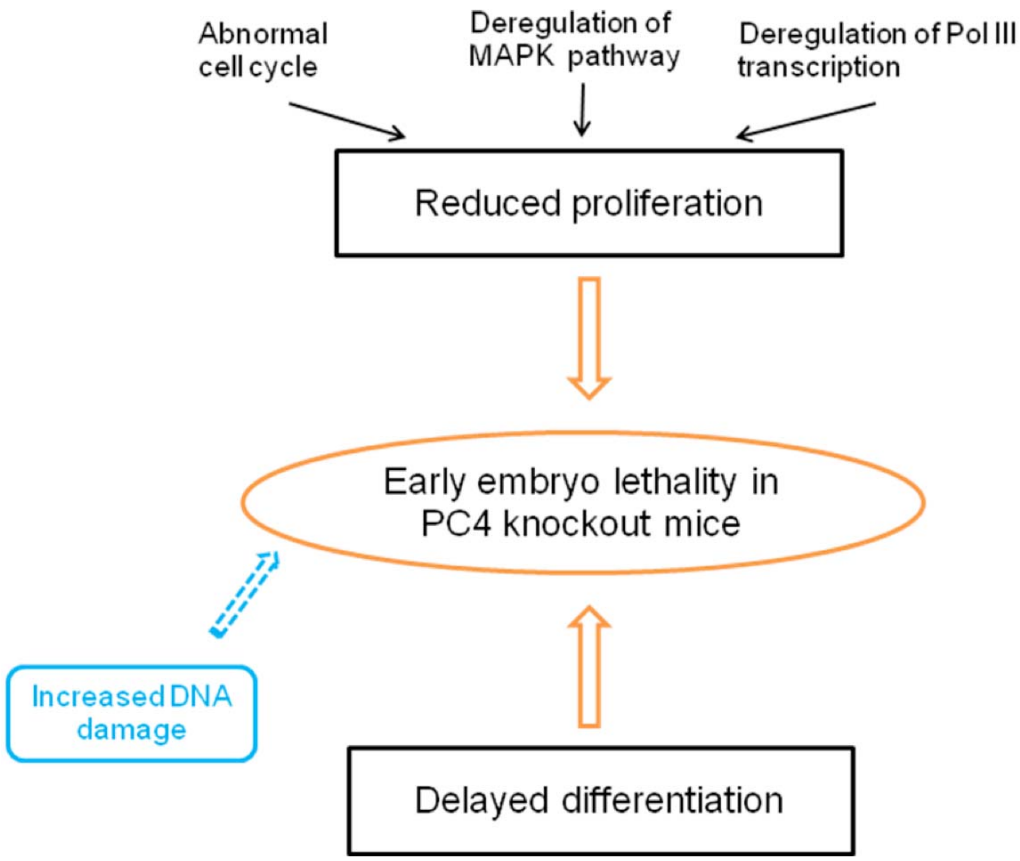

Figure 35: Diagram of possible mechanisms underlying early embryo lethal phenotype of PC4 knockout mice.

5. REFERENCES

Albert TK, Grote K, Boeing S, Stelzer G, Schepers A et al. (2007) Global distribution of negative cofactor 2 subunit-alpha on human promoters. Proc Natl Acad Sci U S A 104(24): 10000-10005.

Asturias FJ (2004) RNA polymerase II structure, and organization of the preinitiation complex. Curr Opin Struct Biol 14(2): 121-129.

Banerjee S, Kumar BR, Kundu TK (2004) General transcriptional coactivator PC4 activates p53 function. Mol Cell Biol 24(5): 2052-2062.

Barr FA, Sillje HH, Nigg EA (2004) Polo-like kinases and the orchestration of cell division. Nat Rev Mol Cell Biol 5(6): 429-440.

Batta K, Kundu TK (2007) Activation of p53 function by human transcriptional coactivator PC4: role of protein-protein interaction, DNA bending, and posttranslational modifications. Mol Cell Biol 27(21): 7603-7614.

Batta K, Yokokawa M, Takeyasu K, Kundu TK (2009) Human transcriptional coactivator PC4 stimulates DNA end joining and activates DSB repair activity. J Mol Biol 385(3): 788-799.

Bjorklund S, Gustafsson CM (2004) The mediator complex. Adv Protein Chem 67: 43-65.

Blazek E, Mittler G, Meisterernst M (2005) The mediator of RNA polymerase II. Chromosoma 113(8): 399-408.

Bode J, Schlake T, Iber M, Schubeler D, Seibler J et al. (2000) The transgeneticist's toolbox: novel methods for the targeted modification of eukaryotic genomes. Biol Chem 381(9-10): 801-813.

Brandsen J, Werten S, van der Vliet PC, Meisterernst M, Kroon J et al. (1997) C-terminal domain of transcription cofactor PC4 reveals dimeric ssDNA binding site. Nat Struct Biol 4(11): 900-903.

Brasset E, Vaury C (2005) Insulators are fundamental components of the eukaryotic genomes. Heredity 94(6): 571-576.

Brook FA, Gardner RL (1997) The origin and efficient derivation of embryonic stem cells in the mouse. Proc Natl Acad Sci U S A 94(11): 5709-5712.

Burns TF, Fei P, Scata KA, Dicker DT, El-Deiry WS (2003) Silencing of the novel p53 target gene Snk/Plk2 leads to mitotic catastrophe in paclitaxel (taxol)-exposed cells. Mol Cell Biol 23(16): 5556-5571.

Cairns CA, White RJ (1998) p53 is a general repressor of RNA polymerase III transcription. Embo J 17(11): 3112-3123.

Calvo O, Manley JL (2001) Evolutionarily conserved interaction between CstF-64 and PC4 links transcription, polyadenylation, and termination. Mol Cell 7(5): 1013-1023.

Calvo O, Manley JL (2005) The transcriptional coactivator PC4/Sub1 has multiple functions in RNA polymerase II transcription. Embo J 24(5): 1009-1020.

Chapman RD, Heidemann M, Albert TK, Mailhammer R, Flatley A et al. (2007) Transcribing RNA polymerase II is phosphorylated at CTD residue serine-7. Science 318(5857): 1780-1782.

Chesnokov I, Chu WM, Botchan MR, Schmid CW (1996) p53 inhibits RNA polymerase III-directed transcription in a promoter-dependent manner. Mol Cell Biol 16(12): 7084-7088.

Chobanian AV, Prescott MF, Haudenschild CC (1984) Recent advances in molecular pathology. The effects of hypertension on the arterial wall. Exp Mol Pathol 41(1): 153-169.

Contreras-Levicoy J, Urbina F, Maldonado E (2008) Schizosaccharomyces pombe positive cofactor 4 stimulates basal transcription from TATA-containing and TATA-less promoters through Mediator and transcription factor IIA. Febs J 275(11): 2873-2883.

Corradetti MN, Inoki K, Guan KL (2005) The stress-inducted proteins RTP801 and RTP801L are negative regulators of the mammalian target of rapamycin pathway. J Biol Chem 280(11): 9769-9772.

Cramer P (2004) RNA polymerase II structure: from core to functional complexes. Curr Opin Genet Dev 14(2): 218-226.

Cramer P, Bushnell DA, Fu J, Gnatt AL, Maier-Davis B et al. (2000) Architecture of RNA polymerase II and implications for the transcription mechanism. Science 288(5466): 640-649.

Crighton D, Woiwode A, Zhang C, Mandavia N, Morton JP et al. (2003) p53 represses RNA polymerase III transcription by targeting TBP and inhibiting promoter occupancy by TFIIIB. Embo J 22(11): 2810-2820.

Das C, Hizume K, Batta K, Kumar BR, Gadad SS et al. (2006) Transcriptional coactivator PC4, a chromatin-associated protein, induces chromatin condensation. Mol Cell Biol 26(22): 8303-8315.

Deng W, Roberts SG (2005) A core promoter element downstream of the TATA box that is recognized by TFIIB. Genes Dev 19(20): 2418-2423.

Egloff S, O'Reilly D, Chapman RD, Taylor A, Tanzhaus K et al. (2007) Serine-7 of the RNA polymerase II CTD is specifically required for snRNA gene expression. Science 318(5857): 1777-1779.

Eisen MB, Spellman PT, Brown PO, Botstein D (1998) Cluster analysis and display of genome-wide expression patterns. Proc Natl Acad Sci U S A 95(25): 14863-14868.

Evans MJ, Kaufman MH (1981) Establishment in culture of pluripotential cells from mouse embryos. Nature 292(5819): 154-156.

Feaver WJ, Gileadi O, Li Y, Kornberg RD (1991) CTD kinase associated with yeast RNA polymerase II initiation factor b. Cell 67(6): 1223-1230.

Fondell JD, Guermah M, Malik S, Roeder RG (1999) Thyroid hormone receptor-associated proteins and general positive cofactors mediate thyroid hormone receptor function in the absence of the TATA box-binding protein-associated factors of TFIID. Proc Natl Acad Sci U S A 96(5): 1959-1964.

Frank DU, Fotheringham LK, Brewer JA, Muglia LJ, Tristani-Firouzi M et al. (2002) An Fgf8 mouse mutant phenocopies human 22q11 deletion syndrome. Development 129(19): 4591-4603.

Fukuda A, Tokonabe S, Hamada M, Matsumoto M, Tsukui T et al. (2003) Alleviation of PC4-mediated transcriptional repression by the ERCC3 helicase activity of general transcription factor TFIIH. J Biol Chem 278(17): 14827-14831.

Fukuda A, Nakadai T, Shimada M, Tsukui T, Matsumoto M et al. (2004) Transcriptional coactivator PC4 stimulates promoter escape and facilitates transcriptional synergy by GAL4-VP16. Mol Cell Biol 24(14): 6525-6535.

Ge H, Roeder RG (1994) Purification, cloning, and characterization of a human coactivator, PC4, that mediates transcriptional activation of class II genes. Cell 78(3): 513-523.

Ge H, Zhao Y, Chait BT, Roeder RG (1994) Phosphorylation negatively regulates the function of coactivator PC4. Proc Natl Acad Sci U S A 91(26): 12691-12695.

Goppelt A, Meisterernst M (1996) Characterization of the basal inhibitor of class II transcription NC2 from Saccharomyces cerevisiae. Nucleic Acids Res 24(22): 4450-4455.

Goppelt A, Stelzer G, Lottspeich F, Meisterernst M (1996) A mechanism for repression of class II gene transcription through specific binding of NC2 to TBP-promoter complexes via heterodimeric histone fold domains. Embo J 15(12): 3105-3116.

Gridasova AA, Henry RW (2005) The p53 tumor suppressor protein represses human snRNA gene transcription by RNA polymerases II and III independently of sequence-specific DNA binding. Mol Cell Biol 25(8): 3247-3260.

Guermah M, Malik S, Roeder RG (1998) Involvement of TFIID and USA components in transcriptional activation of the human immunodeficiency virus promoter by NF-kappaB and Sp1. Mol Cell Biol 18(6): 3234-3244.

Guo H, Gao C, Mi Z, Zhang J, Kuo PC (2007) Characterization of the PC4 binding domain and its interactions with HNF4alpha. J Biochem 141(5): 635-640.

Haile DT, Parvin JD (1999) Activation of transcription in vitro by the BRCA1 carboxyl-terminal domain. J Biol Chem 274(4): 2113-2117.

Halle JP, Stelzer G, Goppelt A, Meisterernst M (1995) Activation of transcription by recombinant upstream stimulatory factor 1 is mediated by a novel positive cofactor. J Biol Chem 270(36): 21307-21311.

Hamatani T, Ko M, Yamada M, Kuji N, Mizusawa Y et al. (2006) Global gene expression profiling of preimplantation embryos. Hum Cell 19(3): 98-117.

Hauf S, Cole RW, LaTerra S, Zimmer C, Schnapp G et al. (2003) The small molecule Hesperadin reveals a role for Aurora B in correcting kinetochore-microtubule attachment and in maintaining the spindle assembly checkpoint. J Cell Biol 161(2): 281-294.

He X, Khan AU, Cheng H, Pappas DL, Jr., Hampsey M et al. (2003) Functional interactions between the transcription and mRNA 3' end processing machineries mediated by Ssu72 and Sub1. Genes Dev 17(8): 1030-1042.

Heng HH, Goetze S, Ye CJ, Liu G, Stevens JB et al. (2004) Chromatin loops are selectively anchored using scaffold/matrix-attachment regions. J Cell Sci 117(Pt 7): 999-1008.

Henry NL, Bushnell DA, Kornberg RD (1996) A yeast transcriptional stimulatory protein similar to human PC4. J Biol Chem 271(36): 21842-21847.

Hixon ML, Obejero-Paz C, Muro-Cacho C, Wagner MW, Millie E et al. (2000) Cks1 mediates vascular smooth muscle cell polyploidization. J Biol Chem 275(51): 40434-40442.

Holloway AF, Occhiodoro F, Mittler G, Meisterernst M, Shannon MF (2000) Functional interaction between the HIV transactivator Tat and the transcriptional coactivator PC4 in T cells. J Biol Chem 275(28): 21668-21677.

Hossain GS, van Thienen JV, Werstuck GH, Zhou J, Sood SK et al. (2003) TDAG51 is induced by homocysteine, promotes detachment-mediated programmed cell death, and contributes to the cevelopment of atherosclerosis in hyperhomocysteinemia. J Biol Chem 278(32): 30317-30327.

Hu T, Yamagishi H, Maeda J, McAnally J, Yamagishi C et al. (2004) Tbx1 regulates fibroblast growth factors in the anterior heart field through a reinforcing autoregulatory loop involving forkhead transcription factors. Development 131(21): 5491-5502.

Inostroza JA, Mermelstein FH, Ha I, Lane WS, Reinberg D (1992) Dr1, a TATA-binding protein-associated phosphoprotein and inhibitor of class II gene transcription. Cell 70(3): 477-489.

Ito M, Okano HJ, Darnell RB, Roeder RG (2002) The TRAP100 component of the TRAP/Mediator complex is essential in broad transcriptional events and development. Embo J 21(13): 3464-3475.

Ito M, Yuan CX, Okano HJ, Darnell RB, Roeder RG (2000) Involvement of the TRAP220 component of the TRAP/SMCC coactivator complex in embryonic development and thyroid hormone action. Mol Cell 5(4): 683-693.

Jayaraman L, Moorthy NC, Murthy KG, Manley JL, Bustin M et al. (1998) High mobility group protein-1 (HMG-1) is a unique activator of p53. Genes Dev 12(4): 462-472.

Johnson SS, Zhang C, Fromm J, Willis IM, Johnson DL (2007) Mammalian Maf1 is a negative regulator of transcription by all three nuclear RNA polymerases. Mol Cell 26(3): 367-379.

Jonker HR, Wechselberger RW, Boelens R, Folkers GE, Kaptein R (2005) Structural properties of the promiscuous VP16 activation domain. Biochemistry 44(3): 827-839.

Jonker HR, Wechselberger RW, Pinkse M, Kaptein R, Folkers GE (2006) Gradual phosphorylation regulates PC4 coactivator function. Febs J 273(7): 1430-1444.

Kaiser K, Stelzer G, Meisterernst M (1995) The coactivator p15 (PC4) initiates transcriptional activation during TFIIA-TFIID-promoter complex formation. Embo J 14(14): 3520-3527.

Kannan P, Tainsky MA (1999) Coactivator PC4 mediates AP-2 transcriptional activity and suppresses ras-induced transformation dependent on AP-2 transcriptional interference. Mol Cell Biol 19(1): 899-908.

Kim YJ, Bjorklund S, Li Y, Sayre MH, Kornberg RD (1994) A multiprotein mediator of transcriptional activation and its interaction with the C-terminal repeat domain of RNA polymerase II. Cell 77(4): 599-608.

Kishore AH, Batta K, Das C, Agarwal S, Kundu TK (2007) p53 regulates its own activator: transcriptional co-activator PC4, a new p53-responsive gene. Biochem J 406(3): 437-444.

Knaus R, Pollock R, Guarente L (1996) Yeast SUB1 is a suppressor of TFIIB mutations and has homology to the human co-activator PC4. Embo J 15(8): 1933-1940.

Koleske AJ, Young RA (1994) An RNA polymerase II holoenzyme responsive to activators. Nature 368(6470): 466-469.

Kornberg RD, Lorch Y (2002) Chromatin and transcription: where do we go from here. Curr Opin Genet Dev 12(2): 249-251.

Kretzschmar M, Meisterernst M, Roeder RG (1993) Identification of human DNA topoisomerase I as a cofactor for activator-dependent transcription by RNA polymerase II. Proc Natl Acad Sci U S A 90(24): 11508-11512.

Kretzschmar M, Kaiser K, Lottspeich F, Meisterernst M (1994) A novel mediator of class II gene transcription with homology to viral immediate-early transcriptional regulators. Cell 78(3): 525-534.

Kuhn R, Schwenk F, Aguet M, Rajewsky K (1995) Inducible gene targeting in mice. Science 269(5229): 1427-1429.

Kumar BR, Swaminathan V, Banerjee S, Kundu TK (2001) p300-mediated acetylation of human transcriptional coactivator PC4 is inhibited by phosphorylation. J Biol Chem 276(20): 16804-16809.

Kunath T, Strumpf D, Rossant J (2004) Early trophoblast determination and stem cell maintenance in the mouse--a review. Placenta 25 Suppl A: S32-38.

Lagrange T, Kapanidis AN, Tang H, Reinberg D, Ebright RH (1998) New core promoter element in RNA polymerase II-dependent transcription: sequence-specific DNA binding by transcription factor IIB. Genes Dev 12(1): 34-44.

Landry J, Sharov AA, Piao Y, Sharova LV, Xiao H et al. (2008) Essential role of chromatin remodeling protein Bptf in early mouse embryos and embryonic stem cells. PLoS Genet 4(10): e1000241.

Lewis BA, Sims RJ, 3rd, Lane WS, Reinberg D (2005) Functional characterization of core promoter elements: DPE-specific transcription requires the protein kinase CK2 and the PC4 coactivator. Mol Cell 18(4): 471-481.

Lin T, Chao C, Saito S, Mazur SJ, Murphy ME et al. (2005) p53 induces differentiation of mouse embryonic stem cells by suppressing Nanog expression. Nat Cell Biol 7(2): 165-171.

Loebel DA, Watson CM, De Young RA, Tam PP (2003) Lineage choice and differentiation in mouse embryos and embryonic stem cells. Dev Biol 264(1): 1-14.

Lu CC, Brennan J, Robertson EJ (2001) From fertilization to gastrulation: axis formation in the mouse embryo. Curr Opin Genet Dev 11(4): 384-392.

Luo Y, Ge H, Stevens S, Xiao H, Roeder RG (1998) Coactivation by OCA-B: definition of critical regions and synergism with general cofactors. Mol Cell Biol 18(7): 3803-3810.

Malik S, Guermah M, Roeder RG (1998) A dynamic model for PC4 coactivator function in RNA polymerase II transcription. Proc Natl Acad Sci U S A 95(5): 2192-2197.

Malik S, Gu W, Wu W, Qin J, Roeder RG (2000) The USA-derived transcriptional coactivator PC2 is a submodule of TRAP/SMCC and acts synergistically with other PCs. Mol Cell 5(4): 753-760.

Marchand M, Schroeder IS, Markossian S, Skoudy A, Negre D et al. (2009) Mouse ES cells over-expressing the transcription factor NeuroD1 show increased differentiation towards endocrine lineages and insulin-expressing cells. Int J Dev Biol 53(4): 569-578.

Martin GR (1981) Isolation of a pluripotent cell line from early mouse embryos cultured in medium conditioned by teratocarcinoma stem cells. Proc Natl Acad Sci U S A 78(12): 7634-7638.

Matsumoto T, Eki T, Hurwitz J (1990) Studies on the initiation and elongation reactions in the simian virus 40 DNA replication system. Proc Natl Acad Sci U S A 87(24): 9712-9716.

Mayer W, Smith A, Fundele R, Haaf T (2000a) Spatial separation of parental genomes in preimplantation mouse embryos. J Cell Biol 148(4): 629-634.

Mayer W, Niveleau A, Walter J, Fundele R, Haaf T (2000b) Demethylation of the zygotic paternal genome. Nature 403(6769): 501-502.

Meinhart A, Kamenski T, Hoeppner S, Baumli S, Cramer P (2005) A structural perspective of CTD function. Genes Dev 19(12): 1401-1415.

Meisterernst M, Roeder RG (1991) Family of proteins that interact with TFIID and regulate promoter activity. Cell 67(3): 557-567.

Meisterernst M, Stelzer G, Roeder RG (1997) Poly(ADP-ribose) polymerase enhances activator-dependent transcription in vitro. Proc Natl Acad Sci U S A 94(6): 2261-2265.

Meisterernst M, Roy AL, Lieu HM, Roeder RG (1991) Activation of class II gene transcription by regulatory factors is potentiated by a novel activity. Cell 66(5): 981-993.

Meraldi P, Honda R, Nigg EA (2004) Aurora kinases link chromosome segregation and cell division to cancer susceptibility. Curr Opin Genet Dev 14(1): 29-36.

Merino A, Madden KR, Lane WS, Champoux JJ, Reinberg D (1993) DNA topoisomerase I is involved in both repression and activation of transcription. Nature 365(6443): 227-232.

Mermelstein F, Yeung K, Cao J, Inostroza JA, Erdjument-Bromage H et al. (1996) Requirement of a corepressor for Dr1-mediated repression of transcription. Genes Dev 10(8): 1033-1048.

Mittler G, Stuhler T, Santolin L, Uhlmann T, Kremmer E et al. (2003) A novel docking site on Mediator is critical for activation by VP16 in mammalian cells. Embo J 22(24): 6494-6504.

Miyashita T, Reed JC (1995) Tumor suppressor p53 is a direct transcriptional activator of the human bax gene. Cell 80(2): 293-299.

Morton JP, Kantidakis T, White RJ (2007) RNA polymerase III transcription is repressed in response to the tumour suppressor ARF. Nucleic Acids Res 35(9): 3046-3052.

Mortusewicz O, Roth W, Li N, Cardoso MC, Meisterernst M et al. (2008) Recruitment of RNA polymerase II cofactor PC4 to DNA damage sites. J Cell Biol 183(5): 769-776.

Murakami Y, Eki T, Hurwitz J (1992) Studies on the initiation of simian virus 40 replication in vitro: RNA primer synthesis and its elongation. Proc Natl Acad Sci U S A 89(3): 952-956.

Myers LC, Kornberg RD (2000) Mediator of transcriptional regulation. Annu Rev Biochem 69: 729-749.

Nakamura T, Arai Y, Umehara H, Masuhara M, Kimura T et al. (2007) PGC7/Stella protects against DNA demethylation in early embryogenesis. Nat Cell Biol 9(1): 64-71.

Niwa H, Miyazaki J, Smith AG (2000) Quantitative expression of Oct-3/4 defines differentiation, dedifferentiation or self-renewal of ES cells. Nat Genet 24(4): 372-376.

Orphanides G, Reinberg D (2002) A unified theory of gene expression. Cell 108(4): 439-451.

Orphanides G, Lagrange T, Reinberg D (1996) The general transcription factors of RNA polymerase II. Genes Dev 10(21): 2657-2683.

Palancade B, Bensaude O (2003) Investigating RNA polymerase II carboxyl-terminal domain (CTD) phosphorylation. Eur J Biochem 270(19): 3859-3870.

Pan ZQ, Ge H, Amin AA, Hurwitz J (1996) Transcription-positive cofactor 4 forms complexes with HSSB (RPA) on single-stranded DNA and influences HSSB-dependent enzymatic synthesis of simian virus 40 DNA. J Biol Chem 271(36): 22111-22116.

Payer B, Saitou M, Barton SC, Thresher R, Dixon JP et al. (2003) Stella is a maternal effect gene required for normal early development in mice. Curr Biol 13(23): 2110-2117.

Pham CT, MacIvor DM, Hug BA, Heusel JW, Ley TJ (1996) Long-range disruption of gene expression by a selectable marker cassette. Proc Natl Acad Sci U S A 93(23): 13090-13095.

Pontano LL, Aggarwal P, Barbash O, Brown EJ, Bassing CH et al. (2008) Genotoxic stress-induced cyclin D1 phosphorylation and proteolysis are required for genomic stability. Mol Cell Biol 28(23): 7245-7258.

Qureshi SA, Jackson SP (1998) Sequence-specific DNA binding by the S. shibatae TFIIB homolog, TFB, and its effect on promoter strength. Mol Cell 1(3): 389-400.

Rajagopalan S, Andreeva A, Teufel DP, Freund SM, Fersht AR (2009) Interaction between the transactivation domain of p53 and PC4 exemplifies acidic activation domains as single-stranded DNA mimics. J Biol Chem 284(32): 21728-21737.

Rebuzzini P, Neri T, Mazzini G, Zuccotti M, Redi CA et al. (2008) Karyotype analysis of the euploid cell population of a mouse embryonic stem cell line revealed a high incidence of chromosome abnormalities that varied during culture. Cytogenet Genome Res 121(1): 18-24.

Rodriguez CI, Buchholz F, Galloway J, Sequerra R, Kasper J et al. (2000) High-efficiency deleter mice show that FLPe is an alternative to Cre-loxP. Nat Genet 25(2): 139-140.

Roeder RG, Rutter WJ (1969) Multiple forms of DNA-dependent RNA polymerase in eukaryotic organisms. Nature 224(5216): 234-237.

Rosonina E, Willis IM, Manley JL (2009) Sub1 functions in osmoregulation and in transcription by both RNA polymerases II and III. Mol Cell Biol 29(8): 2308-2321.

Santos F, Hendrich B, Reik W, Dean W (2002) Dynamic reprogramming of DNA methylation in the early mouse embryo. Dev Biol 241(1): 172-182.

Santos F, Peters AH, Otte AP, Reik W, Dean W (2005) Dynamic chromatin modifications characterise the first cell cycle in mouse embryos. Dev Biol 280(1): 225-236.

Schang LM, Hwang GJ, Dynlacht BD, Speicher DW, Bantly A et al. (2000) Human PC4 is a substrate-specific inhibitor of RNA polymerase II phosphorylation. J Biol Chem 275(9): 6071-6074.

Scherf M, Epple A, Werner T (2005) The next generation of literature analysis: integration of genomic analysis into text mining. Brief Bioinform 6(3): 287-297.

Schluesche P, Stelzer G, Piaia E, Lamb DC, Meisterernst M (2007) NC2 mobilizes TBP on core promoter TATA boxes. Nat Struct Mol Biol 14(12): 1196-1201.

Schnutgen F, Doerflinger N, Calleja C, Wendling O, Chambon P et al. (2003) A directional strategy for monitoring Cre-mediated recombination at the cellular level in the mouse. Nat Biotechnol 21(5): 562-565.

Schwartz GK, Shah MA (2005) Targeting the cell cycle: a new approach to cancer therapy. J Clin Oncol 23(36): 9408-9421.

Schwenk F, Baron U, Rajewsky K (1995) A cre-transgenic mouse strain for the ubiquitous deletion of loxP-flanked gene segments including deletion in germ cells. Nucleic Acids Res 23(24): 5080-5081.

Shin HJ, Baek KH, Jeon AH, Park MT, Lee SJ et al. (2003) Dual roles of human BubR1, a mitotic checkpoint kinase, in the monitoring of chromosomal instability. Cancer Cell 4(6): 483-497.

Siliciano JD, Canman CE, Taya Y, Sakaguchi K, Appella E et al. (1997) DNA damage induces phosphorylation of the amino terminus of p53. Genes Dev 11(24): 3471-3481.

Simmons DG, Cross JC (2005) Determinants of trophoblast lineage and cell subtype specification in the mouse placenta. Dev Biol 284(1): 12-24.

Singaravelu K, Devalaraja-Narashimha K, Lastovica B, Padanilam BJ (2009) PERP, a p53 proapoptotic target, mediates apoptotic cell death in renal ischemia. Am J Physiol Renal Physiol 296(4): F847-858.

Smale ST, Kadonaga JT (2003) The RNA polymerase II core promoter. Annu Rev Biochem 72: 449-479.

Stein T, Crighton D, Boyle JM, Varley JM, White RJ (2002) RNA polymerase III transcription can be derepressed by oncogenes or mutations that compromise p53 function in tumours and Li-Fraumeni syndrome. Oncogene 21(19): 2961-2970.

Stewart CL, Schuetze S, Vanek M, Wagner EF (1987) Expression of retroviral vectors in transgenic mice obtained by embryo infection. Embo J 6(2): 383-388.

Tam PP, Loebel DA (2007) Gene function in mouse embryogenesis: get set for gastrulation. Nat Rev Genet 8(5): 368-381.

Tam PP, Loebel DA, Tanaka SS (2006) Building the mouse gastrula: signals, asymmetry and lineages. Curr Opin Genet Dev 16(4): 419-425.

Tanaka S, Kunath T, Hadjantonakis AK, Nagy A, Rossant J (1998) Promotion of trophoblast stem cell proliferation by FGF4. Science 282(5396): 2072-2075.

Tavenet A, Suleau A, Dubreuil G, Ferrari R, Ducrot C et al. (2009) Genome-wide location analysis reveals a role for Sub1 in RNA polymerase III transcription. Proc Natl Acad Sci U S A 106(34): 14265-14270.

Thomas MC, Chiang CM (2006) The general transcription machinery and general cofactors. Crit Rev Biochem Mol Biol 41(3): 105-178.

Tudor M, Murray PJ, Onufryk C, Jaenisch R, Young RA (1999) Ubiquitous expression and embryonic requirement for RNA polymerase II coactivator subunit Srb7 in mice. Genes Dev 13(18): 2365-2368.

Ullah Z, Lee CY, Depamphilis ML (2009) Cip/Kip cyclin-dependent protein kinase inhibitors and the road to polyploidy. Cell Div 4: 10.

Wang JY, Sarker AH, Cooper PK, Volkert MR (2004) The single-strand DNA binding activity of human PC4 prevents mutagenesis and killing by oxidative DNA damage. Mol Cell Biol 24(13): 6084-6093.

Wang W, Huang L, Huang Y, Yin JW, Berk AJ et al. (2009) Mediator MED23 links insulin signaling to the adipogenesis transcription cascade. Dev Cell 16(5): 764-771.

Wang Y, Baskerville S, Shenoy A, Babiarz JE, Baehner L et al. (2008) Embryonic stem cell-specific microRNAs regulate the G1-S transition and promote rapid proliferation. Nat Genet 40(12): 1478-1483.

Wang Z, Roeder RG (1998) DNA topoisomerase I and PC4 can interact with human TFIIIC to promote both accurate termination and transcription reinitiation by RNA polymerase III. Mol Cell 1(5): 749-757.

Wang ZQ, Auer B, Stingl L, Berghammer H, Haidacher D et al. (1995) Mice lacking ADPRT and poly(ADP-ribosyl)ation develop normally but are susceptible to skin disease. Genes Dev 9(5): 509-520.

Weger S, Wendland M, Kleinschmidt JA, Heilbronn R (1999) The adeno-associated virus type 2 regulatory proteins rep78 and rep68 interact with the transcriptional coactivator PC4. J Virol 73(1): 260-269.

Werten S, Moras D (2006) A global transcription cofactor bound to juxtaposed strands of unwound DNA. Nat Struct Mol Biol 13(2): 181-182.

Werten S, Wechselberger R, Boelens R, van der Vliet PC, Kaptein R (1999) Identification of the single-stranded DNA binding surface of the transcriptional coactivator PC4 by NMR. J Biol Chem 274(6): 3693-3699.

Werten S, Langen FW, van Schaik R, Timmers HT, Meisterernst M et al. (1998a) High-affinity DNA binding by the C-terminal domain of the transcriptional coactivator PC4 requires simultaneous interaction with two opposing unpaired strands and results in helix destabilization. J Mol Biol 276(2): 367-377.

Werten S, Stelzer G, Goppelt A, Langen FM, Gros P et al. (1998b) Interaction of PC4 with melted DNA inhibits transcription. Embo J 17(17): 5103-5111.

Wu SY, Chiang CM (1998) Properties of PC4 and an RNA polymerase II complex in directing activated and basal transcription in vitro. J Biol Chem 273(20): 12492-12498.

Wu SY, Kershnar E, Chiang CM (1998) TAFII-independent activation mediated by human TBP in the presence of the positive cofactor PC4. Embo J 17(15): 4478-4490.

Wu SY, Thomas MC, Hou SY, Likhite V, Chiang CM (1999a) Isolation of mouse TFIID and functional characterization of TBP and TFIID in mediating estrogen receptor and chromatin transcription. J Biol Chem 274(33): 23480-23490.

Wu WH, Pinto I, Chen BS, Hampsey M (1999b) Mutational analysis of yeast TFIIB. A functional relationship between Ssu72 and Sub1/Tsp1 defined by allele-specific interactions with TFIIB. Genetics 153(2): 643-652.

Young AP, Longmore GD (2004) Differential regulation of apoptotic genes by Rb in human versus mouse cells. Oncogene 23(15): 2587-2599.

Zhong L, Wang Y, Kannan P, Tainsky MA (2003) Functional characterization of the interacting domains of the positive coactivator PC4 with the transcription factor AP-2alpha. Gene 320: 155-164.

Zhou HM, Wang J, Rogers R, Conway SJ (2008) Lineage-specific responses to reduced embryonic Pax3 expression levels. Dev Biol 315(2): 369-382.

Zhu Y, Qi C, Jia Y, Nye JS, Rao MS et al. (2000) Deletion of PBP/PPARBP, the gene for nuclear receptor coactivator peroxisome proliferator-activated receptor-binding protein, results in embryonic lethality. J Biol Chem 275(20): 14779-14782.

6. APPENDIX

6.1 List of abbreviations

%	percentage
°C	degree Celsius
[α^{32}P]dCTP	cytidine 5´-alpha 32P triphosphate
aa	amino acid
bp	base pair
Cat. No.	catalogue number
cDNA	complementary deoxyribonucleic acid
CTD	carboxy-terminal domain of RNA polymerase II
C-terminal	carboxy-terminal
dH_2O	distilled water
dNTP	deoxynucleoside triphosphate
DMEM	Dulbecco's Modified Eagle Medium
DNA	deoxyribonucleic acid
ds	double-stranded
g	gram
mg	milligram
µg	microgram
HSV-tk	herpes simplex virus thymidine kinase
IF	immunofluorescence
ID	identification number
kDa	kilo Dalton
kb	kilobase
L	liter
ml	milliliter
µl	microliter
M	molar
mM	millimolar
mir	microRNA
mRNA	messenger RNA
N-terminal	aminoterminal
NaCl	sodiumchloride
PC4	positive transcription cofactor 4
PC4-CTD	carboxy-terminal domain of PC4
PCR	polymerase chain reaction
RNA	ribonucleic acid
±SD	standard diviation
siRNA	small interfering RNA
ss	single-stranded
U	unit
V	volt(s)
kV	kilovolt(s)
µF	microfarad(s)
WB	Western blot

6.2 Microarray data

Table 9: Genes more than two fold downregulated after PC4 knockdown in HeLa cells

Gene symbol	Gene Title	Fold Change
SUB1	SUB1 homolog (S. cerevisiae)	18.3
SPINK5	serine peptidase inhibitor, Kazal type 5	3.6
EIF4EBP2	Eukaryotic translation initiation factor 4E binding protein 2	2.6
IFI44	interferon-induced protein 44	2.8
C1S	complement component 1, s subcomponent	2.6
C3	complement component 3	2.6
RP1-32F7.2	hypothetical protein FLJ37659	2.7
KCNK3	potassium channel, subfamily K, member 3	2.7
POPDC3	popeye domain containing 3	2.1
GPNMB	glycoprotein (transmembrane) nmb	3.3
CA9	carbonic anhydrase IX	2.7
LOC339745	hypothetical protein LOC339745	2.2
TNFRSF11B	tumor necrosis factor receptor superfamily, member 11b (osteoprotegerin)	2.1

Table 10: Genes more than two fold upregulated after PC4 knockdown in HeLa cells

Gene symbol	Gene Title	Fold Change
C19orf6	chromosome 19 open reading frame 6	23.0
PTK9	PTK9 protein tyrosine kinase 9	13.4
HSP90AB1	heat shock protein 90kDa alpha (cytosolic), class B member 1	11.4
SLC39A6	solute carrier family 39 (zinc transporter), member 6	9.5
VPS35	vacuolar protein sorting 35 (yeast)	7.8
CDCP1	CUB domain containing protein 1	7.7
WDR1	WD repeat domain 1	6.4
P4HB	procollagen-proline, 2-oxoglutarate 4-dioxygenase (proline 4-hydroxylase), beta polypeptide	6.1
DAPK3	death-associated protein kinase 3	6.0
HSP90B1	heat shock protein 90kDa beta (Grp94), member 1	5.9
SPTBN1	spectrin, beta, non-erythrocytic 1	5.7
FUS	fusion (involved in t(12;16) in malignant liposarcoma)	5.5
PTBP1	polypyrimidine tract binding protein 1	5.3
GRK5	G protein-coupled receptor kinase 5	5.1
INPP5A	inositol polyphosphate-5-phosphatase, 40kDa	5.1
RAD21	RAD21 homolog (S. pombe)	5.1
LIX1L	Lix1 homolog (mouse) like	5.0
BUB1	BUB1 budding uninhibited by benzimidazoles 1 homolog (yeast)	4.8

PIP5K1A	phosphatidylinositol-4-phosphate 5-kinase, type I, alpha	4.6
WDR68	WD repeat domain 68	4.6
PSPC1	paraspeckle component 1	4.4
RXRB	retinoid X receptor, beta	4.3
PTPLB	protein tyrosine phosphatase-like (proline instead of catalytic arginine), member b	4.3
MET	met proto-oncogene (hepatocyte growth factor receptor)	4.3
PITPNC1	Phosphatidylinositol transfer protein, cytoplasmic 1	4.1
THBS1	thrombospondin 1	4.0
NEK9	NIMA (never in mitosis gene a)- related kinase 9	3.8
SYTL5	synaptotagmin-like 5	3.8
SKP2	S-phase kinase-associated protein 2 (p45)	3.8
CBFB	core-binding factor, beta subunit	3.7
HIPK2	Homeodomain interacting protein kinase 2	3.7
TAGLN	transgelin	3.6
MATR3	matrin 3	3.6
FAM60A	family with sequence similarity 60, member A	3.6
PTRF	polymerase I and transcript release factor	3.6
HRB	HIV-1 Rev binding protein	3.6
MAZ	MYC-associated zinc finger protein (purine-binding transcription factor)	3.6
VIL2	villin 2 (ezrin)	3.5
CARS	cysteinyl-tRNA synthetase	3.5
ABR	active BCR-related gene	3.5
FAM62B	family with sequence similarity 62 (C2 domain containing) member B	3.4
SPFH1	SPFH domain family, member 1	3.4
SP1	Sp1 transcription factor	3.4
CASP2	caspase 2, apoptosis-related cysteine peptidase (neural precursor cell expressed, developmentally down-regulated 2)	3.4
BHLHB2	basic helix-loop-helix domain containing, class B, 2	3.4
RERE	arginine-glutamic acid dipeptide (RE) repeats	3.4
CDV3	CDV3 homolog (mouse)	3.4
MGC23985	similar to AVLV472	3.3
USP31	ubiquitin specific peptidase 31	3.3
SPG7	spastic paraplegia 7, paraplegin (pure and complicated autosomal recessive)	3.2
C9orf86	chromosome 9 open reading frame 86	3.2
FXR1	fragile X mental retardation, autosomal homolog 1	3.2
KIAA1458	KIAA1458	3.1
TMPO	thymopoietin	3.1
FGFR1	fibroblast growth factor receptor 1 (fms-related tyrosine kinase 2, Pfeiffer syndrome)	3.0
M6PR	mannose-6-phosphate receptor (cation dependent)	2.9
RSN	restin (Reed-Steinberg cell-expressed intermediate filament-associated protein)	2.9
BCL2L1	BCL2-like 1	2.9
CAB39	calcium binding protein 39	2.7
C3orf37	Chromosome 3 open reading frame 37	2.7
WAC	WW domain containing adaptor with coiled-coil	2.7
RP6-213H19.1	serine/threonine protein kinase MST4 /// serine/threonine protein kinase MST4	2.7

CYCS	cytochrome c, somatic	2.7
MOBK1B	MOB1, Mps One Binder kinase activator-like 1B (yeast)	2.6
CALD1	caldesmon 1	2.6
ARL2BP	ADP-ribosylation factor-like 2 binding protein	2.6
MRPL30	mitochondrial ribosomal protein L30	2.6
MAPKAPK2	mitogen-activated protein kinase-activated protein kinase 2	2.6
HERC4	hect domain and RLD 4	2.6
GLUL	glutamate-ammonia ligase (glutamine synthetase)	2.6
CYB5R3	cytochrome b5 reductase 3	2.6
RANBP2	RAN binding protein 2	2.5
HIP1	huntingtin interacting protein 1	2.5
DSG2	desmoglein 2	2.5
LOC653890	similar to serine/threonine/tyrosine interacting protein	2.5
MSRB3	methionine sulfoxide reductase B3	2.5
TAF6L	TAF6-like RNA polymerase II, p300/CBP-associated factor (PCAF)-associated factor, 65kDa	2.4
CLSPN	claspin homolog (Xenopus laevis)	2.4
TAF9B	TAF9B RNA polymerase II, TATA box binding protein (TBP)-associated factor, 31kDa /// similar to TBP-associated factor 9L	2.4
RAB11FIP1	RAB11 family interacting protein 1 (class I)	2.4
PDK4	pyruvate dehydrogenase kinase, isozyme 4	2.4
CAV2	caveolin 2	2.4
XTP3TPA	XTP3-transactivated protein A	2.4
SMAD3	SMAD, mothers against DPP homolog 3 (Drosophila)	2.4
SLC10A3	solute carrier family 10 (sodium/bile acid cotransporter family), member 3	2.4
GSTCD	glutathione S-transferase, C-terminal domain containing	2.4
CDC2L5	cell division cycle 2-like 5 (cholinesterase-related cell division controller)	2.4
SFPQ	Splicing factor proline/glutamine-rich (polypyrimidine tract binding protein associated)	2.3
C5orf22	chromosome 5 open reading frame 22	2.3
SQLE	squalene epoxidase	2.3
FAM120A	family with sequence similarity 120A	2.3
C5orf13	chromosome 5 open reading frame 13	2.3
CPNE3	copine III	2.3
NFIB	nuclear factor I/B	2.2
MT1F	metallothionein 1F (functional)	2.2
RICTOR	rapamycin-insensitive companion of mTOR	2.2
ANKHD1 /// MASK-BP3	ankyrin repeat and KH domain containing 1 /// MASK-4E-BP3 alternate reading frame gene	2.2
ODZ2	odz, odd Oz/ten-m homolog 2 (Drosophila)	2.1
HSPH1	heat shock 105kDa/110kDa protein 1	2.1
C16orf35	chromosome 16 open reading frame 35	2.1
UBE2M	ubiquitin-conjugating enzyme E2M (UBC12 homolog, yeast)	2.1
SVH	SVH protein	2.1
RAP2A	RAP2A, member of RAS oncogene family	2.1
DDX3X	DEAD (Asp-Glu-Ala-Asp) box polypeptide 3, X-linked	2.1
TMOD3	tropomodulin 3 (ubiquitous)	2.1
C9orf19	chromosome 9 open reading frame 19	2.1

ARHGAP18	Rho GTPase activating protein 18	2.1
AP1S3	adaptor-related protein complex 1, sigma 3 subunit	2.1
NUSAP1	nucleolar and spindle associated protein 1	2.0
ADAM9	ADAM metallopeptidase domain 9 (meltrin gamma)	2.0

CURRICULUM VITAE

Personal data:

Full Name	Na Li
Gender	Female
Date of Birth	15.04.1979
Nationality	Chinese
Marital Status	Married

Dissertation:

Since June 2005 (Jun. 2005-May. 2008) Laboratory of Prof. Dr. Michael Meisterernst,
Institute of Molecular Immunology,
Helmholtz-Zentrum München

(Jun. 2008- present) Laboratory of Prof. Dr. Michael Meisterernst,
Institute of Molecular Tumor Biology,
Medical Faculty of the WWU Münster

Title of the thesis: Critical role of transcription cofactor PC4 in mammals

University education:

Sept. 1997- Jul. 2001 Bachelor's education in biological science, School of Life science,
Northeast Normal University, China

Sept. 2001- Sep. 2004 Master's education in cell biology, Institute of Genetics and Cytology,
Northeast Normal University, China

Title of Master thesis: Modified heparin can inhibit P-selectin-mediated adhesion of leucocytes

School education:

Sept. 1985-Jul. 1991 Shiyan Elementary School of Xin Zheng in Henan Province, China

Sept. 1991-Jul. 1994 Yuanling Junior High School of Xin Zheng in Henan Province, China

Sept. 1994-Jul. 1997 The first Senior High School of Xin Zheng in Henan Province, China

Munich, 11.01.2010